

The role of xenoestrogens in the initiation of primary biliary cirrhosis

Andrew Axon, BSc



Thesis submitted in fulfilment of the requirements for the degree of
Doctor of Philosophy

Newcastle University

Faculty of Medical Sciences

Institute of Cellular Medicine

September 2011

Declaration

I hereby declare that this thesis has been composed by myself and has not been accepted in any previous application for a degree. The work has been performed by myself unless otherwise stated. All sources of information have been appropriately acknowledged by means of reference.

Andrew Axon

Abstract

Introduction

Primary biliary cirrhosis (PBC) is a chronic cholestatic liver disease common in postmenopausal women, characterised by the presence of serum antimitochondrial antibodies. Exposure to environmental xenobiotics and estrogenic drugs has been linked to an increased incidence of PBC and cholestasis respectively. We hypothesized that exposure to environmental xenoestrogens may be a risk factor for PBC.

Methods

A screening system by which compounds could be tested for transcriptional estrogenic activity was developed and validated. Compounds were screened for human estrogenic activity by dual luciferase reporter assay and by measurement of the induction of a known estrogen responsive gene, TFF1. The effects of exposure to xenoestrogens on mitochondrial function was assessed by MTS assay and by measurement of TMRM localization. In vivo effects of exposure to xenoestrogens was examined in a range of mouse models.

Results

A number of xenoestrogens were identified, notably the azo dyes sunset yellow and tartrazine, however, neither of these tested positive in the classical mouse uterotrophic assay. Further investigations suggested that these compounds might have a higher affinity and/or specificity for ER β , which may not be critical for sexual development and therefore potentially explains the findings of the *in vivo* assay. Both sunset yellow and tartrazine caused a significant decrease in hepatocyte TMRM localization and sunset yellow caused a reduction in MTS

reduction in primary rat hepatocytes, suggesting these compounds have a detrimental effect on mitochondrial function.

In a mouse model of chronic exposure, tartrazine was found to significantly increase portal tract inflammation (PTI), collagen deposition and increase serum ALP activity, all of which are biomarkers of cholestatic liver injury. SYBR-Green qRT-PCR analysis revealed that both estrogen and tartrazine cause significant changes in the expression MRP 1-6 and other drug/bile salt transport proteins in the mouse liver, indicating a potential mechanism for the observed cholestasis. The expression of hepatic 3a11 was inhibited in this model implying antagonism of the pregnane X receptor.

Conclusions

These findings suggest that exposure to tartrazine, or other xenoestrogens may cause ER β activation and PXR antagonism in the liver, resulting in altered transporter expression and a cholestatic injury. If this liver insult was coupled with damage/alteration to mitochondrial reductase enzyme function, and/or other genetic/environmental factors, it may be an initiating factor in PBC.

For Grandma, Granddad, Nana and Jack.

Acknowledgements

I would like to say a huge thank you to everybody who has helped to make this thesis a possibility.

First and foremost, I would like to thank the British Toxicology Society and the Health Protection Agency for their financial contributions, without which this project would never have started.

I would like to say a huge thank you to Prof. Matt Wright, whose riotous and unrelenting enthusiasm has been indispensable over the last 3 years. Recognition must also go to the other members of my supervisory team, Prof. Peter Blain and Prof. Faith Williams.

Team Wright past and present, Karen Wallace, Helen Tovey, Emma Fairhall, Stephen Hill, Isabella Swidenbank and Philip Probert, plus honorary member Fiona Oakey. Thank you for the moral support and guidance, and also for making every aspect of scientific research a little bit more fun!

Finally I would like to thank my family, who have persevered through the last 20 years of my education, and have been there with every imaginable type of support at every step of the way. Mum, Dad, Matt and Dan, I could not have done this without you. Unfortunately my grandparents did not manage to see me complete this degree, but I know they would have been immensely proud, so for that reason I would like to dedicate this thesis to them.

Table of contents

1. Introduction	1
1.1. The liver, anatomy and function	2
1.1.1. Anatomy and position	2
1.1.1. Blood supply	2
1.2. Cells of the liver	5
1.2.1. Hepatocyte	5
1.2.2. Hepatic sinusoidal endothelial cells	6
1.2.3. Stellate cell	6
1.2.4. Cholangiocyte	6
1.2.5. Kupffer cell	7
1.2.6. PIT cell	7
1.3. Functional Units	9
1.3.1. Liver lobule	9
1.3.2. Liver acinus	9
1.3.3. Portal tract	10
1.4. Functions of the liver	13
1.4.1. Glycogen formation, storage and release	13
1.4.2. Biotransformation	13
1.4.3. Bilirubin metabolism	15
1.4.4. Amino acid and protein metabolism	15
1.4.5. Lipid metabolism	15
1.4.6. Hormone metabolism	16
1.4.7. Xenobiotic metabolism	16
1.5. Biliary system	17
1.6. Cholestasis	20
1.7. Primary biliary cirrhosis	22
1.7.1. Diagnosis of PBC	23
1.7.2. Therapeutic strategies in PBC	26
1.7.3. PBC as an autoimmune disease	30

1.7.4. Xenobiotic exposure and PBC	32
1.7.5. Estrogens and PBC	33
1.8. Estrogen	34
1.8.1. Mechanisms of estrogen signalling.....	36
1.8.2. Estrogen receptor	36
1.8.3. Modulation of estrogen signalling	39
1.8.4. Selective estrogen receptor modulators (SERM).....	39
1.8.5. Selective estrogen receptor degraders (SERD).....	40
1.8.6. Measurement of estrogenic activity	40
1.8.7. Measurement of an estrogen inducible gene.....	42
1.8.8. <i>In vivo</i> analysis of estrogenic activity by mouse uterine bioassay.....	42
1.8.9. Estrogen signalling and cholestasis.....	42
1.8.10. Xenoestrogens and PBC	45
2. Chapter 2 - Materials and Methods	46
2.1. Animals.....	47
2.1.1. Rats.	47
2.1.2. Foetal tissue	47
2.1.3. C57Bl6 wild type mice	47
2.1.4. Prepubescent C57Bl6 mice	48
2.1.5. Mouse uterine bioassay.....	48
2.1.6. Serum enzyme assays	48
2.2. Cell Culture.....	49
2.2.1. Primary rat hepatocyte isolation.....	49
2.2.2. Preparation of cell cultures from the rat biliary structure.....	50
2.2.3. Culture of adherent cell lines	51
2.2.4. Long-term storage of cells	51
2.2.5. Revival of cell stocks	52
2.2.6. Assessment of cell viability and number	52
2.2.7. Charcoal/dextran treated foetal bovine serum	52
2.3. Cell Transfection.....	53
2.3.1. Transfection using polyethylenimine.....	53

2.3.2. Transfection using Effectene reagent	54
2.3.3. Transfection using GeneJuice transfection reagent.....	55
2.3.4. Assessment of transfection efficiency.....	55
2.4. Assay Systems.....	58
2.4.1. Tetramethylrhodamine Methyl ester (TMRM) analysis of mitochondrial polarisation.....	58
2.4.2. MTS assay.....	60
2.4.3. Dual-Glo reporter assay system	60
2.4.4. Measurement of serum antibody titre against pyruvate dehydrogenase (PDC) by ELISA.....	63
2.5. Plasmid DNA Constructs.....	64
2.5.1. Transformation of competent <i>E.coli</i>	64
2.5.2. Storage of transformed bacterial cultures	64
2.5.3. Plasmid DNA miniprep.....	65
2.5.4. Plasmid DNA maxiprep.....	66
2.6. Isolation and quantification of protein samples.....	68
2.6.1. Isolation of protein from cell samples.....	68
2.6.2. Determination of protein concentration by Lowry protein assay.....	68
2.7. SDS-page and western blotting	71
2.7.1. SDS-page gel electrophoresis	71
2.7.2. Sample preparation	72
2.7.3. Western blotting.....	72
2.7.4. Immunodetection	73
2.8. Isolation and quantification nucleic acids	74
2.8.1. TRIzol purification of RNA.....	74
2.8.2. Concentration, purity and integrity of nucleotides	75
2.9. Reverse transcription- polymerase chain reaction (RT-PCR).....	76
2.9.1. cDNA synthesis by reverse transcription	76
2.9.2. DNase treatment and removal of RNA	78
2.9.3. Polymerase chain reaction.....	78
2.9.4. Primer Design	81
2.9.5. Agarose gel electrophoresis	81

2.9.6. SYBR-Green quantitative RT-PCR (qRT-PCR)	82
2.10. Immuno-histochemistry and Immuno-cytochemistry.....	89
2.10.1. Tissue preparation	89
2.10.2. Proteinase K antigen retrieval	89
2.10.3. Sodium citrate antigen retrieval.....	89
2.10.4. Immunostaining.....	90
2.10.5. Haematoxylin and eosin (H & E) staining.....	91
2.10.6. Sirius red staining	91
2.10.7. Immuno-cytochemistry.....	92
2.10.8. DAPI staining of DNA.....	92
2.11. Calculation of half maximal effective concentration (EC₅₀) and half maximal inhibitory concentration (IC₅₀).....	96
3. Chapter 3 – Results.....	98
3.1. Development of a screening system for transcriptional estrogenic activity	99
3.1.1. Construction of an estrogen receptor luciferase reporter construct ...	100
3.1.1.1. pGL3-Promoter vector	100
3.1.1.2. Estrogen response element insert	101
3.1.1.3. Construction of a (ERE) ₃ -Luciferase construct	101
3.1.2. (ERE) ₃ -Luciferase reporter construct is estrogen responsive	104
3.1.3. (ERE) ₃ -pGL3-Promoter construct (ERLuc5) is specific for estrogen receptors α and β	107
3.1.4. Estrogen mediated expression of trefoil factor 1.....	110
3.1.4.1. TFF1 mRNA is expressed in MCF-7 cells.....	110
3.1.4.2. Estrogen increases TFF1 expression is in MCF-7 but not MDA cell lines	110
3.1.4.3. Treatment with the anti-estrogen, tamoxifen, inhibits TFF1 mRNA expression in MCF-7 cells	113
3.1.5. Chapter 3.1 discussion	115
3.2. Screening for transcriptional estrogenic activity of xenobiotics	116

3.2.1. Screening for transcriptional estrogenic activity by dual luciferase assay.....	117
3.2.2. Xenobiotic mediated increase in luciferase activity is inhibited by ICI182780.....	122
3.2.3. Dose-response study of xenobiotic mediated transcriptional estrogenic activity.....	126
3.2.4. Screening for transcriptional estrogenic activity by measurement of TFF1 expression in MCF-7 cells	132
3.2.5. Screening for transcriptional xenoestrogenic activity in primary rat hepatocytes by dual luciferase reporter assay.....	136
3.2.6. (ERE) ₃ -pGL3-Promoter is responsive to both ER α and ER β	140
3.2.7. Chapter 3.2 discussion	144
3.3. Effect of xenoestrogen exposure on mitochondrial function and polarisation.....	145
3.3.1. Mitochondrial reductase activity in primary rat hepatocytes in response to xenoestrogen exposure.	146
3.3.2. Measurement of mitochondrial polarisation in rat hepatocytes by live TMRM localisation following exposure to xenoestrogens	154
3.3.3. Chapter 3.3 discussion.	156
3.4. <i>in vivo</i> exposure to xenoestrogens.....	158
3.4.1. Expression of estrogen receptors <i>in vivo</i>	159
3.4.2. Acute exposure to estrogen causes portal tract inflammation in the mouse.....	160
3.4.2.1. Inflammatory infiltrate around the portal contract are of a mixed population which contain some NIMP positive cells	165
3.4.3. Tartrazine and sunset yellow do not test positive for estrogenic activity by mouse uterine bioassay	170
3.4.4. In vivo model of xenoestrogen exposure on liver function in the mouse	172
3.4.4.1. Administration of E2 and tartrazine both cause elevated serum ALP activity in the mouse	172
3.4.4.2. E2 and Tartrazine both cause increased PTI in the mouse	175

3.4.4.3. Treatment with E2 and tartrazine both cause increased collagen deposition around the portal tracts of the mouse liver.....	177
3.4.4.4. Estrogen and xenoestrogen exposure causes altered bile/drug transport protein expression in the mouse liver.....	180
3.4.4.5. Exposure to estrogen causes increased serum AMA titre in the mouse	186
3.4.5. Chapter 3.4 discussion	190
3.5. Isolation, characterisation and proliferation of cells isolated from the intrahepatic biliary structure.....	193
3.5.1. Isolation of cell cultures from the intrahepatic biliary structure.....	194
3.5.2. Cell cultures isolated from the intrahepatic biliary structure contained an OV-6 positive progenitor, giving rise to cholangiocytes and fibroblasts	197
3.5.3. Cell cultures isolated from the intrahepatic biliary structure of the rat express common pluripotency/progenitor factors	201
3.5.4. Estrogen causes increased proliferation of biliary cell cultures.....	203
3.5.5. Chapter 3.5 discussion	209
4. General discussion	211
5. References	220
6. Communication and Awards.....	233
7. Publications and Abstracts.....	234

List of figures

1.1	The liver structure	4
1.2	Liver cells	8
1.3	The liver lobule.....	11
1.4	Liver ascinus and portal tract	12
1.5	Biliary system and function.....	19
1.6	Primary biliary cirrhosis	25
1.7	Estrogen receptor signalling.....	38
1.8	Estrogen cholestasis	44
2.1	pEGFP-N1.....	57
2.2	Trimethylrhodamine methylester	59
2.3	Assay systems	62
2.4	Lowry protein assay	70
2.5	Reverse transcription	77
2.6	Polymerase chain reaction	80
2.7	SYBR Green qRT-PCR.....	84
3.1	(ERE) ₃ -pGL3-luciferase construct	103
3.2	MCF-7 dual luciferase assay	106
3.3	Specificity of (ERE) ₃ -pGL3-promoter luciferase construct	109
3.4	TFF1 induction in MCF-7 cells	112

3.5	TFF1 expression dose response	114
3.6	Xenoestrogen screening 1	119
3.7	Xenoestrogen screening 2	121
3.8	Antagonism of xenoestrogen activity by ICI182780	124
3.9	Estrogenic activity of 10nM concentration of steroid hormones	125
3.10	Dose response studies of xenoestrogenic activity 1	127
3.11	Dose response studies of xenoestrogenic activity 2	128
3.12	Dose response studies of xenoestrogenic activity 3	129
3.13	Xenoestrogen mediated TFF1 induction	134
3.14	Expression of TFF1 following treatment with 10nM steroid hormones	135
3.15	Expression of the rat ER	138
3.16	Xenoestrogen screening in primary rat hepatocytes	139
3.17	Ectopic expression and activation of the hER in MDA cells	142
3.18	Ectopic expression and activation of the hER in H69 cells	143
3.19	MTS activity in primary rat hepatocytes following xenoestrogen exposure	147
3.20	Dose response study of MTS reduction in primary rat hepatocytes treated with sunset yellow	149
3.21	Dose response study of MTS reduction in primary rat hepatocytes treated with tartrazine	150
3.22	Effect of modulators on mitochondrial function on sunset yellow mediated effects on MTS reduction	153
3.23	TMRM integrity in primary rat hepatocytes following treatment with xenoestrogens	155
3.24	Mouse estrogen receptor expression and E2 induced PTI	161
3.25	Expression of ER α in the mouse liver by IHC	163

3.26	Expression of ER β in the mouse liver by IHC.....	164
3.27	Detection of cells expressing the NIMP antigen in PTI in the mouse liver	167
3.28	No cells expressing the F4/80 antigen were detected in the PTI in the mouse liver.....	168
3.29	No cells expressing the CD3 antigen were detected in the PTI in the mouse liver.....	169
3.30	Uterotropic effects of xenoestrogen exposure in the mouse	171
3.31	Treatment with E2 and tartrazine cause elevated serum ALP activity in the mouse	174
3.32	Typical PTI in the mouse liver following treatment with E2 and tartrazine	176
3.33	Typical sirius red staining in the mouse liver following treatment with E2 and tartrazine	178
3.34	Analysis of portal tract injury following treatment with xenoestrogens..	179
3.35	Expression of Abcc family of transport proteins in the mouse liver following treatment with xenoestrogens	182
3.36	SYBR Green qRT-PCR analysis of gene expression in the mouse liver following treatment with xenoestrogens	185
3.37	Serum AMA activity in the mouse following treatment with xenoestrogens	188
3.38	Correlation between serum AMA activity and severity of cholestatic liver injury	189
3.39	Mixed cell cultures isolated from the rat biliary structure	196
3.40	ICC study of mixed cell cultures isolated from the rat intrahepatic biliary structure.....	199

3.41	Profile of CK19, albumin and vimentin expression in biliary cell cultures throughout culture	200
3.42	Profile of the expression of pluripotency factors and the ER in biliary cell cultures	202
3.43	Effect of E2 on the proliferation of biliary cell cultures by cell count.....	204
3.44	Effect of E2 on the proliferation of biliary cell cultures by total actin.....	206
3.45	Effect of E2 on the differentiation of biliary cell cultures	208

1. Introduction

1.1. The liver, anatomy and function

1.1.1. Anatomy and position

The liver is the largest gland in the human body, it performs an extensive number of diverse functions, many of which are essential for health and survival. The liver is located in the right upper quadrant of the abdominal cavity and is of reddish-brown appearance, it is the shape of a rounded wedge and in a normal adult has a mass of between 1.2 and 1.6kg^{17, 18}.

The human liver is usually described to have three distinct surfaces, the superior, inferior and posterior. The superior surface is attached to the underside of the diaphragm and the anterior abdominal wall by the falciform ligament, along the line of which the liver is divided into the right and left lobes(Fig 1.1A). The right lobe is much larger in size than the left by a ratio of approximately 6:1. The inferior and posterior surfaces are themselves divided into 4 lobes by 5 fossæ^{17, 18}.

1.1.1. Blood supply

The liver receives a dual blood supply, 75% of which comes via the hepatic portal vein, delivering venous blood drained from the gastrointestinal tract and its associated organs. The remaining 25% of the blood supply to the liver is via the hepatic artery, providing the liver with a supply of oxygenated arterial blood. Both these blood vessels, along with the common bile duct, enter the organ at

the region named the *Porta hepatis*, an area under the surface of the left side of the right lobe.

The blood supply empties into central veins within the liver lobules which converge to form hepatic veins, the blood then leaves the liver and is drained via the inferior vena cava^{17, 18} (Fig 1.1B)

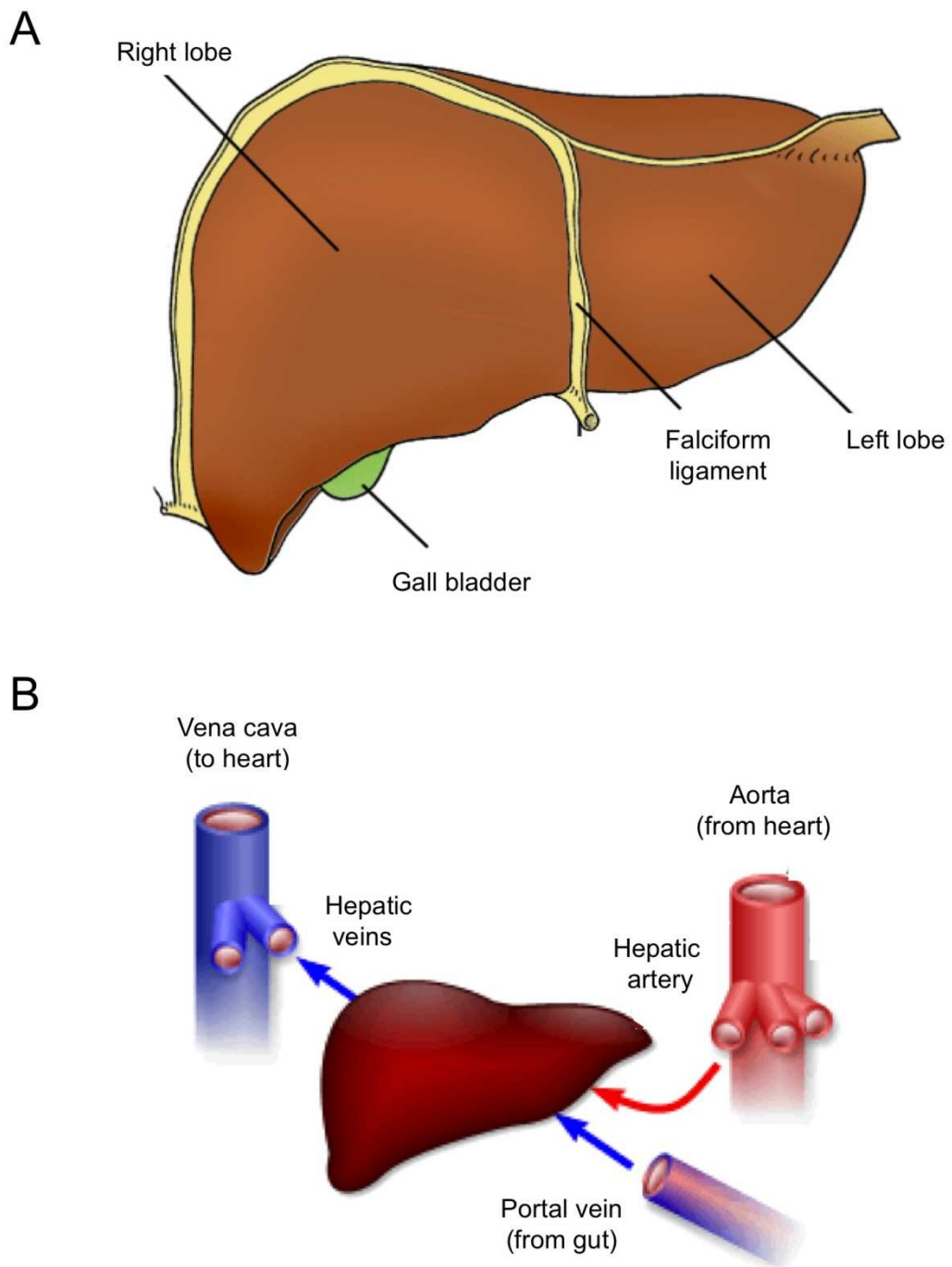


Figure 1.1 – The liver structure. A. Anterior view of the human liver. Adapted from Structure and function of the liver, e-Learning unit, St Georges, University of London⁵. B. Detail of dual blood supply to the human liver, Adapted from www.blobs.org⁹

1.2. Cells of the liver

1.2.1. Hepatocyte

Hepatocytes are the largest and most abundant cell type in the liver, the 300 billion hepatocytes that form a typical adult human liver constitute approximately 80% of the total liver mass¹⁷. The hepatocyte is a polygonal epithelial cell, with a typical lifespan of 150-200 days¹⁷. A hepatocyte can be considered to have 3 distinct surfaces that are clearly defined by both morphology and function. Around a third of the surface of a typical hepatocyte membrane constitutes the sinusoidal surface. The sinusoidal (basolateral) surface is specialised for absorptive and secretory functions by the presence of numerous microvilli some of which project into the space of Disse. Approximately 15% of the hepatocyte surface forms the canalicular (apical) membrane, this is the secretory pole of the hepatocyte forming the bile canaliculi. The remaining 50% of the hepatocyte forms a smooth intercellular fissure, which is in contact with the space of Disse and sealed from the bile canaliculi by tight junctions. Both intermediate junctions and desmosomes, known collectively as adhering junctions, link neighbouring hepatocytes. These structures contain gap junctions facilitating intercellular exchange between neighbouring cells. The hepatocyte expresses a wide variety of cell membrane transport proteins allowing it to perform its absorptive and secretory roles¹⁷(Fig 1.2A).

1.2.2. Hepatic sinusoidal endothelial cells

Hepatic sinusoidal endothelial cells constitute 15-20% of the total cell number in the liver, but only around 3% of the liver volume¹⁷. They are flat cells supported by a fine layer of extracellular matrix. Endothelial cells form the continuous lining of the sinusoid, where portal and arterial blood are combined¹⁷.

1.2.3. Stellate cell

Stellate cells, first described by Ito in 1951, make up 3-8% of the total liver cell number and lay in the area between the hepatocytes and the sinusoidal endothelial cells, known as the space of Disse¹⁷. Stellate cells are at their most abundant in zone III of the ascinus. In their normal phenotype, stellate cells contain an abundance of vitamin A as droplets within the cytoplasm. In response to injury the stellate cell may transdifferentiate to a myofibroblast phenotype¹⁹. When this occurs the stellate cell will shed its retinoids and begin to secrete vast quantities of extracellular matrix proteins (notably collagen type I, III and IV)¹⁹. This response of the stellate cell to injury may persist, and is thought to be the underlying causative mechanism of hepatic fibrosis¹⁷(Fig 1.2B).

1.2.4. Cholangiocyte

Biliary epithelial cells or cholangiocytes form the bile duct epithelium, their structure varies dependant upon the type and size of bile duct in which they are located. Biliary epithelial cells are predominantly concerned with the transport

of bile, from where it is collected from the apical membrane of the hepatocyte, to where it leaves the liver via the common bile duct. Like hepatocytes, biliary epithelial cells express a range of transport proteins that are essential in the production of bile¹⁷.

1.2.5. Kupffer cell

First described by K.W von Kupffer in 1898, Kupffer cells are the resident sinusoidal macrophages and constitute 8-12% of the total liver cells¹⁷. Kupffer cells are thought to be derived from monocytes, and released from stem cells within the bone marrow, they are most abundant in the periportal areas¹⁷. The most significant functions of this cell type are phagocytosis and clearance of toxins, antigens and antigen-antibody complexes¹⁷.

1.2.6. PIT cell

PIT cells are lymphocytes with large granules and rod-cored vesicles. They are natural killer cells found in the liver, particularly in the sinusoids and space of Disse. PIT cells are principally involved in the destruction of tumour, foreign and necrotic cells¹⁷.

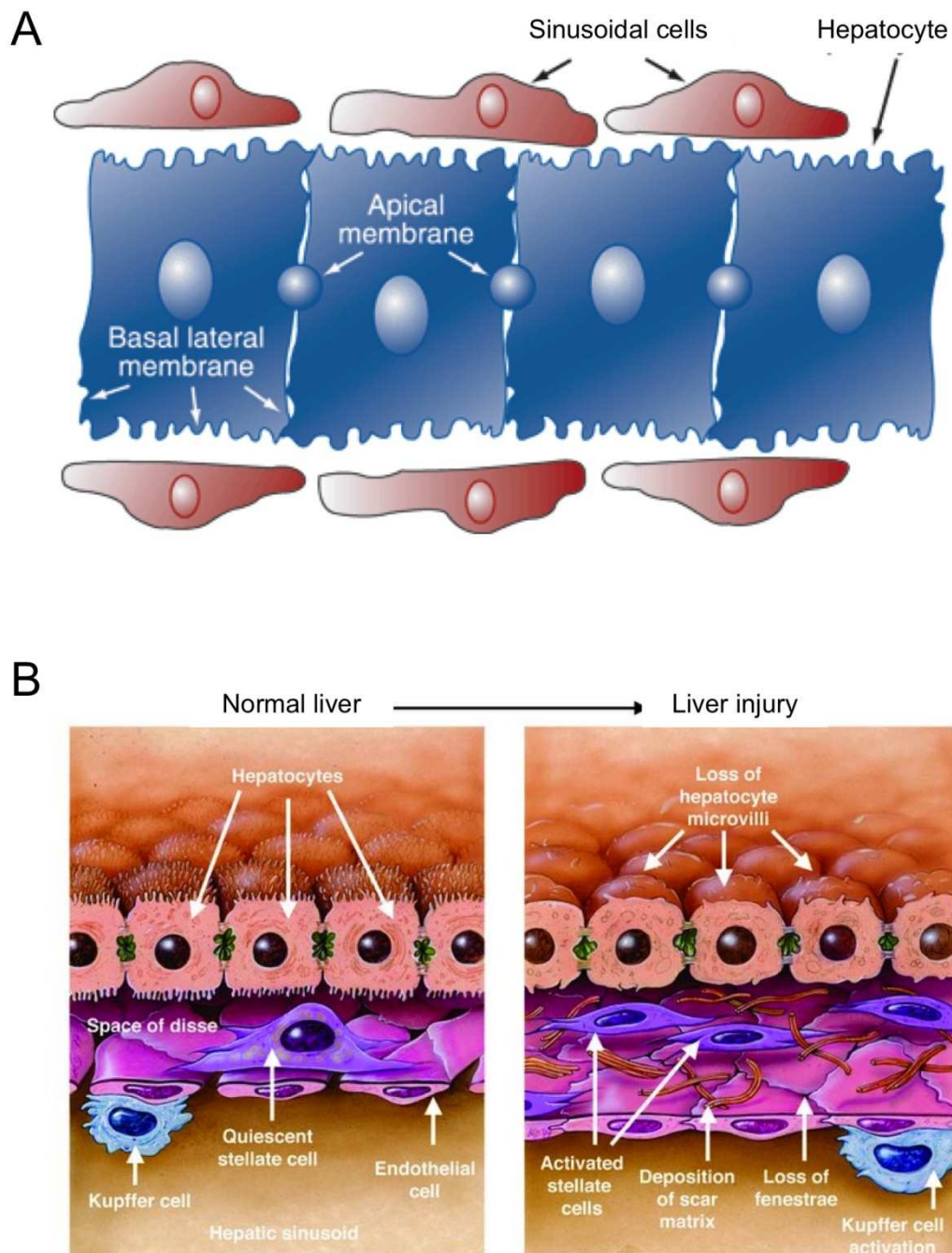


Figure 1.2 – Liver Cells. A. Hepatocellular membranes. Diagram of the orientation and position of the hepatocyte relative to the sinusoid and the apical membrane which forms the bile canaliculus. Adapted from *Use of cultured cells to study alcohol metabolism*, Clemens, D.L.⁸. **B. Cellular events in hepatic fibrosis.** Artistic representation of the cellular events leading to hepatic fibrosis, including the activation of stellate cells and deposition of collagen. Figure modified from *Mac the knife? Macrophages– the double-edged sword of hepatic fibrosis*, Friedman, S.L.¹⁵.

1.3. Functional Units

There is no standard way of describing the functional unit of the liver, as its arrangement will vary depending on the perspective from which it is studied. The functional liver unit is usually described using one of two different models, the lobule or the acinus.

1.3.1. Liver lobule

The liver lobule, first described by Kiernan focuses on the blood flow and bile drainage through the liver, it can be viewed as a hexagonal unit of 6 portal tracts surrounding a central vein. There are typically 1.0-1.5 million of these lobules in the adult liver^{17, 20}(Fig 1.3).

1.3.2. Liver acinus

The liver acinus describes a smaller functional unit than the lobule that is better used to illustrate the metabolic and secretory roles of the liver. First described by Rappaport, the acinus describes a field with the portal tract at its centre, radiating to the central vein. The acinus itself can be separated into 3 zones, with zone I being the closest to a portal tract, and therefore the richest in O₂ and zone III closest to the central vein^{17, 21}(Fig 1.4A).

1.3.3. Portal tract

The portal tract is a distinctive arrangement of branches of the hepatic artery, portal vein, bile ducts and lymphatic vessels. These vessels, along with a branch of the vagus nerve, are encased in perivascular connective tissue. The portal tract is directly surrounded by a continuous layer of specialised hepatocytes which is designated the *limiting plate*^{17, 22}(Fig 1.4B).

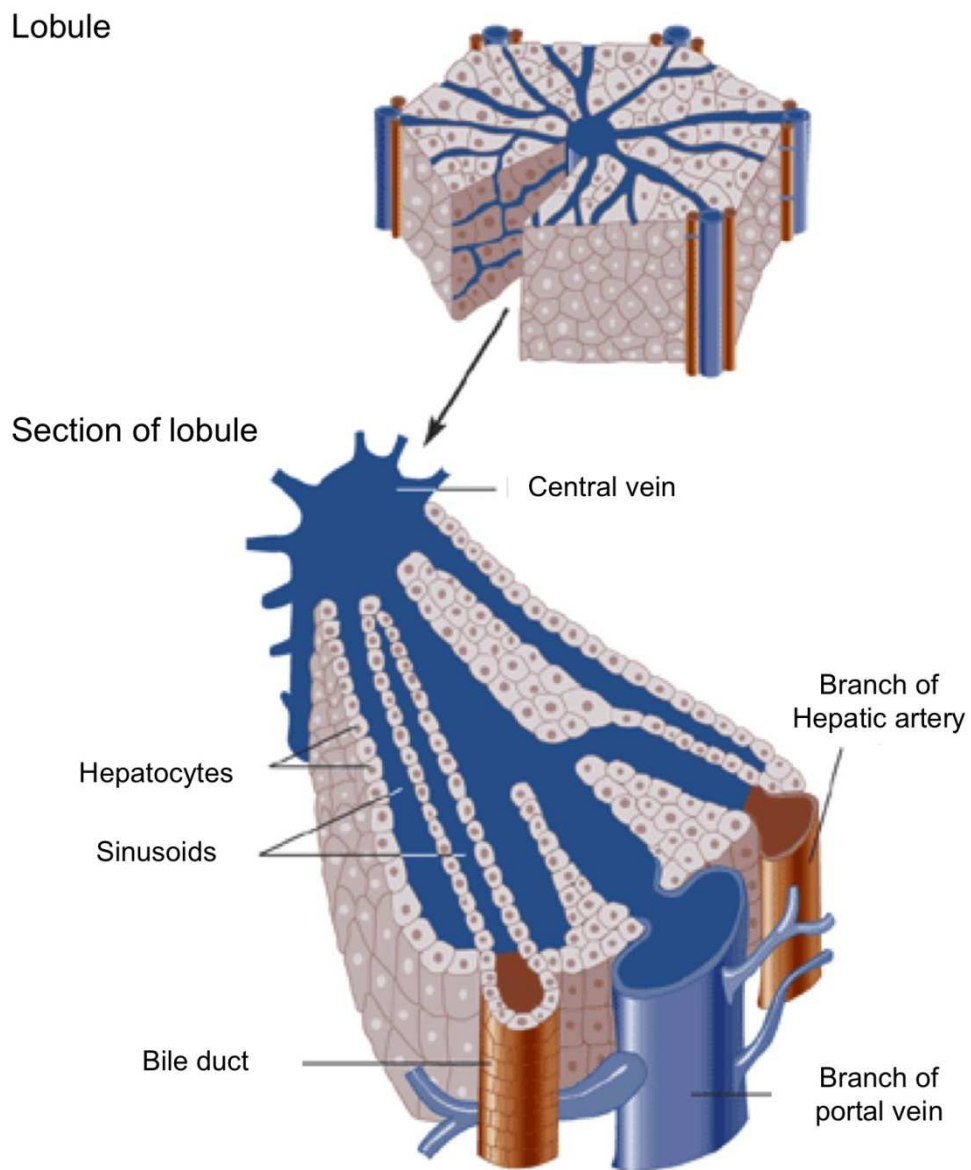


Figure 1.3 – The liver lobule. The structure of the liver lobule. Blood enters the lobule through branches of the portal vein and hepatic artery and flows through the sinusoid passing the absorptive surface of the hepatocytes before leaving the liver via the central vein. Adapted from *Energy availability and alcohol-related liver pathology*, Cunningham, C.C.⁹

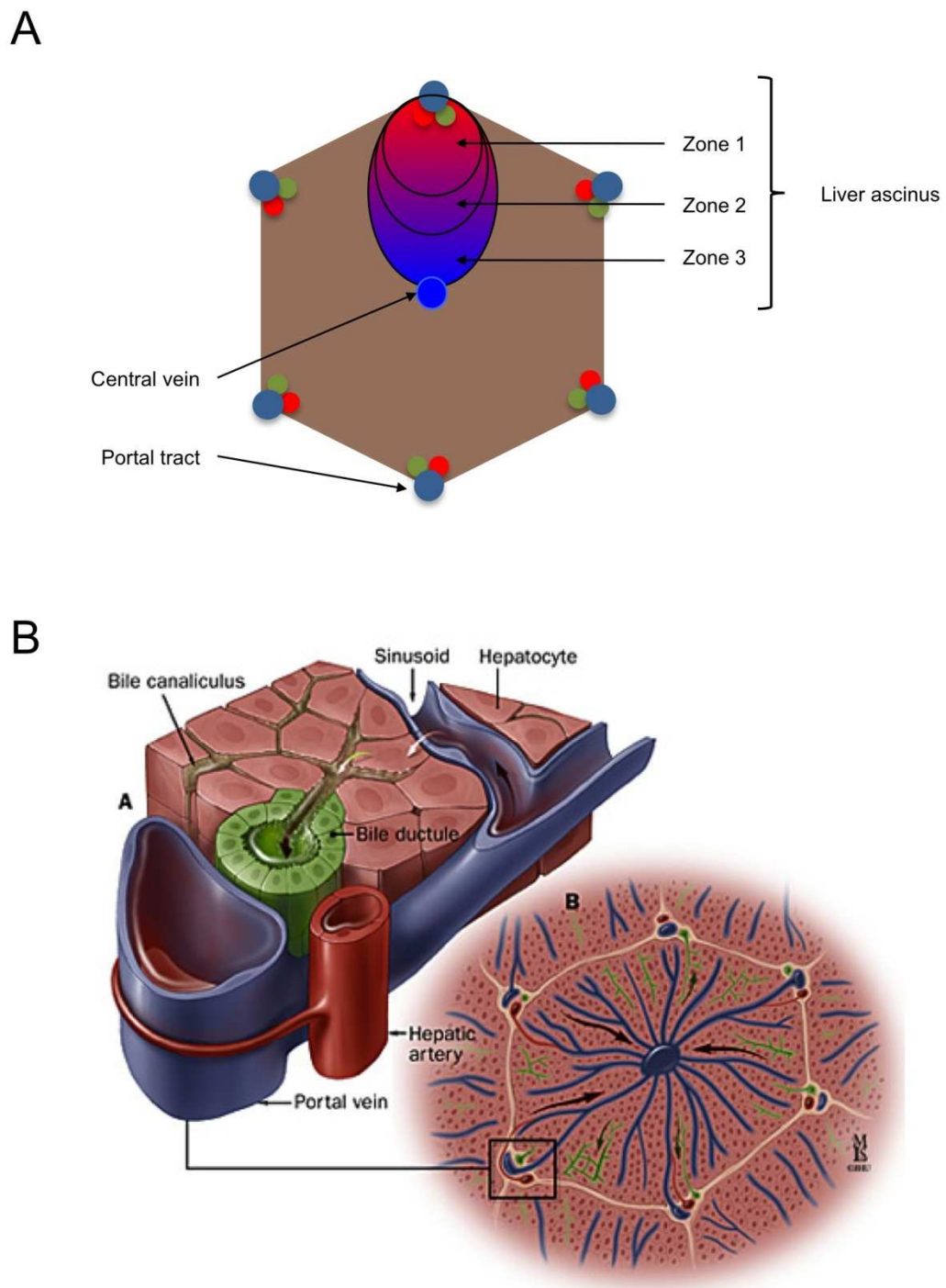


Figure 1.4 – Liver ascinus and portal tract. A. The liver ascinus. Diagram of the liver ascinus, the area between a specific portal tract and the central vein. Shown are the three ascinar zones, defined by their relative blood oxygen levels. **B. The portal tract.** Magnified view of a portal tract (A) relative to the liver lobule (B), modified from *John Hopkins Medical, Gastroenterology and Hepatology*.

1.4. Functions of the liver

1.4.1. Glycogen formation, storage and release

One of the major functions of the liver is storage of chemical energy in the form of glycogen. When dietary carbohydrates are catabolised, causing glucose to accumulate in the blood, insulin secretion from the pancreas is initiated. As blood enters the liver, insulin stimulates the liver to take up glucose. Glucose molecules are then modified to form chains of glycogen, which are stored within the hepatocytes. Providing blood levels of both glucose and insulin remain high, the liver will continue to store glycogen. Stored glycogen may comprise up to 8% of the total wet liver weight (around 80g), this is enough to maintain glucose homeostasis for up to 10 hours¹⁷.

When blood glucose levels decrease during periods of fasting, the pancreas will begin to secrete increasing amounts of glucagon, a hormone which stimulates the release of glucose into the blood¹⁷.

1.4.2. Biotransformation

The liver is the main site of elimination of both endogenous and exogenous substances from the body that are either not required or are potentially harmful. The detoxifying roles of the liver have long been established but the mechanisms utilised in the conversion of toxic substances are now termed

metabolism, because of the potential for the same processes to create harmful products from toxic substances¹⁷.

Many of the metabolic activities performed by the liver are biotransformation reactions. This refers to the biochemical alteration of a substance, which allows the conversion of lipophilic substances to excretable water-soluble metabolites. Biotransformation of both endogenous and exogenous substances may occur in many different organs, but mostly occurs in the liver^{23, 24}.

The process of biotransformation occurs in two steps, or phases. Phase 1 reactions, also termed functionalisation reactions, generally increase the water solubility of a compound, often through formation of a hydrophilic group on the target (hydroxyl, carboxyl, sulphhydryl or amine group) by one of 4 processes: oxidation, reduction, hydrolysis or hydration. A large proportion of the phase 1 oxidation reactions are performed by enzymes from the cytochrome P450 family (CYP). There are an extensive number of different CYP enzymes, derived from over 50 separate genes with different substrate specificities. CYP are the major enzymes involved in drug metabolism and bioactivation, because of the varying expression of CYP between individuals they are highly implicated in some cases of adverse drug reactions and non-response to treatment due to varying metabolism, detoxification or bioactivation^{23, 24}.

In phase 2 reactions, the product formed in phase 1 is conjugated with an endogenous substance by specific transferase enzymes. Phase 1 metabolites may be conjugated with glucuronic, sulphate, acetic or amino acids, S-adenosyl

methionine or mercaptopuric acid derivatives. The resulting conjugates are highly hydrophilic and therefore readily excretable via the urine or bile^{23, 24}.

1.4.3. Bilirubin metabolism

Bilirubin is an organic anion, produced from the breakdown of haem, primarily from erythrocytes in the spleen. Bilirubin is an apolar lipophilic substance and is potentially toxic, it is bound to serum albumin and transported to liver where it is detoxified by hepatocytes^{17, 23, 24}.

Bilirubin is transported across the sinusoidal membrane of the hepatocyte, at which point the albumin is separated. The free bilirubin is detoxified by conjugation with glucuronic acid in the smooth endoplasmic reticulum, mediated by UDP-glucuronyltransferase. The product of this reaction is water-soluble secondary bilirubin that is eliminated through the bile^{17, 23, 24} (Fig 1.5A).

1.4.4. Amino acid and protein metabolism

There is an average turnover of approximately 650g/day of the body's amino acid pool. The majority of the degradation of amino acids occurs in the liver through transamination and oxidative deamination reactions^{17, 23, 24}.

1.4.5. Lipid metabolism

The liver performs a variety of different functions in the metabolism of lipids, these include the uptake, oxidation and transformation of free fatty acids and

the synthesis of plasma lipoproteins essential for transport of lipids in the aqueous environment of the blood. The liver can also synthesise glucose from the glycerol molecule found in the triglycerides stored in fatty tissue, through the process of lipolysis^{17, 23, 24}.

85% of the body's supply of cholesterol is also formed in the liver, cholesterol is critical in the formation of cell membranes, and is the initial substrate in the biosynthesis of bile acids via cytochrome p-450 mediated oxidation, vitamin D and steroid hormones^{17, 23, 24}.

1.4.6. Hormone metabolism

The liver contributes towards the inactivation of hormones and subsequently the maintenance of hormonal homeostasis. The elimination of the steroid hormones – glucocorticoids, androgens and estrogens occurs primarily in the liver via an array of enzymatic reactions which increases their polarity to aid excretion in the bile or urine. Steroid hormones may be sulphated by sulphotransferase enzymes, glucuronidated by uridine diphosphate-glucuronosyltransferases or hydroxylated by cytochrome p-450 mono-oxygenase enzymes^{17, 23-25}.

1.4.7. Xenobiotic metabolism

Any xenobiotic in the gastrointestinal tract and some in the blood system will travel directly to the liver because of its functional role and position. This makes the liver the major site of xenobiotic, and therefore drug, metabolism. The metabolic enzymes used in the detoxification of endogenous substances are

also utilised in the metabolism, clearance and also bioactivation of xenobiotics^{17, 23, 24}.

The metabolic function of the liver may also be altered by exposure to xenobiotics, which may induce or inhibit expression or function of certain metabolising enzymes^{17, 23, 24}.

1.5. Biliary system

Hepatocytes actively transport bile acids from the blood in a process facilitated by transporters at the hepatocyte basolateral membrane¹⁶, following uptake into the hepatocytes, bile acids may be modified within the hepatocytes forming the component parts of bile. The newly formed bile salts are actively transported across the apical membrane of the hepatocyte, into the channel formed between two neighbouring cells, sealed by tight junctions. This has the effect of concentrating the bile salts in what is termed canaliculi, the osmotic gradient produced by this action is sufficient that water simultaneously diffuses into the canaliculi, producing bile. The newly formed bile is moved along the tiny canaliculi by the peristaltic movement of the actin-myosin network lying beneath the canalicular membrane of the hepatocytes. The canaliculi converge into an extension connecting them together, this intermediate ductule is referred to as the canal of Hering²⁶. From the canal of Hering onwards, the bile ductules have their own specialised epithelial lining, formed from cholangiocytes. The bile flows from the canal of Hering into the preductules, the smallest duct of the biliary tract (5-20µm in diameter). From the preductules onwards, the ducts get

progressively larger in size. Terminal ductules join interlobular bile ducts that run along the portal tracts collecting into a channel which drains through a network of small intrahepatic bile ducts, before converging in the common bile duct (CBD) and subsequent transport of bile away from the liver ²⁶.

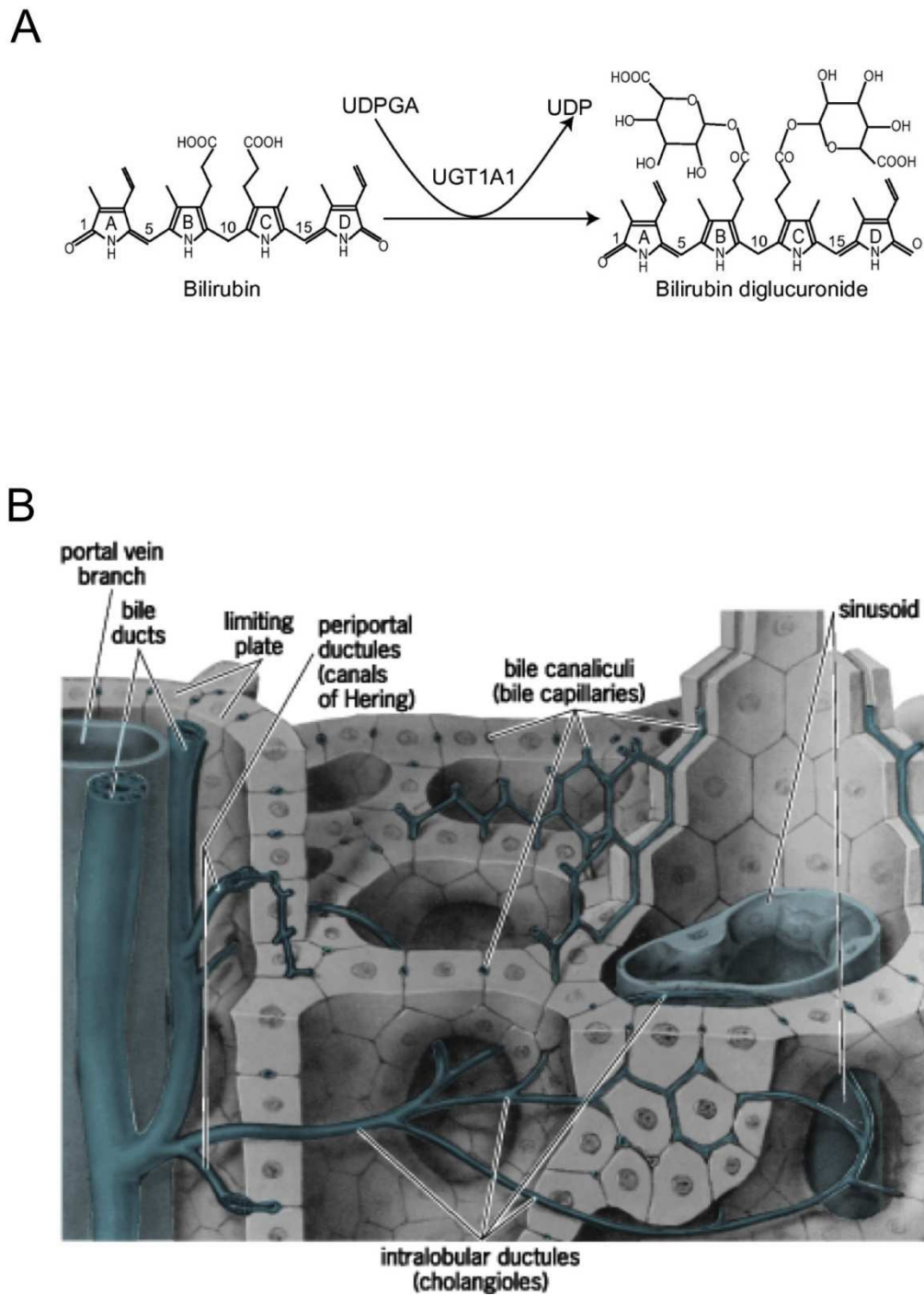


Figure 1.5 – Biliary system and function. A; Bilirubin metabolism Schematic of the metabolism of bilirubin to bilirubin diglucuronide by UGT1A1 adapted from *Adaptive evolution of multiple-variable exons and structural diversity of drug-metabolizing enzymes*, Li, C. Wu, Q.¹⁰. **B; Bile flow.** Diagram showing the network of bile ducts which transport the bile formed by hepatocytes away through the bile canaliculi to the larger bile ducts in the portal tract, adapted from accessscience.com¹⁴.

1.6. Cholestasis

Cholestatic liver disease refers to a condition that occurs as a result of an interruption or impairment to the normal flow of bile through the liver. Bile is a naturally occurring yellow alkaline fluid, normally around pH 8, which is essential for the digestion of dietary lipids. Bile is formed by hepatocytes and transported through the network of intrahepatic bile ducts within the liver. The newly formed bile exits via the common bile duct, up to 50ml of bile is stored in the gall bladder of an adult. When required, the bile is released into the duodenum where it acts as a surfactant to aid the digestion of dietary fats. Bile salts have both a hydrophobic and hydrophilic pole allowing them to interact between lipids and the aqueous environment of the small intestine. Bile aids the dispersion of the fat into micelles, thus creating a much larger surface area for other digestive enzymes to act upon¹⁷.

Occasionally the normal flow of bile through the liver may become interrupted, resulting in a disease condition known broadly as cholestasis. Taken from the Greek *chole* (bile) and *stasis* (standing still), cholestasis may arise from any of a large number of different situations. Common circumstances in which cholestasis may occur include physical obstruction or damage to the common bile duct, obstetric cholestasis, gallstones, primary biliary cirrhosis or as a side effect of some prescription drugs^{27 28}. The result of cholestasis is an elevation of the serum concentration of bile acids which causes the symptoms of pruritus, an intense itching of the skin, fatigue, lethargy and jaundice²⁸.

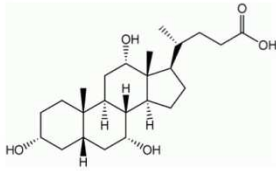
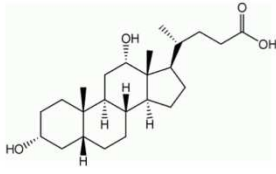
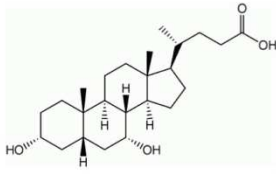
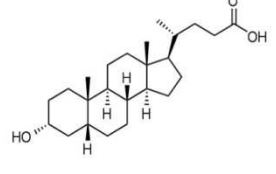
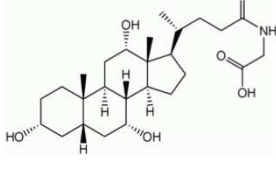
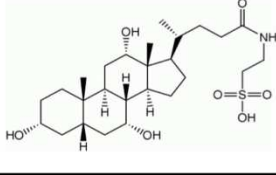
Bile acid	Structure	Description
Cholic acid		Along with chenodeoxycholic acid, one of the primary bile acids in humans, its production acts as a rate limiting step in the production of bile acid synthesis.
Deoxycholic acid		A secondary bile acid produced metabolically by intestinal bacteria from cholic acid.
Chenodeoxycholic acid		A primary bile acid, synthesised in the liver from cholesterol.
Lithocholic acid		A secondary bile acid, synthesised from chenodeoxycholic acid by bacterial metabolism in the colon.
Glycocholic acid		Formed from the conjugation of the primary bile acid, cholic acid, with glycine.
Taurocholic acid		Formed from the conjugation of cholic acid with taurine.

Table 1.1 –Bile acids. A summary of the common bile acids which constitute bile, showing their chemical structure and relevant information.

1.7. Primary biliary cirrhosis

Primary biliary cirrhosis (PBC) is a chronic, slowly progressive form of cholestatic liver disease of unknown cause, characterised by persistent, irreversible inflammation and destruction of small intrahepatic bile ducts, which may result in cirrhosis and ultimately failure of the liver^{29, 30}(Fig 1.6). Whilst a significant proportion of PBC patients are asymptomatic at the time of diagnosis, others complain of debilitating fatigue and pruritus, often preceding any indication of impaired liver function^{31, 32}. Previous research and clinical observation has highlighted a broad array of immune mediated symptoms and phenomena, synonymous with an autoimmune aetiology³³.

In PBC, cholestasis is accompanied by a persistent inflammation of the small interlobular and septal bile ducts (those less than 100µm in diameter). This causes severe, persistent and irreversible damage to the biliary epithelial cells that form the epithelial lining of the ductules. PBC may ultimately result in the total destruction, or “vanishing” of the ducts. Interestingly this effect seems specific to the smaller bile ducts, with the medium and large type remaining undamaged³⁴. The disease state may progress from localised fibrosis, to cirrhosis and in the most severe cases total failure of the liver³⁵. 90% of cases of PBC are observed in women, nearly always in those between the age of 40 and 59 at the time of presentation³⁶.

1.7.1. Diagnosis of PBC

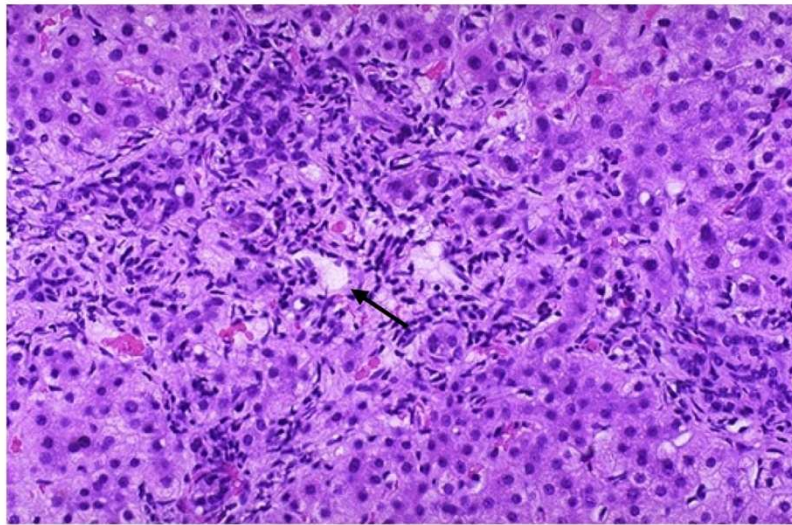
Suspicion of PBC arises when cholestasis is observed in postmenopausal women that is not caused by mechanical cholestasis, which is confirmed by ultrasound examination. Accompanying the usual symptoms of cholestasis, elevated serum alkaline phosphatase (ALP), aspartate aminotransferase (AST) and bilirubin may be observed²³. The gold standard in diagnosis of PBC is by liver biopsy, which will reveal the unique inflammatory infiltration of the small bile ducts, and possibly granulomas and copper deposits which collect in the liver along with other components of bile, as a result of the cholestasis. It is also important to note that some clinical signs of PBC currently used as diagnostic markers are not present in all cases, nor are they always concordant with the severity of liver damage³².

Diagnosis of PBC may also be based upon the identification of serum antimitochondrial antibodies (AMA), 95% of Caucasian PBC patients have AMA specific for mitochondrial pyruvate dehydrogenase complex enzymes, primarily the E2 subunit (PDC-E2). The presence of AMA in PBC forms the basis of the suggestion that PBC may be an autoimmune disease³⁷. The enzymatic reactions catalysed by PDC enzymes are summarised in Fig 1.6B.

As up to 50% of PBC patients do not outwardly show any symptoms at the time of diagnosis, the disease may be identified only through biochemical markers flagged by chance, or as a result of routine check up³⁵. Identification of PBC by physical examination may not be possible until the disease has progressed into

the latter phases, at which point portal hypertension and pigmentation of the skin, caused by exaggerated melanin deposition, may be observed. Upon progression, the physical indices of liver failure; enlarged liver, spleen and ascites may be seen ³².

A



B

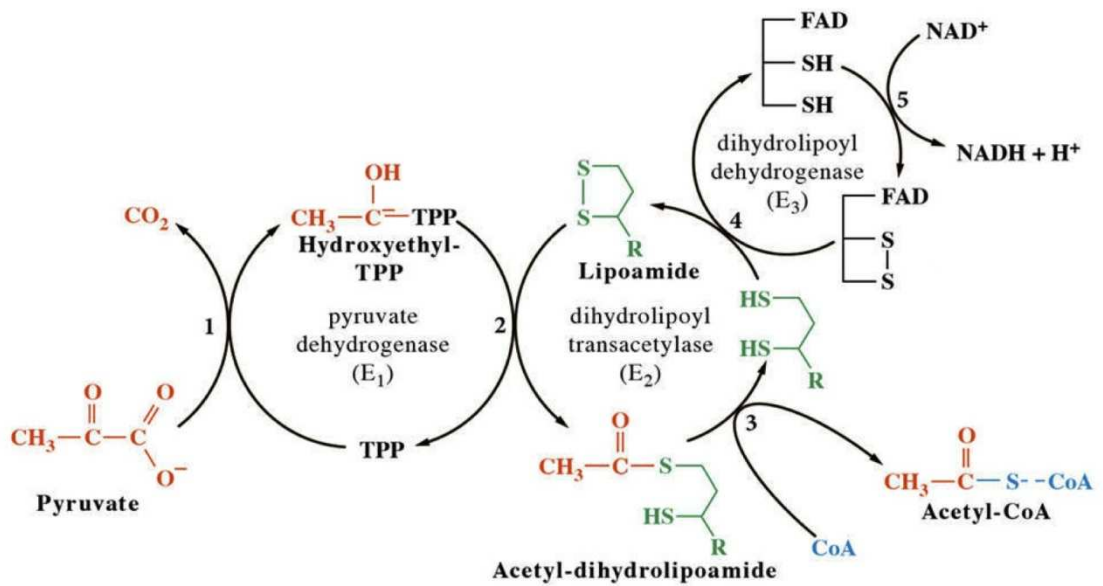


Figure 1.6 – Primary biliary cirrhosis. A. PBC histology. Haematoxylin and Eosin stained Tissue section from the liver of a PBC patient showing the inflammatory cell infiltrate and damage/ destruction of the bile duct epithelium and disappearing bile duct (arrow), taken from The Liver Centre⁶. **B.** Pyruvate dehydrogenase complex reactions. Schematic of the reactions catalysed by PDC enzymes to convert pyruvate to Acetyl-CoA and NADH, adapted from *Pyruvate dehydrogenase multienzyme complex*¹²

1.7.2. Therapeutic strategies in PBC

Effective drug treatments for PBC are limited and currently no cure for the disease has been identified³⁸. Therapeutic strategies mainly focus on the management of the symptoms of the disease. The most common treatments are administration of the naturally occurring bile salt ursodeoxycholic acid (UDCA), immunosuppression or a combination of the two.

First observed by Lueschner in 1981, treatment with 13-15mg/kg body weight of UDCA has been shown to improve serum biochemical markers of PBC³⁹, increase 10 year patient survival⁴⁰ and reduce the fibrosis seen in the early stages of disease progression⁴¹. The exact mechanism by which UDCA exerts a positive effect is unclear, it is likely that it causes a modification of the recycling bile acid pool, resulting in a more hydrophilic environment. The net result of UDCA treatment may be to promote the formation of bile with a lower concentration of the more harmful naturally occurring bile salts.

Another treatment strategy employed in PBC is immunosuppression. The rationale for use of immunosuppressive treatment is based upon the identification of the autoimmune hallmarks of PBC. A variety of different strategies have been investigated, using common immunosuppressive drugs⁴².

Corticosteroids: prednisolone treatment has been shown to improve serum ALP and AST, but no change in the serum bilirubin levels or severity of pruritus has been observed⁴³.

Azathioprin: Treatment with the classical immunosuppressant drug azathioprin has yet to show any significant effects in cases of PBC⁴⁴.

Cyclosporin A: Mixed reports surround the effectiveness of cyclosporin A in PBC, a small study of a cohort of 20 patients suggests an improvement in histology following 2 years of treatment.⁴⁵ The widespread use of cyclosporine A would be ill advised due to its potential for severe side effects.

D-penicillamine: A common characteristic of PBC is the accumulation of copper in the bile, with this in mind the copper chelator, d-penicillamine, has been previously trialled. D-penicillamine also has immunosuppressive and anti fibrotic properties and would seem to be an attractive therapeutic option. Over 6 studies totalling 748 patients, no positive therapeutic effect was observed but 30% of patients experienced severe side effects⁴⁶.

Methotrexate: Commonly used for immunosuppressive purposes, and also effective at providing symptomatic relief in rheumatoid arthritis, methotrexate therapy has been previously tested in PBC. In a study of 60 patients, low dose (7.5mg/week) led to an improvement of biochemical markers with the exception of bilirubin. No effect was seen regarding the overall severity of the disease, necessity for transplantation or patient survival⁴⁷.

In principle immunosuppressant therapy seems to be a good strategy for PBC, but only a few drugs offer any improvement, and even those effects are mainly upon patient serum biochemistry, not on disease severity or progression.

With immunosuppression proving ineffective, UDCA remains the primary strategy for treatment of PBC, but sometimes patients do not respond to UDCA alone. Non-responders are defined as those who show unaltered progression of PBC to cirrhosis and portal hypertension despite UDCA therapy, in these cases combination therapy may be considered⁴².

Steroids and UDCA: In a randomised study of 30 patients receiving 10mg/day of prednisolone alongside UDCA, a significant improvement in inflammatory activity was observed⁴⁸. UDCA accompanied by 9mg/day budesonide showed both biochemical and histological improvements amongst 39 patients⁴⁹.

Sulindac and UDCA: Over 12 months of treatment with a combination of sulindac and UDCA, again both biochemical and histological improvements were observed⁵⁰.

Colchicine and UDCA: Two studies in the 1990's^{51, 52} of combination therapy using colchicine and UDCA totalling 118 patients resulted only in mild biochemical improvements.

Other drug therapeutic strategies are limited, although one possible alternative is treatment with a selective estrogen receptor modulator (SERM). Tamoxifen has previously been suggested as a potential treatment, based on clinical data from patients who were diagnosed with PBC and also subsequently administered tamoxifen for the treatment of breast cancer³⁴. The macrolide

antibiotic, Rifampicin, has also been trialled in PBC patients and showed moderate success in management of symptoms⁵³.

The mechanism of action in the case of both tamoxifen and rifampicin may possibly be due to the anti inflammatory action of the activation of the orphan nuclear receptor transcription factor, the pregnane X receptor (PXR). Both of these drugs are known PXR agonists^{54 55} and PXR activators such as rifampicin have previously been shown to be beneficial in experimental models of fibrotic liver disease⁵⁶⁻⁵⁸. It is also possible that the increased P450 expression resulting from PXR activation increases the level of bile acid metabolism and clearance⁵³.

Where no other treatment method has proven effective and the condition is progressing to end stage liver failure, transplant may be the only remaining option. The appropriate timing of transplant in cases of PBC can be judged based on serum bilirubin levels, it has been suggested that post transplant survival is at a peak if surgery is performed before serum bilirubin levels exceed 170 μ mol/l⁵⁹. Liver transplant is most successful in cases of PBC compared to other liver diseases, with an expected 85% survival rate³².

1.7.3. PBC as an autoimmune disease

The cause of the initial inflammatory response, which initiates the development of PBC is currently unknown, it is still widely accepted that PBC is of autoimmune pathogenesis. Whilst PBC undoubtedly exhibits several hallmarks indicative of a classic autoimmune condition, more recent work has begun to challenge this concept suggesting that there is a more complex pathway involved²⁹.

PBC is widely thought of as an autoimmune condition, often characterised by the detection of anti-mitochondrial antibodies AMA. AMA are specifically targeted at oxoacid dehydrogenase complex (OADC) antigens^{37, 60}. The OADC family of mitochondrial proteins consists of three major subunits, pyruvate dehydrogenase (PDC), branched chain ketoacid dehydrogenase (BCKD) and ketoglutarate dehydrogenase (ODG). Each enzyme consists of three unique subunits, each with a specific enzymatic activity: E1 (decarboxylase), E2 (dihydro lipoamide acyltransferase) and E3 (lipoamide dehydrogenase)⁶¹. These antigens are enzymes found localised within the inner mitochondrial matrix, which catalyze oxidative decarboxylation reactions.

In around 90% of caucasians, PBC patient sera AMA activity is solely directed upon pyruvate dehydrogenase complex E2 subunit (PDC-E2)^{29, 62}. In approximately 50% of PBC patients, serum AMA are also cross reactive with epitopes upon the E2 subunit of both BCKD and OGD. Bile AMA are always directed towards the same epitopes as their serum AMA counterparts^{63, 64}.

In cases of PBC a MHC class II antigen has been identified upon the cholangiocyte membrane. It is possible that the recognition of this antigen initiates an intense and localised immune response mediated by circulating T cells, resulting in persistent portal infiltrate, inflammation and the subsequent destruction of the duct⁶⁵.

The evidence supporting PBC to be a classical autoimmune disease, although well documented, is not without opposition. Firstly OADC are present in all nucleated cells and AMA are widely distributed throughout the body, yet the response is organ specific and localised predominately to the small bile ducts. Secondly AMA are not present in all cases of PBC, suggesting they cannot be solely responsible for the condition.⁶⁵

Unlike other “classical” autoimmune diseases PBC has never been convincingly described in children, and as previously highlighted, and as described previously, PBC patients do not respond effectively to treatment with immunosuppressant drugs⁶⁶.

1.7.4. Xenobiotic exposure and PBC

In recent years, emerging research has linked exposure to environmental xenobiotics as a potentially causative agent in the development of PBC.

It has been suggested that following exposure, a xenobiotic may either conjugate with or entirely replace the E2 component of PDC forming an unrecognised structure. It has been suggested that this altered protein may initiate an antibody response against the newly created conjugate and also against the native form, suggesting a loss of self-tolerance to PDC-E2. It has been shown that AMA positive patient serum reacts with synthetically modified PDC-E2 proteins conjugated with xenobiotics with higher affinity than the native form.

A good illustration of this process, known as molecular mimicry, is the xenobiotic induced liver disease halothane hepatitis, sometimes seen following exposure to the volatile anaesthetic, halothane. Halothane exposure may result in the formation of trifluoroacetylated (TFA) proteins which can induce an immune response against not only themselves but the host PDC-E2, this example also suggests that PDC-E2 may be susceptible to this type of modification⁶⁷.

It has been widely reported that exposure to particular groups of xenobiotics and environmental toxins may increase an individuals susceptibility to developing PBC. Correlations have previously been made linking tobacco

smoke, cosmetic products, and exposure to many other environmental contaminants with a heightened risk of developing the disease. Supporting this idea, cluster analysis has shown that there is also a higher prevalence of the disease near some heavily industrial areas and toxic waste disposal⁶⁸⁻⁷⁰.

A good example of a xenobiotic that may be implicated in PBC is 2-octynoic acid, a chemical widely found in cosmetics including perfume, lipstick and also in common food flavourings. It has been shown that this particular xenobiotic has the potential to conjugate to the lipoly domain of PDC-E2 forming a modified protein. This 2-octynoic acid conjugated PDC-E2 complex is more highly reactive with PBC patient sera than that of controls⁶⁸.

1.7.5. Estrogens and PBC

Estrogen signalling may be linked to an array of cholestatic liver conditions. Estrogenic compounds, such as hormonal contraceptives and also high levels of circulating estrogen such as those seen in pregnancy, can result in cholestatic liver diseases, including pregnancy cholestasis and PBC^{28, 71}. The incidence of estrogen cholestasis varies with geographical location and ethnicity. Most notably is the incidence of intrahepatic cholestsasis of pregnancy which is most common in Chile and has been attributed to both genetic and environmental factors⁷².

1.8. Estrogen

Estrogens are a group of steroid hormones, usually described as the primary female sex hormones, summarised in Table 1.2. Estrogens are primarily implicated in the process of female sexual development and regulation of the menstrual cycle, but are also present in males and have a wide variety of other functions including regulation of cellular growth and differentiation¹⁻³.

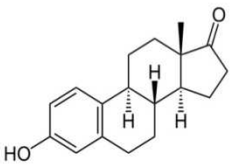
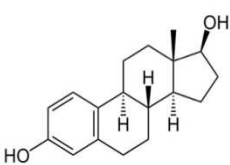
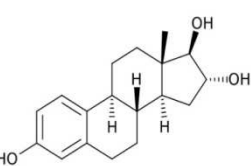
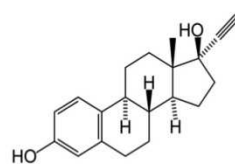
Name (abbreviation)	Structure	Description
Estrone (E1)		The least abundant of the naturally occurring estrogens, estrone is the predominant estrogen in post menopausal women
Estradiol (E2)		Estradiol is the major estrogen in humans and the most abundant in females. It is also present in males as a metabolite of testosterone.
Estriol (E3)		Estrone is only produced in significant amounts during pregnancy, as it is synthesized by the placenta
Ethinyl Estradiol (EE)		Ethinyl estradiol is a orally bioactive derivative of estradiol, used as an estrogenic drug. It is used in almost all modern oral contraceptives.

Table 1.2 – Estrogens. Chemical structures and relevant information regarding the 3 naturally occurring estrogens and the modified synthetic estrogen, ethinyl estradiol.¹⁻³.

1.8.1. Mechanisms of estrogen signalling

The classical estrogen signalling pathway is via direct binding of a ligand to the estrogen receptor (ER), and subsequent translocalisation and binding to estrogen response elements (ERE) in the regulatory regions of estrogen responsive genes. The ligand-ER-ERE complex is then joined by various co regulators, which initiate transcriptional responses to estrogen signalling. The consensus ERE is a 5-base pair (bp) palindrome separated by a 3-bp spacer: GGTCAnnnTGACC⁷³⁻⁷⁶.

Another mechanism by which estrogen may modulate gene transcription is by transcription factor crosstalk, where ERs interact with other transcription factors, such as activator protein-1 (AP-1) and specificity protein-1 (SP-1)⁷⁷.

It is also understood that estrogen signalling may occur through non-genomic mechanisms, taking place much more rapidly, hence sometimes referred to as rapid signalling. This form of signalling has been shown to utilise a variety of membrane bound proteins including protein kinases A and C, MAP kinase, and membrane localised ERs, forming signalling cascades^{78, 79}.

More recently an orphan G protein-coupled receptor (GPR) GPR30 was shown to mediate nongenomic estrogen signalling through interaction with the novel ER variant ER α 36, which acts as an extranuclear ER^{80, 81} (Fig 1.7).

1.8.2. Estrogen receptor

There are two subtypes of the human estrogen receptor (ER), ER α and ER β , each is derived from a distinctly separate gene. Of the two forms there are many different splice variants forming numerous unique ERs, each may differ in its action, tissue distribution or affinity for ligand, usually described as an affinity for the naturally occurring estrogen, 17 β - estradiol (E2). Both ER α and ER β share similar functional domains and significant sequence homology^{73, 74, 76, 82}.

The ER consists of six distinct domains, named A-F. The combined A and B domain encodes activation function 1 (AF1) and is located closest to the N terminal, this area is implicated in estrogen related transcriptional activity. The C domain is the DNA binding region of the ER and has the greatest sequence homology between α and β forms (97%). The D domain is a hinge region. The ligand-binding domain (LBD) is the E region encodes activation function 2 (AF2) this area 55% conserved between the two receptor types. AF2 within LBD constitutes the ligand dependent transcriptional regulatory function of ER. The function of the F domain, located nearest to the C terminal, is not fully understood, but it is believed that this area plays a regulatory role in ER dimerisation and transcriptional activity⁸³.

In the classical estrogen signalling mechanism, ligand binding to ER induces dimerisation of the receptor. The two forms of ER can form homodimers, each with independent activities, or influence each others activity via heterodimerisation. The subsequent DNA interaction and recruitment of co activators, causes the change in the transcription of estrogen responsive genes⁸⁴.

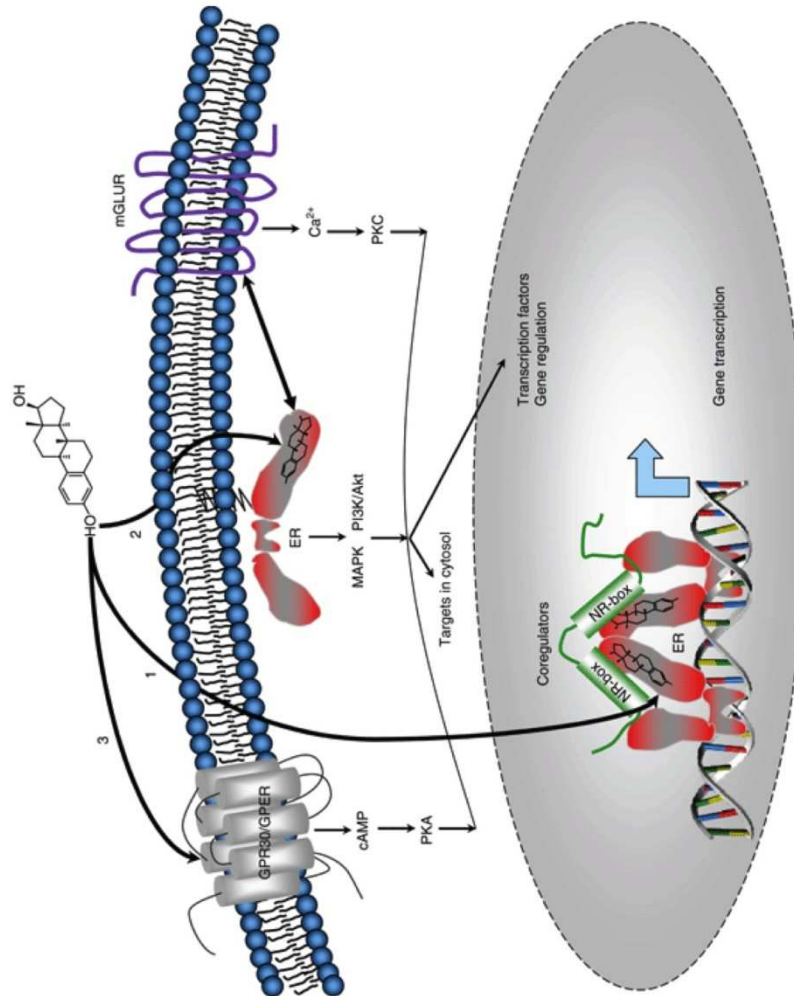


Figure 1.7 – Estrogen receptor signalling. Diagram showing common mechanisms of estrogen receptor signalling “Classical” pathway of binding of estrogen to nuclear estrogen receptor and binding to estrogen response elements (1) Binding of estrogen to membrane localised estrogen receptors and subsequent interaction with of MAP/ P13 kinases or G-protein coupled receptors mediating rapid signalling mechanisms (2,3). Adapted from *Estrogen Receptors: Therapies Targeted to Receptor Subtypes*¹¹

1.8.3. Modulation of estrogen signalling

Estrogen signalling has been a therapeutic target for many years, alterations of the level of estrogen signalling or modulation of parts of the estrogen signalling pathways have long been used in the treatment of many different conditions. From the oral administration of synthetic estrogens for contraceptive purposes, to inhibition ER activity by use of ER antagonists in the treatment of breast cancer, there are a large number of drugs available for influencing estrogen signalling.

There is a comprehensive range of estrogenic drugs available which act as a ligand for the ER, a commonly used estrogenic drug is ethinyl estradiol (EE). EE is an orally bioactive estrogenic drug, commonly used in almost all formulations of combined oral contraceptives. When administered orally the liver rapidly inactivates E2. The structure of EE is modified by a substitution of estrane for ethinyl at C17, forming an estrogen which is much more resistant to metabolism^{85, 86}.

1.8.4. Selective estrogen receptor modulators (SERM)

Inhibition of estrogen signalling is usually achieved by administration of an ER antagonist. Two of the first drugs classified as estrogen receptor antagonists were tamoxifen and raloxifene. These drugs were developed to competitively displace estradiol from ER in breast cancer cells. It quickly became apparent that the pharmacology of these drugs was more complicated. The effects of

these early drugs were observed to differ between different tissues, having the ability to exert either partial or full antagonist activities⁸⁷. In the late 1980s, Gottardis and Jordan showed by a series of xenograft models of breast cancer, that tamoxifen initially functioned as an antagonist, but over time the tumours developed resistance to the drug, and eventually recognised the ligand-ER complex as an antagonist⁸⁷. It was for this reason that drugs such as tamoxifen became known as selective estrogen receptor modulators (SERM) rather than as ER antagonists⁸⁷.

1.8.5. Selective estrogen receptor degraders (SERD)

Some of the newer drugs that have been designed to decrease the level of estrogen signalling, such as fulvestrant (ICI 182780), are termed selective estrogen receptor degraders (SERD). As the name suggests, SERD interact with ER and influence ER turnover. As with some SERM, fulvestrant has a high affinity for both ER α and ER β , but only increases turnover of ER α . This is a good example of how despite the highly conserved sequence homology between the two different receptor subtypes, they can have distinctly diverse functions⁸⁷.

1.8.6. Measurement of estrogenic activity

It may be necessary to assess the degree of estrogenic activity of a certain compound or substance. There are different established methods by which this

can be done, most of which focus on the classical estrogen signalling pathway and subsequent effect upon gene transcription.

1.8.7. Measurement of an estrogen inducible gene

A common method by which estrogenic activity can be assessed is by *in vitro* analysis of the transcription level of a known estrogen inducible gene in an estrogen responsive cell line. An example of this is to measure the induction of Trefoil Factor 1 (TFF1, previously termed pS2) mRNA induction in the estrogen responsive breast cancer cell line, MCF7^{88, 89}.

1.8.8. *In vivo* analysis of estrogenic activity by mouse uterine bioassay

The classical method by which estrogenic activity is assessed, and often defined, is by mouse uterine bioassay. This method involves the administration of the substance of interest to prepuberal female mice, usually 19 days of age^{90, 91}. The animals receive either vehicle control or treatment by intra peritoneal injection for up to for 5 days, at which point they are euthanised. The uterus of each mouse it then excised and its wet weight relative to body mass is calculated. A classical estrogenic substance will cause a significant increase in the weight of uterus, along with other uterotropic changes, including an increase in depth of the uterine epithelium^{90, 91}.

1.8.9. Estrogen signalling and cholestasis

Estrogen signalling influences transcription of many genes, some of which may be important in cholestatic liver diseases such as PBC. Particularly significant are the changes of expression of the hepatocyte transport proteins, bile salt

export pump (BSEP) and p-glycoprotein (p-GP). Expression of both of these transporters has been reported to decrease following treatment with estrogen in the rat. This change in transporter expression may also cause impaired flow of bile from the liver and therefore cholestasis. This suggests a potential mechanism explaining estrogen induced cholestasis ¹⁶(Fig 1.8).

It is understood that ER activation can increase expression of the ER in certain cell types⁹². It has been shown that estrogen administration, and in cholestasis and PBC there is an increase in ER (particularly the ER β) expression in cholangiocytes⁹². This activity could form the basis of a positive feedback loop, in which estrogen cholestasis causes an increase in receptor expression, intensifying the severity of the condition ⁹².

A

	Day 0	Day 5
	(before treatment)	Controls / EE treated
Weights (g)	(n = 10)	(n = 11)/(n = 11)
Body (body wt)	230±20	231±26/223±26
Liver	11.0±1.4	8.3±1.2/13.9±2.3
Bile flow	(n = 10)	(n = 10)/(n = 11)
(μl/min × g liver)	2.0±0.3	2.1±0.4/0.7±0.2
(μl/min × 100 g body wt.)	9.5±1.5	7.6±1.7/4.6±1.4
Serum parameters	(n = 10)	(n = 13)/(n = 14)
Bile acids (μmol/liter)	3.4±1.7	1.4±0.6/15.7±10.1
Cholesterol (mmol/liter)	2.3±0.4	1.9±0.6/0.6±0.2
Bilirubin (μmol/liter)	2.8±1.3	3.0±1.3/3.6±1.9
Alkaline phosphatase (U/liter)	316±78	284±80/684±180
Leucineaminopeptidase (U/liter)	50±8	50±8/47±7
Liver homogenates	(n = 7)	(n = 13)/(n = 13)
Protein (mg/g liver)	124±4	143±9/128±11
DNA (mg/g liver)	2.5±0.4	2.7±0.3/2.5±0.3

B

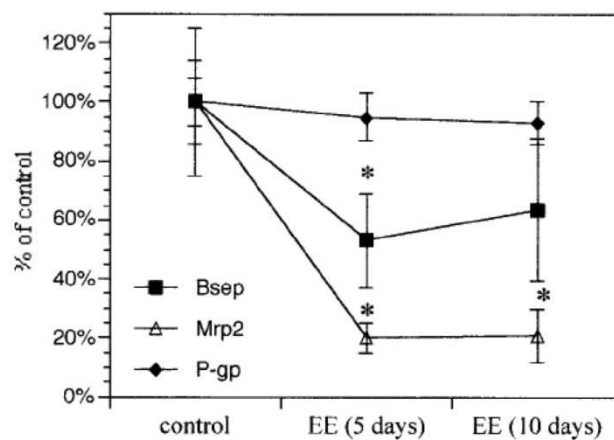


Figure 1.8 – Estrogen Cholestasis. A. Estrogen cholestasis in the rat. Basic parameters of ethinyl estradiol induced cholestasis in the rat following treatment with 5mg/kg EE, adapted from *Ethinylestradiol treatment induces multiple canalicular membrane transport alterations in rat liver*, Bossard et al.¹³ **B. Effect of EE on membrane transport proteins in the rat liver.** Data showing the altered expression of hepatic transporter proteins in the rat liver following treatment with 5mg/kg EE, adapted from *Expression of the bile salt export pump is maintained after chronic cholestasis in the rat*. Lee et al.¹⁶

1.8.10. Xenoestrogens and PBC

A large number of environmental pollutants and xenobiotics are known to have estrogenic activity. Known xenoestrogens include various pesticides, insecticides and weed killers such as DDT, and tartrazine, a common food additive, and compounds routinely found in cosmetics such as the family of parabens which are widely used as preservatives^{93 94}. Given the links which have been formed between xenobiotic exposure and PBC, we hypothesised that the cholestasis seen in PBC could be related to estrogenic activity of these xenobiotics.

2. Chapter 2 - Materials and Methods

2.1. Animals

2.1.1. Rats

Sprague-Dawley rats were purchased from Harlan or Charles River (both UK) and were housed in the Comparative Biology Centre at Newcastle University. Rats were kept in an air-conditioned environment of $20^{\circ}\text{C} \pm 3^{\circ}\text{C}$ with a controlled humidity of $50\% \pm 10\%$ and a 12hr light/dark cycle. Animals were cared for as per Home Office regulations.

2.1.2. Foetal tissue

Female rats were mated, taking the time of formation of the vaginal plug as time of conception. Between 12 and 16 days of gestation foetuses were obtained from pregnant females after CO_2 asphyxiation and cervical dislocation. Foetuses were pooled and snap frozen in liquid nitrogen prior to homogenisation and RNA isolation.

2.1.3. C57Bl6 wild type mice

Mice were purchased from Harlan or Charles River (both UK) and housed in the Comparative Biology Centre at Newcastle University. Mice were kept in an air-conditioned environment of $20^{\circ}\text{C} \pm 3^{\circ}\text{C}$ with a controlled humidity of $50\% \pm 10\%$ and a 12-hour light/dark cycle. Animals were cared for as per Home Office regulations.

2.1.4. Prepubescent C57Bl6 mice

For investigations utilising prepubescent C57Bl6 mice, breeding cages of the ratio 2 females: 1 male were established within the Comparative Biology Centre at Newcastle University, the date of birth of each litter was recorded. Animals used for study were identified by an ear notch and remained with the rest of the litter until old enough to be weaned.

2.1.5. Mouse uterine bioassay

Female mice were sexed and identified by ear notching before 19 days of age, on day 19 animals were administered treatment by a single daily intra peritoneal injection on 4 consecutive days. On day 5, animals were sacrificed by Schedule I method and their uteri harvested for analysis.

2.1.6. Serum enzyme assays

Serum samples were collected by tail bleeding, and by terminal bleed after autopsy. Blood was allowed to clot and then centrifuged at 13 000rpm, the serum was collected and analysed by the Clinical Biochemistry Department at the Royal Victoria Infirmary, Newcastle.

2.2. Cell Culture

2.2.1. Primary rat hepatocyte isolation

Male Sprague-Dawley rats (150 - 200g) were anaesthetised by *i.p.* administration of 100mg/kg Sagatal (sodium pentobarbital) solution. An incision was made along the midline of the animal, a 19G cannula was inserted into the portal vein and secured with 2 ligatures, the vena cava was then severed to allow perfusate to exit. The liver was first perfused with 300mls of 25mM ethylene glycol tetraacetic acid (EGTA) solution in Earle's balanced salt solution (EBSS) (without Mg^{2+} and Ca^{2+} , with $NaHCO_3$). Whilst the organ blanched it was excised from the animal and placed in a sterile 10cm Petri dish. The liver was then perfused with 200mls EBSS (without Mg^{2+} and Ca^{2+} , with $NaHCO_3$) at 37°C. Finally the liver was perfused with 0.5mg/ml collagenase A from *Clostridium histolyticum* solution in EBSS at 37°C, this perfusate was re-circulated until the optimum level of digestion was achieved.

The perfused liver was disrupted into the remaining collagenase A solution, the liberated cells were then passed through a 75 μ M nylon mesh and suspended in William's Medium E (WME). The isolated cells were centrifuged at 50g for 5 minutes before washing in WME and one further centrifugation and re-suspension in WME. Cells were counted using a haemocytometer and cell viability determined by trypan blue exclusion. Cell yield routinely exceeded 500×10^6 cells per liver and viability > 90%.

Primary rat hepatocytes were seeded in WME supplemented with 80U/ml penicillin, 80U/ml streptomycin, 2mM L-glutamine, 1% (v/v) insulin transferrin selenium solution (ITS) (final concentrations: 10 µg/ml insulin from bovine pancreas, 55 µg/ml human transferrin, 50 ng/ml sodium selenite) and 10% (v/v) foetal bovine serum (FBS) for up to 24hrs whilst they adhered. Hepatocytes were then maintained in serum free WME supplemented with 80U/ml penicillin, 80U/ml streptomycin, 2mM L-glutamine and 1% (v/v) ITS (final concentrations: 10 µg/ml insulin from bovine pancreas, 55 µg/ml human transferrin, 50 ng/ml sodium selenite). Cell culture media was replaced every 24 hours.

2.2.2. Preparation of cell cultures from the rat biliary structure

Following rat hepatocyte isolation, the remaining tissue was incubated in a 1mg/ml solution of collagenase A at 37°C and agitated by shaking at 250rpm for 1 hour. The liberated biliary structure was then disrupted into small pieces using a scalpel, then incubated in 1mg/ml solution of pronase at 37°C and agitated by shaking at 250rpm for 1 hour. The cell suspension was passed through a 75µM nylon mesh and centrifuged at 2000rpm for 5 min. The cell pellet was suspended in Dulbecco's modified eagles medium, supplemented with 80U/ml penicillin, 80U/ml streptomycin, 2mM L-glutamine and 10% (v/v) FBS. The cell pellet from one rat liver was typically seeded into 4 6-well tissue culture plates, dependant upon size of cell pellet. The cell culture media was renewed every 24 hours.

2.2.3. Culture of adherent cell lines

MCF-7 and MDA cell lines were cultured as a monolayer and upon reaching 70-80% confluence, were passaged. Cell culture media was aspirated from the cells and they were washed twice in sterile 1 x phosphate buffered saline (PBS - 0.01 M phosphate buffer, 0.0027 M potassium chloride and 0.137 M sodium chloride, pH 7.4, at 25 °C) (75cm² flask 10mls, 6 well plate 2ml/well) to remove any remaining culture media. Sufficient 1 x trypsin-EDTA solution, diluted in 1 x PBS was added to cover the cells (4mls per 75cm² flask and 0.5ml/well of a 6 well plate) for up to fifteen minutes under standard cell culture conditions. Careful impact to the cell culture vessel was used to encourage detachment. Once cells were sufficiently detached trypsin activity was inhibited by addition an equal volume of serum-supplemented culture media to the cell suspension. The cell suspension was removed to a 50ml Falcon tube and centrifuged at 1500rpm for 5 minutes. The supernatant was discarded and the remaining cell pellet was re-suspended in fresh media. Cells were then seeded accordingly for cell maintenance or experimental protocols as described.

2.2.4. Long-term storage of cells

Cell stocks for all cell lines used were periodically frozen and stored long term in liquid nitrogen. Cells were detached, pelleted and suspended in freezing media (90% (v/v) FBS 10% (v/v) DMSO), typically 2mls per pellet from each confluent 75cm² tissue culture flask. The cell suspension was divided into sterile cryogenic storage vials (1.5ml/cryovial). Aliquots were frozen at a controlled rate

using an isopropyl alcohol filled freezing device (Mr Frosty™, Nalgene). Once cooled to -80°C, the cell stocks were transferred to liquid nitrogen for long-term storage.

2.2.5. Revival of cell stocks

Cryogenically stored cell stocks were removed from liquid nitrogen and thawed at 37°C. The cell suspension was added to 10x its volume of the appropriate cell culture media, pre warmed to 37°C in a 50ml falcon tube. The cells were pelleted by centrifugation for 5 minutes at 1500rpm and the supernatant was discarded. The cell pellet was re-suspended in fresh cell culture media and transferred to a cell culture flask. Viable cells were allowed 24 hours to attach before changing the culture media. Cells were then cultured as described previously.

2.2.6. Assessment of cell viability and number

For routine cell culture purposes, cell viability was assessed by the ability of a cell to exclude trypan blue. 100 µl of a cell suspension was added to an equal volume of 0.4% trypan blue solution and 200µl of fresh culture media to give a final concentration of 0.1% (w/v) trypan blue. A small volume of the cell suspension was loaded onto a haemocytometer. Counts of both the total cell number and number of non-viable cells were performed in order to calculate the concentration of the cell suspension and the percentage viability.

2.2.7. Charcoal/dextran treated foetal bovine serum

Foetal bovine serum naturally contains a variety of steroid hormones and other low molecular weight compounds, which may vary from one batch to the next. For investigations into steroid hormone signalling it is often necessary to culture cells with FBS that has been depleted of endogenous hormones to reduce the high background level of nuclear receptor activity. This can be achieved by pre-treating the serum with activated charcoal / dextran.

20g of activated charcoal and 0.2g Dextran T70 (both from Sigma UK) were suspended in 250ml diH₂O and incubated at room temperature for 10 min. The charcoal suspension was then centrifuged at 7000rpm for 15min at 4°C. The supernatant was then removed and the process repeated once more. The charcoal/dextran was then re-suspended in 200ml FBS in a conical flask and incubated at 55°C for 40 min with vigorous shaking. The serum was then centrifuged at 10000rpm for 30min at 4°C. The supernatant was retained and centrifuged again under the same conditions. The media was then sterilised by passing through a 0.2µ filter unit.

2.3. Cell Transfection

2.3.1. Transfection using polyethylenimine

MCF-7 cells were routinely transiently transfected using polyethylenimine (PEI) (from Polysciences inc). Cells were seeded equally in 6 well tissue culture plates and allowed to grow to around 60-70% confluence, immediately before

transfection the cell culture media was removed and replaced with 1ml of fresh media per well of a 6 well plate.

For a typical transfection in 1 well of a 6 well plate, 1.5µg of total plasmid DNA was placed in a centrifuge tube with 1ml of serum-free media. 10µl of 1mg/ml PEI solution in 20mM HEPES buffer (pH 7.5) was added and the solution was then vortex mixed for 10 seconds. The transfection master mix was then incubated for 30 min at room temperature before adding drop wise to the cell culture. Transfected cell cultures were incubated under standard conditions for 24 hours before changing the culture media and proceeding with the investigation.

2.3.2. Transfection using Effectene reagent

MDA and H69 cells were transfected using Effectene transfection reagent. Cells were seeded into 6 well tissue culture plates and allowed to grow to 60-70% confluence. Immediately before transfection the cell culture media was removed and replaced with 1.5ml of fresh media. Typically one well of a 6 well plate was transfected with 1.5µg of total plasmid DNA. The plasmid DNA, buffer EC and enhancer solution were mixed to a ratio of 1µg DNA to 150µl EC and 10µl enhancer solution before being vortex mixed for 10 seconds and incubated at room temperature for 5 minutes. 15µl of Effectene solution was added per 1µg plasmid DNA, this was vortexed again and incubated at room temperature for 20 minutes. The DNA/effectene transfection master mix was added to the

cultures in a drop wise manner, the cells were then incubated for 24 hours under standard cell culture conditions.

2.3.3. Transfection using GeneJuice transfection reagent

Primary rat hepatocytes were routinely transfected using GeneJuice transfection reagent (from Novagen). Following isolation, primary rat hepatocytes were seeded at a density of 7.5×10^5 cells per well of a 6 well plate. Typically 1.5 μ g of total plasmid DNA was transfected in each well of a 6 well plate, a transfection master mix was made at a ratio of 100 μ l serum free culture media and 3 μ l GeneJuice transfection reagent to each 1 μ g of plasmid DNA.

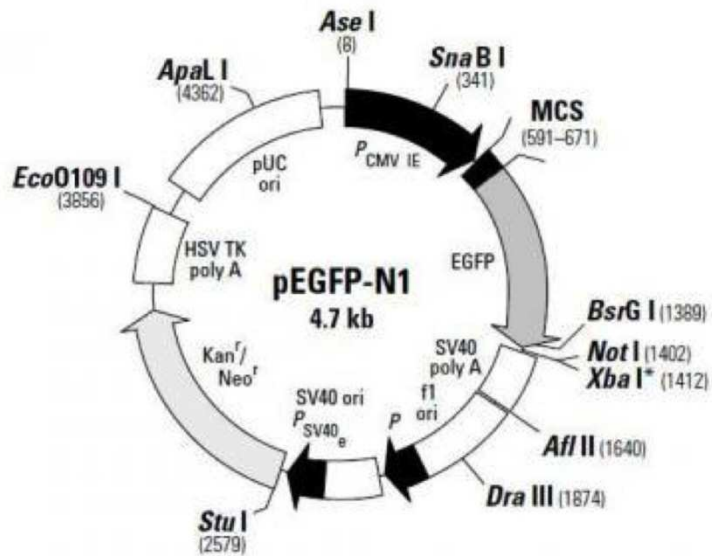
For each well of a 6 well plate to be transfected 150 μ l serum free culture media was added to 4.5 μ l of GeneJuice in a sterile tube and thoroughly mixed by vortexing before incubating for 5 min at room temperature. To this 1.5 μ g of total plasmid DNA was added and mixed by inverting several times. The transfection master mix was added directly to the cells in culture media in a drop-wise manner. Cells were then incubated for 24 hours.

2.3.4. Assessment of transfection efficiency

Cell cultures were transfected using the appropriate method as described previously with the green fluorescent protein expression plasmid peGFP-N1 (eGFP). Cells were transfected for 24 hours before visualising by fluorescence microscopy, cells positive for eGFP were counted and expressed as a

percentage of the total number of cells per field of view. The average transfection efficiency of 3 fields of view was then calculated. (Fig 2.1)

A



B

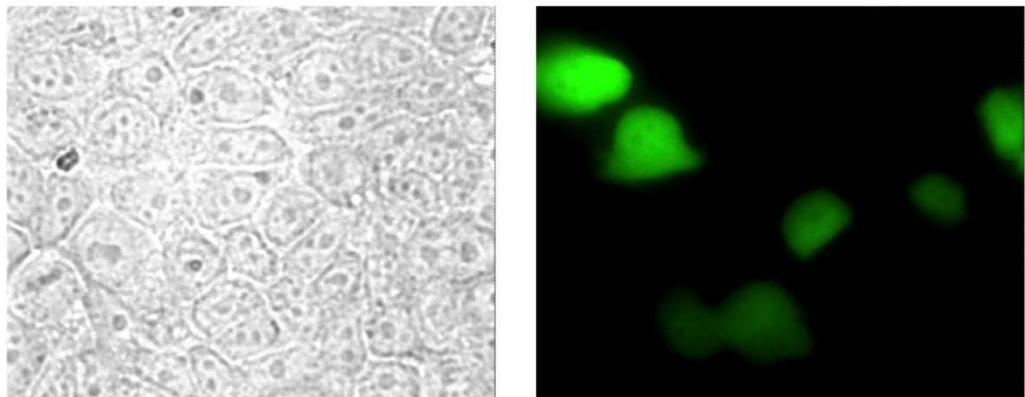


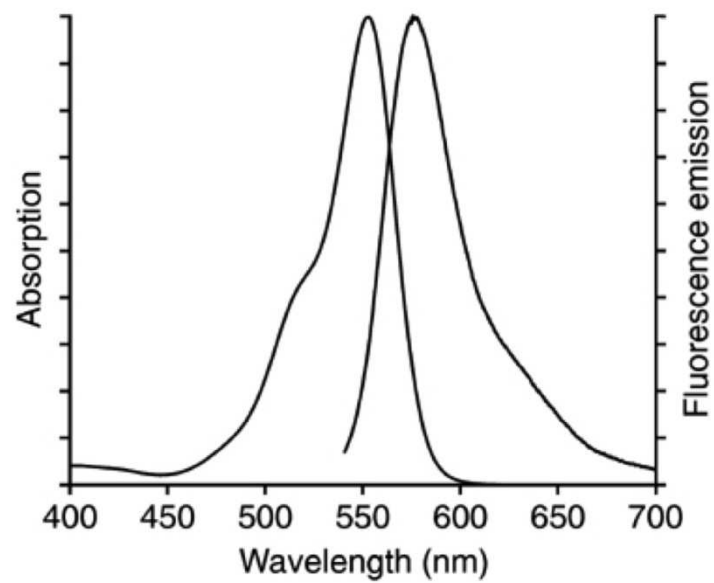
Figure 2.1 - pEGFP-N1. A –pEGFP-N1 plasmid map. The basic plasmid map for pEGFP-N1 plasmid which encodes green fluorescent protein (GFP) used for transfection efficiency studies⁴. **B – pEGFP-N1 transfected MCF-7 cells.** Bright field and FITC images of GFP transfected MCF-7 estrogen responsive breast carcinoma cell culture.

2.4. Assay Systems

2.4.1. Tetramethylrhodamine Methylester (TMRM) analysis of mitochondrial polarisation

TMRM is a fluorescent dye which accumulates in polarised mitochondria of a cell. Excited TMRM emits in the red spectrum at 573nm (Fig 2.2A). Cells were seeded in 96 well imaging plates (Greiner) and cultured as previously described, before loading with TMRM (Sigma, UK) dissolved in DMSO. The concentration of TMRM was optimised for each individual cell type, The TMRM was added directly to the culture media before incubation for 1hr to allow uptake of the dye. After dye loading, the media was removed, cells were washed with sterile 37°C 1 x PBS and fresh, pre war med culture media was added. The cells were then treated as required and the localisation of the TMRM was observed by imaging every 15 min using a high throughput automated imaging system. (Attovision Pathway, BD biosciences) The intensity of TMRM fluorescence was analysed using the Velocity imaging software (Fig 2.2B)

A



B

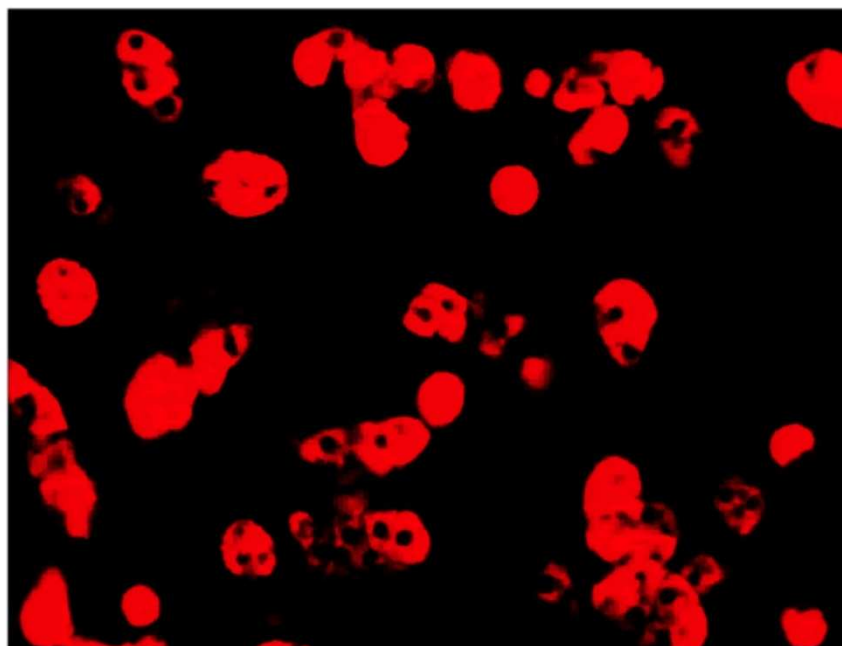


Figure 2.2 – Trimethylrhodamine methylester. A. Excitation and emission of TMRM. Graph of the excitation and emission wavelengths of Trimethylrhodamine methylester (TMRM). **B. TMRM loaded primary rat hepatocytes.** Culture of primary rat hepatocytes loaded with 250 μ M TMRM, visualised on the Attovision pathway imaging system.

2.4.2. MTS assay

3-(4,5-dimethylthiazol-2-yl)-5-(3-carboxymethoxyphenyl)-2-(4-sulfophenyl)-2H-tetrazolium (MTS) is a tetrazolium compound which is used to measure mitochondrial reductase enzyme activity. MTS undergoes reduction by NADPH the product of which is a soluble formazan product which is an indigo colour and can be measured by absorbance at 490nm (Fig 2.3A).

Cells were seeded in 96 well tissue culture plates and cultured as described previously. Following treatment, 10µl MTS reagent (CellTiter 96[®] AQueous Non-Radioactive Cell Proliferation Assay, Promega, UK) was added to each well. Cells were incubated for 2-4 hours before reading the absorbance at 490nm using a 96 well plate spectrophotometer (molecular devices spectraMAX 250).

2.4.3. Dual-Glo reporter assay system

For luciferase reporter gene assays, a dual reporter systems was used, this method is designed to increase experimental accuracy and limit experimental variability between replicates. The technique requires that two individual reporter enzymes, luciferase and renilla, are simultaneously expressed within a single system. The Dual-Glo assay system, obtained from Promega, exploits the luciferase activities of both firefly (*Photinus pyralis*) and renilla (*Renilla reniformis*, sea pansy) luciferase enzymes. Normally, firefly luciferase is expressed under the control of the target gene being studied. A plasmid encoding the renilla under the control of a constantly active promoter is

simultaneously transfected. A difference in the structure of the two luciferase enzymes allows the level of expression of each in a sample to be determined independently (Fig 2.3B,C). The level of firefly luciferase activity in the sample is first determined by addition of the substrate, luciferin. The firefly luciferase reaction is then quenched and the renilla reaction is initiated simultaneously by the addition of the Stop and Glo substrate.

Culture media was removed from transfected cells, which were then washed in 1 x PBS before addition of 1 x passive lysis buffer to each well (150µl/well of 6 well plate), lysis of the cells was encouraged by placing on an orbital shaking plate for 5 min. The Dual-Glo assay reagents were prepared in concordance with the manufacturers instructions. 100µl of the cell sample was added to an equal volume of luciferase substrate in a clear micro centrifuge tube and mixed by pipetting. The luciferase activity was then measured using a bench top luminometer. Firefly luciferase activity was then quenched by addition of 100µl Stop and Glo reagent. The activity of the renilla luciferase was then measured. In all experiments the relative luciferase of the experimental plasmid DNA construct (e.g. 3xERE luciferase) was normalised to the level of expression of the renilla luciferase levels by dividing the firefly measurement by the renilla value after subtraction of background luminescence. All values were then further normalised to the no treatment control and data expressed as a fold change in normalised luciferase activity in response to individual treatments.

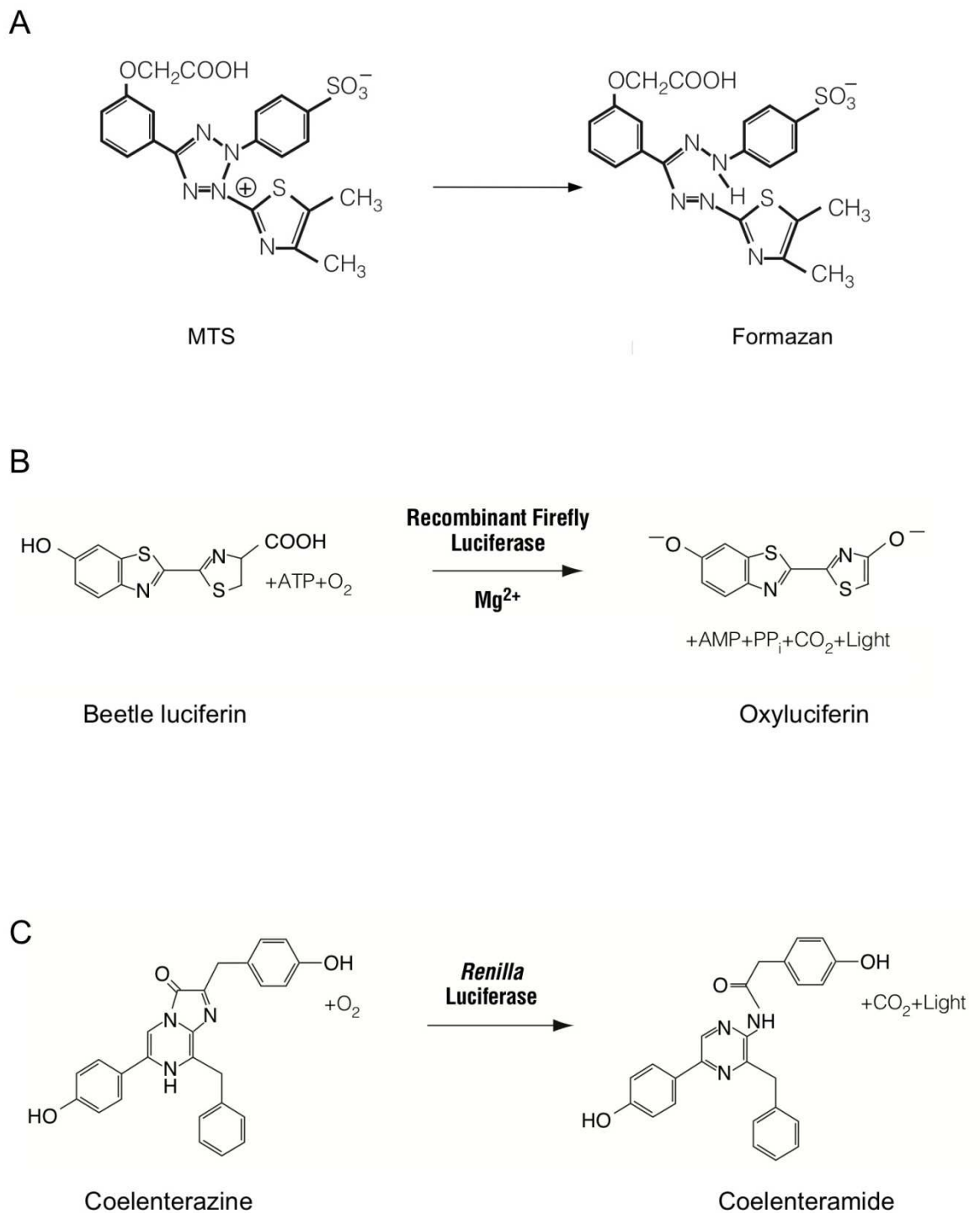


Figure 2.3 – Assay systems. A. MTS reduction. Reaction diagram of the reduction of MTS to formazan as utilised by the Promega aqueous cell titre assay system. **B. Firefly luciferase reaction.** Reaction pathway of the conversion of Beetle luciferin to oxyluciferin catalysed by firefly luciferase. **C. Renilla luciferase reaction** Reaction pathway of the conversion of coelenterazine to coelenteramide catalysed by *Renilla* luciferase.

2.4.4. Measurement of serum antibody titre against pyruvate dehydrogenase (PDC) by ELISA

Serum antibody activity against PDC was assessed by enzyme –linked immunosorbant assay (ELISA). The ELISA technique previously described by Jones *et al*⁹⁵ is an established method for quantifying antibody binding to PDC.

Wells of a microtitre plate were coated with 100µl of isolated murine PDC protein solution diluted to 5µg/ml in coating buffer (35mM NaHCO₃, 15mM Na₂CO₃, pH 9.6) overnight at 4°C. Non-specific binding sites were then blocked by incubation with 150µl/well PBSA (PBS + 5% (w/v) BSA) for 30min at 20°C. Following a wash step with PBSTw (PBS + 0.05% (v/v) Tween 20), wells were incubated with mouse sample sera diluted 1:100 in PBSATw (PBS +0.05% (v/v) Tween 20 + 0.5% (w/v) BSA) for 3 hours at 20°C. The plate was washed 3 times before incubation with goat anti mouse IgG peroxidase-conjugated secondary antibody for 90min at 20°C. following one further wash step, bound peroxidase activity was determined by addition of 100µl/well of developer (0.43mg/ml o-phenylenediamine (OPD), 0.012% (v/v) H₂O₂ in 0.1M citrate buffer (19.2g/L citric acid monohydrate in dH₂O) for 15min before stopping the reaction with 100µl 2M H₂SO₄. Absorbance was read at 492nm on a plate reader.

2.5. Plasmid DNA Constructs

2.5.1. Transformation of competent *E.coli*

Plasmid DNA was synthesised via transformation and cloning of TOP10 competent *E.coli* (Invitrogen). The bacterial cells were stored long term at -80°C and defrosted on ice before use. 50-100ng of plasmid DNA was introduced to 10µl of TOP10 cell suspension, and incubated on ice for 30 minutes. The *E.coli* were then heat shocked by heating to 42°C for 30 seconds before removing to ice for a further 2 minutes. 250µl of sterile S.O.C media was then added and the culture was incubated in an orbital rotating incubator for 1 hour at 37°C. 5 and 50µl of the transformed cells were then spread onto LB-agar plates containing the appropriate antibiotic selection markers for the plasmid (ampicillin 100µg/ml or kanamycin 50µg/ml). The plates were incubated for 8 hours or overnight at 37°C, a single, well-defined colony was selected and used to inoculate 5mls of lysogeny broth (LB, Miller formulation – 10g tryptone, 5g yeast extract, 10g NaCl per litre) containing the appropriate antibiotic selection. Following overnight incubation the culture was subjected to plasmid mini prep protocol or used to inoculate a larger volume of LB, typically 100ml, for plasmid maxiprep purposes.

2.5.2. Storage of transformed bacterial cultures

Glycerol stocks were prepared for safe long-term storage of transformed bacterial cultures. 500µl of the LB culture was added to 500µl of a sterile 70:30

LB:glycerol mixture. The glycerol stock was immediately stored at -80°C. Glycerol stocks were used to produce more plasmid DNA when required, 20µl of the stock was streaked onto an LB-agar plate with the corresponding antibiotic selection marker and incubated at 37°C for 8 hours or overnight. A single, defined colony was selected to grow the bacterial cultures as previously described.

2.5.3. Plasmid DNA miniprep

Plasmid purification by miniprep describes the alkaline lysis of bacterial cell walls followed by the isolation of plasmid DNA from the lysate by a process of binding and eluting the plasmid DNA to anion-exchange resin, and then eluting by washing with a high-salt buffer. Miniprep is designed for the purification of plasmid DNA from up to 5ml of a bacterial culture. Qiagen miniprep kits were used, following the manufacturers instructions. Briefly, 2mls of overnight culture was placed in a microcentrifuge tube, and the bacterial cells were pelleted by centrifugation at 10 000rpm for 1 minute, the supernatant was then discarded. The pellet was re-suspended in 250µl of buffer P1 (containing RNase), to which 250µl of buffer P2 was added and mixed by numerous gentle inversions until complete lysis was achieved. Buffer N3 was added and mixed immediately by repeated inversions. The sample was then centrifuged at 13 000rpm for 10 minutes to form a compact white pellet. The remaining supernatant was removed and added to a Qiaprep column, which was centrifuged for 60 seconds. The flow through was discarded and the column was washed by addition of 500µl of buffer PB and centrifuged once more. A final wash was

performed by addition of 750µl of buffer PE another 60 second centrifugation. All the wash buffers were discarded and the Qiaspin columns were centrifuged for a further 60 seconds to ensure complete removal of all PE buffer. The Qiaspin column was transferred to a sterile RNase-free microcentrifuge tube to collect the plasmid DNA. 50µl of sterile H₂O was added to the column. A final centrifugation of the column at 13000 rpm for 60 seconds eluted the plasmid DNA.

2.5.4. Plasmid DNA maxiprep

Plasmid DNA maxiprep was performed using proprietary kits from Qiagen, following the manufacturers instructions. In brief, 100ml of a bacterial culture was centrifuged at 6000rpm for 20 minutes at 4°C to pellet the cells. The supernatant was discarded before the bacterial pellet was re-suspend in 10ml of Buffer P1 (containing RNase), 10ml of buffer P2 was then added and mixed by repeated inversion. The suspension was incubated at room temperature for 5 minutes before adding 10ml of chilled buffer P3 and mixing again by inversion. This mixture was incubated for 20 minutes on ice and then centrifuged again at 6000rpm for 20 minutes at 4°C. Following centrifugation, the supernatant was then applied to an equilibrated Qiagen-tip 500 column. Two 30ml washes of the column with buffer QC were performed and the flow through was discarded. 15ml of buffer QF was the applied to the column and the eluted plasmid was collected. The plasmid DNA was then precipitated by addition 10mls of 100% sterile isopropanol. The DNA was then pelleted by centrifugation at 6000rpm for 30 minutes at 4°C, the supernatant was again

discarded. The DNA pellet was washed by resuspension in 5mls of sterile 70% EtOH and centrifuged for a further 10 minutes at 10 000rpm. The supernatant was removed and the pellet allowed to air dry before dissolving in an appropriate volume of nuclease free H₂O.

2.6. Isolation and quantification of protein samples

2.6.1. Isolation of protein from cell samples

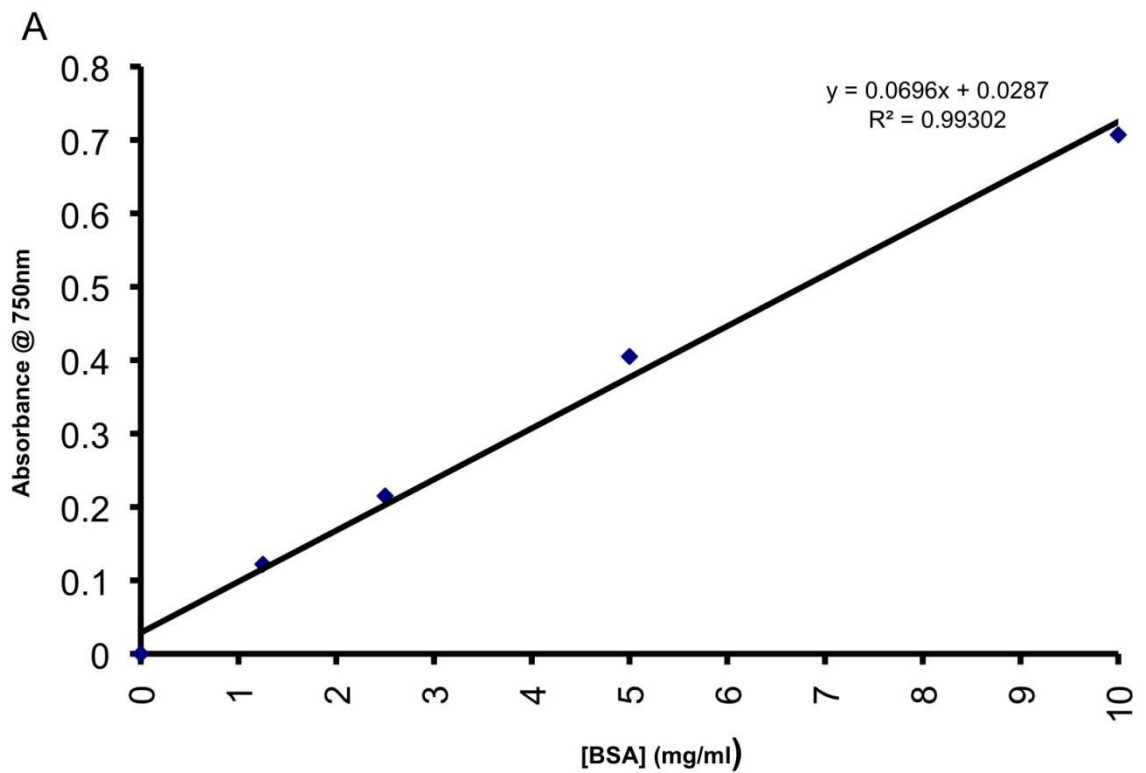
Culture media was removed from cell samples, which when were washed twice in 1 x PBS. Cells were then detached by scraping into chilled 1 x PBS (1 ml per well of a 6 well plate), transferred to a sterile micro centrifuge tube and centrifuged at 13 000 rpm for 1 minute. The supernatant was discarded and the cell pellet was re-suspended in an appropriate volume of 20mM Tris buffer (pH 7.4). Protein samples were stored long term at -80°C.

2.6.2. Determination of protein concentration by Lowry protein assay

The concentration of total protein in a sample was determined using the method first described by Lowry. Bovine serum albumin (BSA) was used to create standards of known protein concentration, creating a standard curve to which an unknown sample was compared. The complete Lowry buffer, termed buffer ABC was prepared immediately before the assay, it composed of 1 x Lowry A (2% w/v NaCO /4% w/v NaOH), B (2% w/v sodium tartrate) and C (1% w/v copper sulphate) mixed at a ratio of 100:1:1 (v:v:v) respectively.

Bovine serum albumin (BSA) standards were prepared by serial dilution of a 20µg/µl BSA stock, diluted in dH₂O. 5ul of each standard or sample was placed in a micro centrifuge tube along with 50µl of dH₂O and 1ml buffer ABC, the standards were then incubated at room temperature for 10 minutes before

addition of 100µl of Folin's reagent (Fluka, UK) (pre-diluted 1:1 with dH₂O). Samples were incubated at room temperature for a further 30 min before transferring to a disposable cuvette. The absorbance of each sample at 750nm was determined by spectrophotometer. The absorbance of the standard concentration samples was used to create a standard curve. The equation of the standard curve was then used to determine the protein concentration of the unknown sample (Fig 2.4A,B).



B

$$1) y = 0.0696x + 0.0287$$

Therefore;

$$2) x = (y - 0.0287) / 0.0696$$

Figure 2.4 – Lowry protein assay. A. Lowry standard curve. A typical standard curve created for the quantification of unknown protein sample concentrations. **B. Lowry calculation.** The equation devised from the standard curve (A) to determine the concentration of an unknown protein sample (x) from its absorption following Lowry assay (y).

2.7. SDS-page and western blotting

2.7.1. SDS-page gel electrophoresis

The separation of proteins within a sample by sodium dodecyl sulphate - polyacrylamide gel electrophoresis (SDS-PAGE) is a commonly used method which was first described by in 1970 by Laemmli. SDS-PAGE allows the separation of proteins by their different molecular weight. The technique requires that the sample be heated in the presence of SDS and dithiothreitol (DTT) to completely denature the proteins, removing any quaternary, tertiary and secondary structures. The linearised proteins are associated with SDS, a negatively charged detergent. The samples are loaded onto a polyacrylamide gel matrix within an electric field, with the positive electrode at the opposite end of the gel to where the samples were loaded. Due to the negative charge of all proteins they migrate towards the positive electrode at a rate dependent on their molecular weight.

The apparatus used for SDS-PAGE electrophoresis was the MINI-PROTEAN tetra cell, from Bio-Rad, UK. Gels were cast to a thickness of 0.75mm or 1mm, dependent on the volume of sample required. Discontinuous gels were prepared by first casting a separating gel. 9-14% acrylamide gels were routinely used based on the molecular weight of the target protein. Separating gels were composed of 9-14% acrylamide, 375mM Tris buffer pH8.8, 0.1% w/v SDS, 0.05% w/v ammonium persulphate and 0.05% v/v TEMED. Once the gels were cast, a layer of 100% isopropanol was applied to the surface of the gel to

achieve a sharp, level edge at the interface of the stacking and separating gels. Gels were left for 20-30 minutes to polymerise before removing the isopropanol and washing with distilled water. A 4% stacking gel, consisting of 4% w/v acrylamide, 125mM Tris buffer pH 6.8, 0.1% w/v SDS, 0.05% w/v ammonium persulphate and 0.1% (v/v) TEMED, was then cast on top of the separating gel. Wells for the samples were formed in the gel using combs placed into the stacking gel layer. The polymerised gels were secured in the electrophoresis tank, and submerged in electrophoresis running buffer (20mM Tris, 160mM glycine and 0.08% w/v SDS, pH 8.3).

2.7.2. Sample preparation

Protein sample concentration was determined by the Lowry method and routinely diluted to 2µg/µl with loading buffer (62.5mM Tris Buffer pH 6.8, 10% v/v glycerol, 2% w/v SDS 100mM DL-Dithiothreitol (DTT) and 0.02% w/v bromophenol blue). Samples were heated to 90°C for 3 min to linearise the protein, an appropriate amount of protein, dependent on the relative level of expression, was loaded to the gel, this was typically between 10-30µg of protein. An electric field of 100V was applied across the gel until a tight and uniform front was achieved at the gel interface, then 150V until the sample front reached the end of the gel. After this the gels were removed and the proteins were either stained or transferred to a nitrocellulose membrane for immunodetection of specific proteins.

2.7.3. Western blotting

Western blotting is the term used to describe the well-established technique of transferring the total protein from a polyacrylamide gel to a nitrocellulose membrane by electro-transfer. Polyacrylamide gels were equilibrated in transfer buffer (25mM Tris, 192 mM glycine and 20% v/v methanol, final pH 8.3) for 5 minutes at 4°C. Gels were placed onto a piece of nitrocellulose membrane and assembled in a transfer cassette. The cassette was placed into the transfer tank and submerged in chilled transfer buffer. Electro transfer was performed at 100V for 2 hours on ice. The negatively charged proteins from the gel migrate towards the positive pole of the transfer tank and onto the positively charged nitrocellulose membrane.

2.7.4. Immunodetection

Following transfer, nitrocellulose membranes were blocked in a solution of 3% milk powder in 1 x TBS-T buffer (0.2M NaCl, 20mM Tris, pH 7.4 and 0.05% (v/v) tween 20) for 1 hour at room temperature or overnight at 4°C. The membranes were then washed three times in TBS-T for 5 minutes per wash. Nitrocellulose membranes were first incubated with an antibody specific for the target protein (primary antibody) for 1 hour at room temperature or overnight at 4°C. after 3 x 5 min washes in TBS-T, a corresponding HRP-conjugated secondary antibody was applied and incubated as before. Antibodies were diluted in incubation buffer (0.3% (w/v) milk powder in TBS-T). The secondary antibody was then discarded and the membranes were thoroughly washed for 30min in 1 x TBS-T with regular changes. The reagents, ECL, ECL-plus and ECL advance (GE healthcare, UK) for chemiluminescent detection HRP activity (corresponding to

target protein position and amount) on the membrane. The reagents were used according to the manufacturers instructions, Reagent 1 and 2 were mixed in equal volumes, applied evenly to the membrane and incubated for 30 seconds. Any excess reagent was removed and the membranes were sealed in catering wrap, ensuring the removal of any air. The membranes were then exposed to x-ray film, which was then developed following standard procedure.

2.8. Isolation and quantification nucleic acids

2.8.1. TRizol purification of RNA

TRizol reagent from Invitrogen was used to isolate RNA from whole tissue and cell samples. 1ml of TRizol was added to each sample (sample not exceeding 10% of volume of TRizol) and the sample was disrupted by homogenising and sonication. The sample/TRizol mixture was then removed to an RNase/DNase free 1.5ml micro centrifuge tube, 200µl of chloroform was added and mixed by vortexing. The sample was then centrifuged at 13000rpm in a bench-top microcentrifuge at 4°C for 15 min. The upper aqueous layer was removed and placed into a clean micro centrifuge tube, to which 500µl of sterile isopropanol was added. The sample was then incubated on ice for 20 minutes. Samples were then centrifuged again at 13000rpm for 15 minutes at 4°C. The supernatant was discarded and the pellet dislodged in 70% ethanol before a final centrifugation (13000rpm, 15min, 4°C). The supernatant was discarded and the pellet was allowed air dry before resuspension in an appropriate

volume of nuclease free H₂O (typically 10-20µl). RNA samples were stored at -80°C.

2.8.2. Concentration, purity and integrity of nucleotides

RNA concentration within a sample was determined by spectrophotometry. A small amount of the RNA sample was diluted in 1:100 in nuclease free H₂O and transferred to a quartz cuvette. The absorbance of the sample was assessed at 260nm, zeroed against pure nuclease free H₂O. RNA concentration was then calculated, assuming an OD of 1.0 unit at 260nm being equivalent to 40µg/ml.

Concentration of total dsDNA in a sample was calculated by spectrophotometry. DNA concentration can be estimated by measuring the absorbance at 260nm (A_{260}), multiplying by the dilution factor, and using the relationship that an A_{260} of 1.0 = 50µg/ml pure dsDNA.

Purity of nucleotide samples and protein contamination was estimated from the A_{260}/A_{280} ratio. An A_{260}/A_{280} ratio between 1.7 and 2.0 generally represents a high-quality sample.

$$\text{DNA Purity } (A_{260}/A_{280}) = A_{260} \text{ reading} \div A_{280} \text{ reading}$$

2.9. Reverse transcription- polymerase chain reaction (RT-PCR)

2.9.1. cDNA synthesis by reverse transcription

First strand cDNA synthesis was performed using moloney murine leukaemia virus (MMLV) reverse transcriptase. MMLV reverse transcriptase is an RNA dependent DNA polymerase used for the efficient synthesis of cDNA from long RNA templates (Fig 2.5). The RNA sample was routinely diluted to a starting concentration of 200ng/μl with nuclease free H₂O. 4μl of the RNA sample was incubated with 1μl of random primers (50ng/μl) (Promega) 90°C for 3 minutes. Samples were then placed on ice. A reverse transcription master mix consisting of 4μl x5 RT buffer (250mM Tris-HCl (pH 8.3 at 25°C), 375mM KCl, 15mM MgCl₂, 50mM DTT), 8μl H₂O, 2μl of 10mM dNTP's and 1μl of MMLV per sample was prepared on ice. 15μl of the master mix was added to each sample and gently mixed by pipetting, the samples were then incubated for 1 hour at 42°C to synthesise the cDNA. cDNA was stored at -20°C.

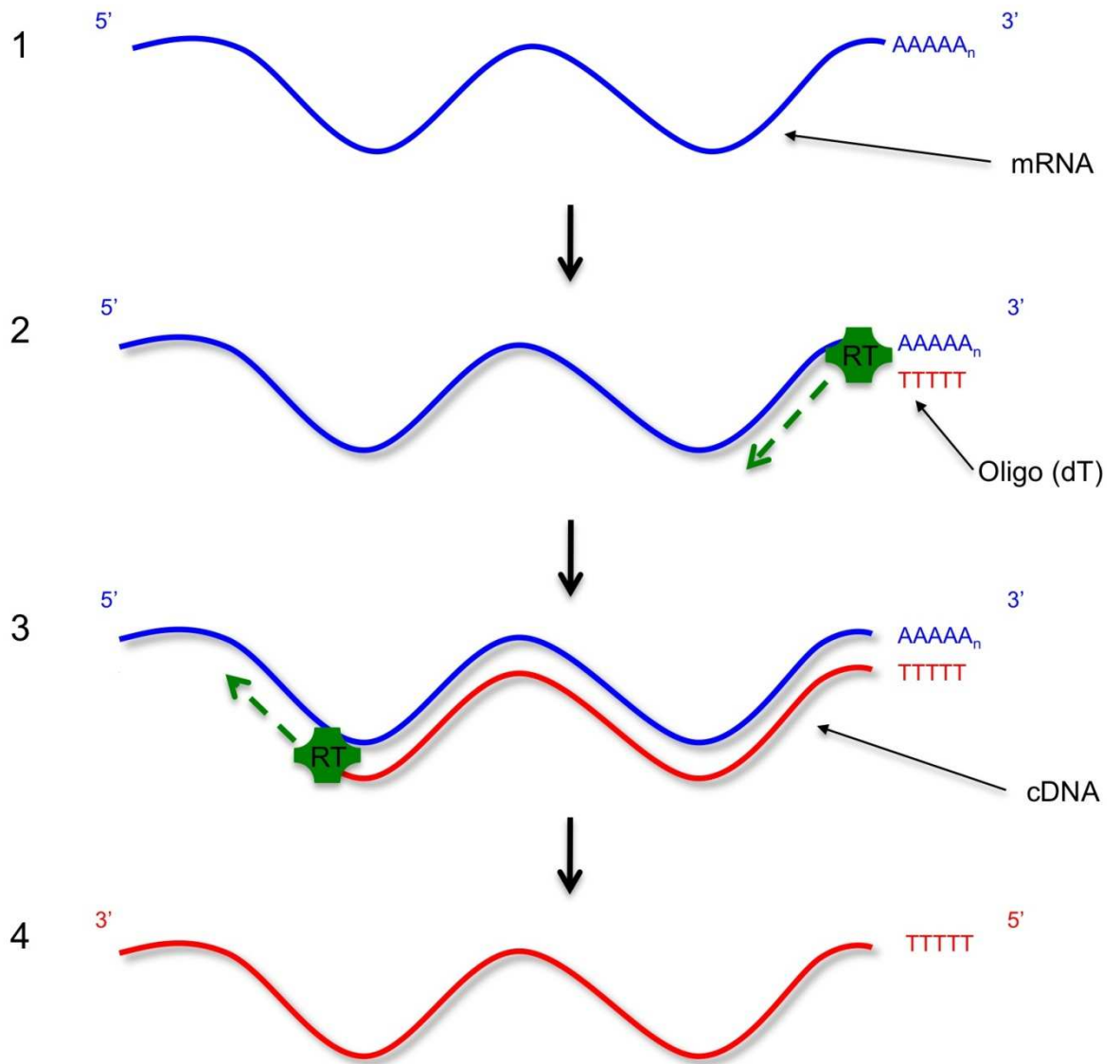


Figure 2.5 – Reverse transcription. Diagram showing the production of single stranded cDNA from mRNA template primed with oligo(dT) by reverse transcription catalysed by reverse transcriptase (RT). Reverse transcription can also be performed using random primers which can prime at various places along the transcript.

2.9.2. DNase treatment and removal of RNA

Isolated RNA was treated with RQ1 RNase-free DNase (Promega, UK) to eliminate any possibility of contaminating genomic DNA being carried through to subsequent PCR based reactions. 0.1x the volume of RNA sample of both RQ1 RNase free DNase and 10x DNase buffer were added to the RNA before incubation at 37°C for 30 min. Following this, 0.1x the volume of sample of DNase stop solution was added before a final incubation at 65°C for 10 min to inhibit the DNase activity.

2.9.3. Polymerase chain reaction

Polymerase chain reaction (PCR) is used to amplify specific DNA sequences, allowing for their detection. Taq polymerase (Taq) is a DNA polymerase named after the bacterium, *Thermus aquaticus* from which it was first isolated. Taq is routinely used in PCR for amplifying short segments of DNA (Fig 2.6). Taq operates at a optimum temperature range of 75-80°C, and can replicate a 1000 base pair strand of DNA in less than 10 seconds at 72°C, annealing temperatures around this range are normally used. It should be noted that Taq has a relatively low replication fidelity as it lacks 3' to 5' exonuclease proofreading activity, and has an error rate of about 1 in 9,000 nucleotides, for applications where a higher degree of accuracy is required, other DNA polymerases were used. A PCR master mix of 10µl 2x Go-Taq Green reagent, 2 µl of each upstream and downstream primers (giving a final working primer concentration of 1µM) and 3µl of nuclease free H₂O, per sample. 2µl (80ng) of

cDNA from each sample was added to a separate PCR microtube, to which 18µl of the PCR master mix was added, mixing gently by pipetting. PCR reactions were performed in a programmable bench top thermocycler, and individual reaction conditions were optimised, a typical cycle was:

Denature at 90°C for 3 min,

35 cycles;

Denature: 1 min at 90°C,

Anneal: 1 min at optimised annealing temperature,

Elongate: 1.5min at 73°C.

Elongate: 8 min at 73°C.

PCR products were stored at 4°C short term, or -80° C for longer periods.

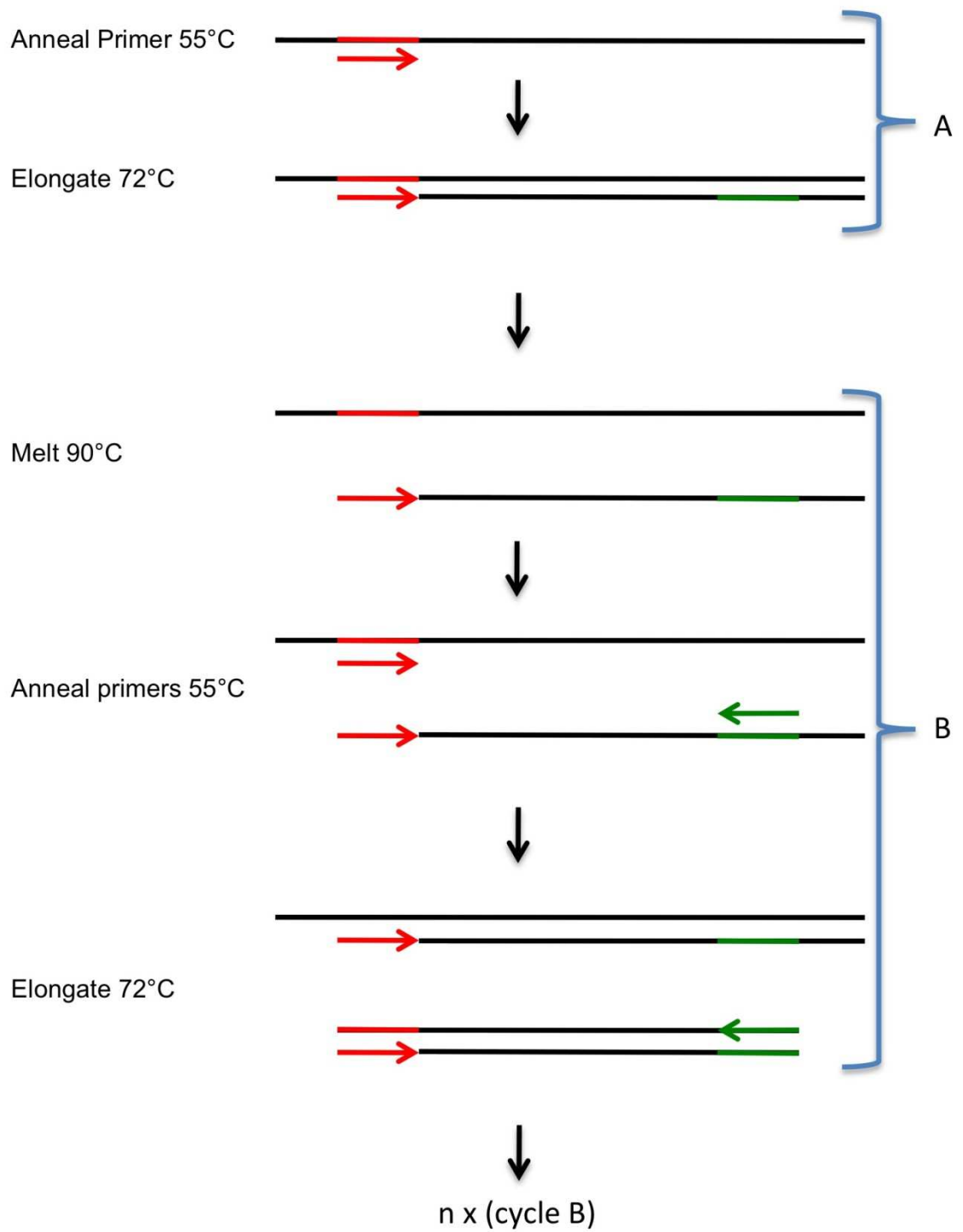


Figure 2.6 – Polymerase chain reaction. Diagram showing the formation of multiple dsDNA copies of a section of a cDNA template from a previous reverse transcription reaction by polymerase chain reaction (PCR).

2.9.4. Primer Design

Primer pairs for PCR were designed using the publically available tool, Primer BLAST (www.ncbi.nlm.nih.gov), where possible primers were designed to have a GC content in the region of 60% and have a length of approx 20 nucleotides. Melting temperature (T_m) was specified to be as close to 60°C as possible, ensuring the GC content of each primer is equal ensures both primers have similar T_m . The annealing temperature for each set of primer pairs was determined by an optimisation process, starting with a temperature 5°C below the specified T_m (55°C).

2.9.5. Agarose gel electrophoresis

Nucleic acids amplified by PCR were separated and identified, according to their length, by agarose gel electrophoresis. This method was used to separate different length nucleic acid acids based on their rate of migration across an agarose gel. The size of a nucleic acid fragment is inversely proportional to the rate at which it will migrate across a polymerised agarose gel towards the positive pole of an electrical field. Samples were compared against a DNA ladder made up from DNA fragments of known sizes. The percentage agarose content of the gel used was dependent upon the size of the target DNA fragment. Typically a target fragment of 150bp may be separated using a 1.5% (w/v) agarose gel. Agarose gels were prepared by adding the required mass of agarose powder (w/v) to 1 x tris-acetate-EDTA acid solution (TAE) (40mM tris, 20mM acetic acid, 1mM EDTA). The mixture was then heated in a

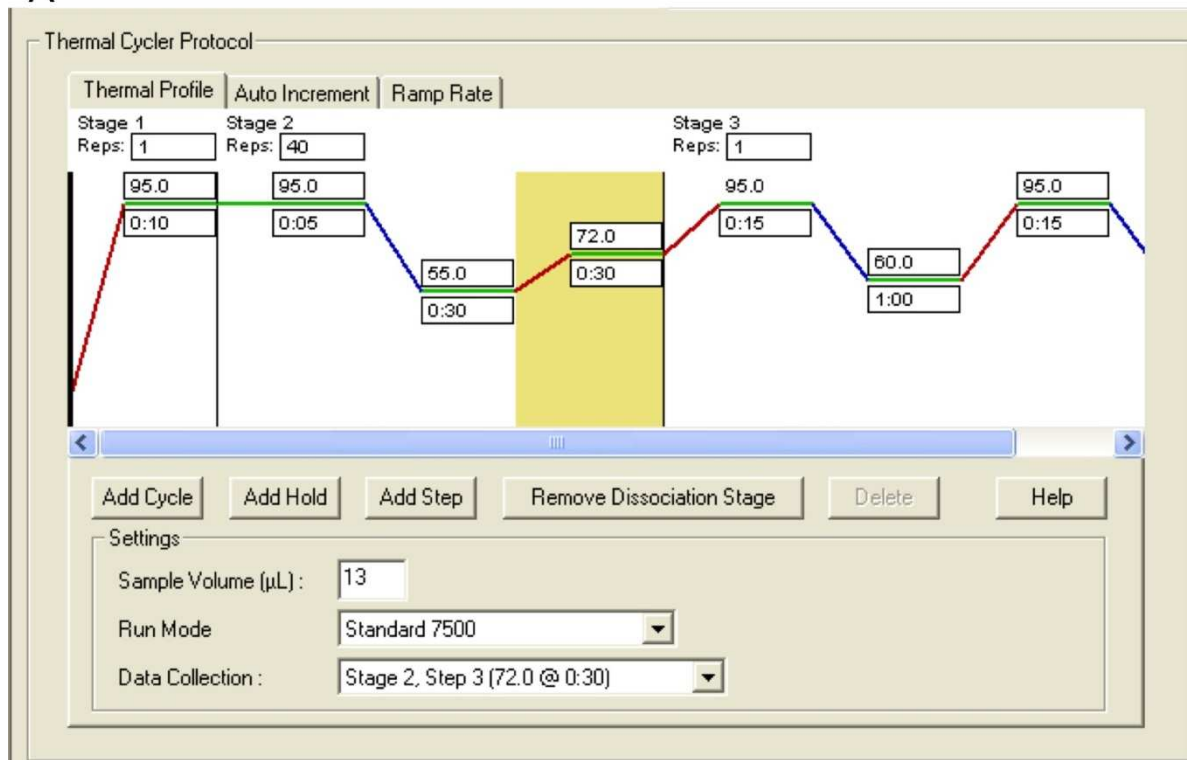
microwave oven until completely melted. The gel solution was then allowed to cool to approximately 60°C before addition of ethidium bromide (EtBr, final concentration 50µg/ml) and carefully mixing. EtBr is a DNA intercalating agent, which once bound to DNA will fluoresce upon exposure to UV light. This allows nucleic acids to be visualised. The agarose gels were cast and sample wells were formed using a comb. Once the gel was set and completely cooled it was positioned in an electrophoresis tank and submerged in 1 x TAE. PCR product samples mixed with 6x loading dye (New England Biolabs, UK) which increases their density so the sample sinks into the well, it also adds colour so the sample migration can be seen by eye. Samples were loaded alongside a DNA ladder standard of appropriate size (New England Biolabs, UK) to aid identification of PCR products. Gels were typically run at 80V until sufficient migration was achieved, before visualisation under UV light.

2.9.6. SYBR-Green quantitative RT-PCR (qRT-PCR)

SYBR Green qRT-PCR is a method that allows for the relative expression of a particular gene to be quantitatively compared between different samples. qPCR is essentially very similar to standard PCR, with the addition of a dye, in this case SYBR-Green, once bound to double stranded DNA (dsDNA) will fluoresce. At the end of the elongation step of the PCR cycle, the level of fluorescence is detected as a measure of the amount of dsDNA present. This is then used to determine the amount of transcript of the target gene present, relative to the other samples. Reaction conditions were optimised individually, and performed in a 13µl reaction volume. For each well of a 96 well PCR plate, 6.5 µl of 2x

SYBR Green Master Mix both upstream and downstream primers to a final concentration of 250nM and a sufficient volume of nuclease free H₂O were combined to make a master mix. 13 µl of master mix was added to each well of the plate. 10ng of each sample was added to individual wells before sealing the plate with optical film. The plates were then briefly centrifuged at 250g to collect all the contents at the bottom of each well. qRT-PCR reactions were performed in an Applied Biosystems 7500 fast thermocycler. Gene expression was then calculated relative to control groups, and normalised against 18S ribosomal RNA to account for any variations. Fold change in gene expression was calculated as 2^{-ddCt} where ddCt is the change in Ct relative to 18s and experimental control (Fig 2.7).

A



B

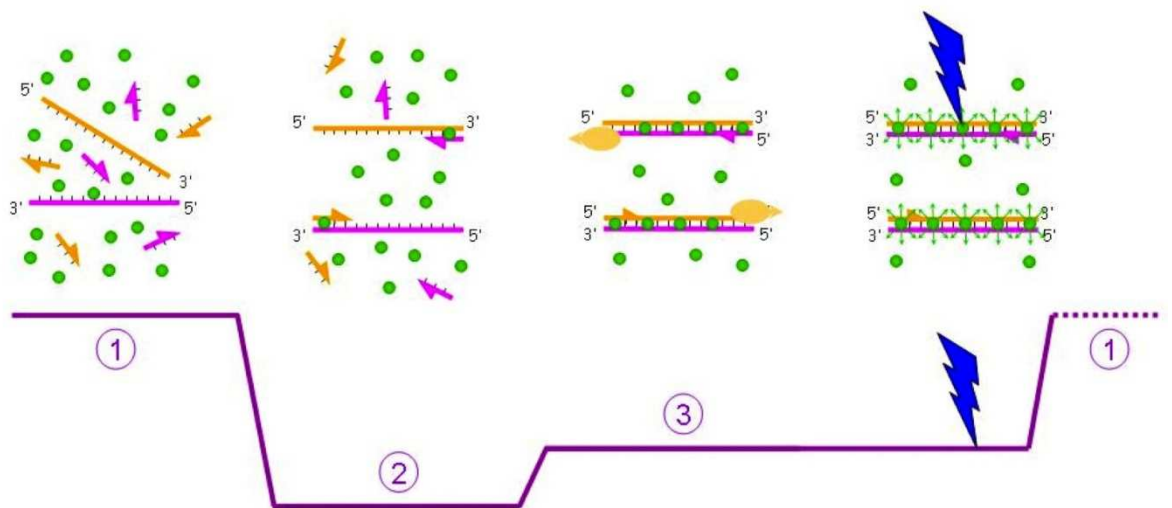


Figure 2.7 – SYBR Green qRT-PCR. A. A screen print of a typical run method used on an ABI 7500 real time thermocycler, to perform SYBR Green quantitative RT-PCR. B. Diagram of the SYBR green qRT-PCR reaction, showing the SYBR green dye (green circles) binding to dsDNA and fluorescing.

Chapter 2 – Materials and Methods

Oligo ID	5'-3' sequence	(°C)	Comments
rAlbuminUS	GTCAGAGGATGAAGTGCTC	57	Will amplify rat albumin (NM_134326.2) cDNA sequence of 471bp.
rAlbuminDS	TTAGCAAGTCTCAGCAGCAG		
rcMYCUS	TCTCGGCCGCTGCCAACTG	58	Will amplify [NM_012603.2] Rattus norvegicus myelocytomatosis oncogene (Myc), cDNA sequence of 204bp
rcMYCDS	TGGGCGAGCTGCTGTGCTTG		
rCK19US	GCTGAAGCCTGGTACCTTACTCAGATT	53	Will amplify rat CK19 cDNA sequence of 230 bp.
rCK19DS	CTGATCACACCCTGGATGTGTGAC		
rER α US	AGTGAAGCCTCAATGATGGG	55	Will amplify rat ESR1 cDNA sequence of 146 bp.
rER α DS	ATCTCCAACCAGGCACACTC		
rER β US	AGGTGCTAATGGTGGGACTG	55	Will amplify rat ESR2 cDNA sequence of 345 bp.
rER β DS	ACTGCTGCTGGGAGGAGATA		
rKLF4US	GGCGGGCTGATGGGCAAGTT	58	Will amplify NM_053713.1 Rattus norvegicus Kruppel-like factor 4 (gut) (Klf4), cDNA sequence of 235bp
rKLF4DS	GCTGGGGTCCAGCGCTCAAG		
rOCT4US	GGTGCAGGCCCGGAAGAGA	58	Will amplify NM_001009178.1 Rattus norvegicus POU class 5 homeobox 1 (Pou5f1), cDNA sequence of 180bp
rOCT4DS	TCCCCTTCTGGCGCCGGTTA		

Chapter 2 – Materials and Methods

rSOX2US	CTTCCCGGAGGCTTGCTGGC	58	Will amplify NM_001109181.1 Rattus norvegicus SRY (sex determining region Y)-box 2 (Sox2), cDNA sequence of 105bp
rSOX2DS	CGCGTAGCTGTCCATGCGCT		
rSOX17US	CAGCACATGCAGGACCATCCCA	52	Will amplify rat (XM_001068621) cDNA sequence of 321bp.
rSOX17DS	GTCCTGCTCCACGCCATCCAA		
rVimentinUS	CGATGTGGACGTTTCCAAGCC	58	Will amplify ref NM_031140.1 Rattus norvegicus vimentin (Vim) cDNA sequence of 226bp
rVimentinDS	ATCCAATTCGCAGGTGAGTG		
hER α US	CCTGATGGCCAAGGCAGGCC	55	Will amplify all 4 human ER α variant transcripts (NM_000125; NM_001122740; NM_00112274 and NM_001122742) cDNA sequences of 221bp.
hER α DS	TGGAGGGGCATCCGTGGAGG		
hER β US	AGCCCCGAGCAGCTAGTGCT	55	Will amplify all 3 human ER β variant transcripts (variant 1, NM_001040275; variant 2, NM_001040276 and variant 3, NM_001437) cDNA sequences of 249bp.
hER β DS	TGATGGGGCTGATGTGGCGC		
rmhGAPDHUS	TGACATCAAGAAGGTGGTGAAG	55	Will amplify rat (NM_017008), human (NM_002046) or mouse (NM_008084) glyceraldehyde 3 phosphate dehydrogenase cDNA sequence of 243bp.
rmhGAPDHDS2	TCTTACTCCTTGAGGCCATGT		
rmh18sUS	CCCGAAGCGTTTACTTTGAA	55	Will amplify cross species (rat, mouse, human) 18s cDNA sequence of 136 bp.
rmh18SDS	CCCTCTTAATCATGGCCTCA		
hTFF1US	GTGCAAATAAGGGCTGCTGT	55	Will amplify human trefoil factor 1 transcript (NM_003225) cDNA sequence of 177bp.
hTFF1DS	CCGAGCTCTGGGACTAATCA		

Chapter 2 – Materials and Methods

m3a11US	ACAAACAAGCAGGGATGGACCTGG	56	Will amplify NM_007818.3, Mus musculus cytochrome P450, family 3, subfamily a, polypeptide 11 (Cyp3a11), cDNA sequence of 152bp.
m3a11DS	AAATGGCAGAGGTTTGGGCC		
mAbcb11US	GTGGCCGTGCTCATCGCCTT	58	Will amplify mouse ATP-binding cassette, sub-family B (MDR/TAP), member 11 (Abcb11) transcript (NM_021022.3) cDNA sequence of 201bp.
mAbcb11DS	TCCAATTCCAGCCACGGTGCG		
mAbcb1bUS	TCCCGCAGTGGCTCTTGAAGC	58	Will amplify mouse ATP-binding cassette, sub-family B (MDR/TAP), member 1B (Abcb1b) (NM_011075.2) cDNA sequence of 150bp.
mAbcb1bDS	AACTCCATCACCCCTCACGTGC		
mAbcc1US	GCAGCGCTGATGGCTCCGAT	60	Will amplify mouse ATP-binding cassette, sub-family C (CFTR/MRP), member 1 (Abcc1) transcript (NM_008576.2) cDNA sequence of 174bp.
mAbcc1DS	TGTAGCCCCGGTCATGGCGA		
mAbcc2US	CGGTGGACGACACTCCCC	60	Will amplify mouse ATP-binding cassette, sub-family C (CFTR/MRP), member 2 (Abcc2) transcript (NM_013806.2) cDNA sequence of 182bp.
mAbcc2DS	CCGTCTCAGCTGGCGGGATG		
mAbcc3US	CTGGCCCACGCGAGGAATGG	60	Will amplify mouse ATP-binding cassette, sub-family C (CFTR/MRP), member 3 (Abcc3) transcript (NM_029600.3) cDNA sequence of 184bp.
mAbcc3DS	TGCGGCCTCCAGGATTCGGA		
mAbcc4US	GTTCCCGGAAGCCGCTGCTT	60	Will amplify all 3 variant of ATP-binding cassette, sub-family C member 4 (Abcc4) transcripts (NM_001033336.3;NM_001163675.1andNM_001163676.1) cDNA sequences of 170bp.
mAbcc4DS	GCGAGCAGAGGTTGGCGTCC		
mAbcc5US	AGCGCTGTACCAGGGCAACA	60	Will amplify both variant mouse ATP-binding cassette, sub-family C (CFTR/MRP), member 5 (Abcc5) (variant 1, NM_013790.2 and variant 2, NM_176839.1) cDNA sequences of 217bp.
mAbcc5DS	TGGTAGTGGTCCGGAAGGGCT		

mAbcc6US	GACCCGGTTGTGGATGGGCG	60	Will amplify mouse ATP-binding cassette, sub-family C (CFTR/MRP), member 6 (Abcc6) transcript (NM_018795.2) cDNA sequence of 216bp.
mAbcc6DS	CAGCAGGTTCCCGACTGGCG		
mIL-1 β US	AAGCCTCGTGCTGTCGGACC	58	Will amplify NM_008361.3 Mus musculus interleukin 1 beta (Il1b), cDNA sequence of 201 bp.
mIL-1 β DS	TCCAGCTGCAGGGTGGGTGT		
mER α US	AAGGGCAGTCACAATGAACC	54	Will amplify mouse ESR1 cDNA sequence of 211 bp.
mER α DS	GCCAGGTCATTCTCCACATT		
mER β US	GGGTGAAGGAGCTACTGCTG	55	Will amplify mouse ESR2 cDNA sequence of 576 bp.
mER β DS	GTGTCAGCTTCCGGCTACTC		
mSlc10a1US	CCTGGCCTTTCCCTAATGGCC	58	Will amplify mouse Slc10a1 solute carrier family 10 (sodium/bile acid cotransporter family), member 1 cDNA sequence of 164bp.
mSlc10a1DS	TGCCCTTCTGCCTCAGTTCATTGC		

Table 2.1 –PCR primer sequences. The designated name, 5'-3' sequence, optimised annealing temperature ($^{\circ}$ C) and description of oligo nucleotides used as PCR primers.

2.10. Immuno-histochemistry and Immuno-cytochemistry

2.10.1. Tissue preparation

Tissue samples were fixed in a solution of 10% formalin 1 x PBS for 24 hours before processing. Tissue samples were processed following a standard protocol, which is a series of wash steps followed by dehydration in EtOH solutions. Tissue samples were embedded in paraffin wax and sections were cut (typically 5µm) and mounted onto slides. Sections were de-waxed in xylene and re-hydrated by a series of washes in ethanol solutions of decreasing concentration (absolute → 90% → 70%) and finally into deionised water.

2.10.2. Proteinase K antigen retrieval

Rehydrated tissue sections were incubated in 10µg/ml proteinase K solution, diluted in 1xPBS for 25 min at 37°C. slides were then rinsed thoroughly in 1 x PBS before continuing with immunostaining protocol.

2.10.3. Sodium citrate antigen retrieval

Rehydrated tissue sections were submerged in 0.01M sodium citrate buffer (pH6) and heated at full power in a microwave oven for 20 min, sections were allowed to cool to room temperature in the citrate buffer.

2.10.4. Immunostaining

Tissue sections were incubated in 3% H₂O₂ solution at room temperature for 10 min to block any endogenous peroxide activity. The sections were then washed for 5 min in 1 x PBS. Non-specific binding of the primary antibody was blocked by pre-incubating sections in 20% (v/v) FBS in 1 x PBS for 20 minutes. After blocking the primary antibody (diluted in 0.05% (v/v) FBS solution) was applied. Sufficient primary antibody was used so that the whole section was evenly covered, the sections were incubated for 1 hour at room temperature or overnight at 4°C. After incubation, sections were washed 3 times for 5 minutes in 1 x PBS, the appropriate HRP conjugated secondary antibody (diluted in 0.05% (v/v) FCS in 1 x PBS) was then applied and incubated for 1 hour at room temperature. The sections were then washed a further 3 times for 5 minutes in 1 x PBS. The antibody binding activity was visualised using diaminobenzidine (DAB) chromogen (Dako, UK) to develop colour essentially as outlined in the manufacturer's instructions. DAB incubation times were optimised for individual antibodies, but were typically between 30 seconds and 15 min. For each set of samples, control sections which were not incubated with a primary antibody were used, to control for non-specific binding of the secondary-HRP antibody had occurred. Following the DAB incubation step, sections were washed immediately in deionised water and counterstained with haematoxylin then washed in acidified water. The stained sections were dehydrated through sequential ethanol solutions of increasing concentration and finally into xylene.

The sections were then mounted in DPX mounting medium (Sigma, UK) and a cover slip was applied.

2.10.5. Haematoxylin and eosin (H & E) staining

For routine examination of tissue histology, sections were H and E stained. Haematoxylin is a blue stain that used to mark the nuclei and eosin is red dye that stains the cytoplasm. Sections were de-waxed in xylene and then re-hydrated sequentially through ethanol as described previously. Sections were then stained in haematoxylin for 1 minute before being thoroughly rinsed in water. The sections were then washed in acidified water for 5 seconds and washed once more in running water. The sections were then stained in eosin for 1 minute and washed in running water again. The sections were then dehydrated through ethanol washes and mounted in Depex.

2.10.6. Sirius red staining

Sirius red stain for collagen was performed by incubating dewaxed paraffin embedded sections in a 1g/L solution of Sirius red dye in saturated aqueous picric acid for 1 hour. Slides were then washed twice in acidified water (5ml glacial acetic acid in 1L dH₂O) before dehydration and mounting as described previously.

2.10.7. Immuno-cytochemistry

The culture media was removed from samples of adherent cells in culture plates and the cells were washed twice in 1 x PBS. The cells were then fixed in situ with a fixative solution (2% v/v formaldehyde / 0.2% v/v glutaraldehyde in 1 x PBS pH 7.4) for 15 minutes at room temperature. The fixative was removed and cells were washed twice for 5 min in 1 x PBS. The cell samples were blocked with a solution of 20% (v/v) FBS in 1 x PBS for 20 min at room temperature, to prevent non-specific protein binding. The blocking solution was removed before incubation for 1 hour with the primary antibody, diluted to the required concentration in antibody incubation buffer (0.05% (v/v) FCS in 1 x PBS). The samples were then washed twice for 5 min in 1 x PBS. The secondary antibody was then added, diluted to the required concentration in antibody incubation buffer and cells were incubated for 1 hour at room temperature (when using fluorescently labelled antibodies, the samples were shielded from light). After incubation, the secondary antibody was removed and cells were washed 4 times in 1 x PBS for 5 min. Samples were then submerged in 1 x PBS and stored at 4°C before imaging.

2.10.8. DAPI staining of DNA

DAPI (4',6-diamidino-2-phenylindole) is fluorescent probe which is permeable to the cell membrane and is used to fluorescently stain cell nuclei. DAPI readily binds AT rich regions of dsDNA, and fluoresces at a maximum of 461nm (blue). Following immunocytochemistry, DAPI was added to the cell samples at a

concentration of 6 μ g/ml and incubated for 10 minutes. Cells were then washed in 1 x PBS.

Antigen	Mwt (kDa)	Dilution	Comments and Source
Albumin	60	1/200 ICC	Rabbit polyclonal IgG.
β -actin	44	1/4000 WB	Mouse monoclonal IgG. Chemicon (MAB1501).
CD3	23	1/100 IHC	Rabbit polyclonal from Abcam. Sodium citrate antigen retrieval.
CK-19	44	1/200 ICC	Mouse monoclonal from Abcam..
ER α	68	1/500 WB 1/50 IHC, ICC	Rabbit polyclonal from Abcam Proteinase K antigen retrieval.
ER β	55	1/1000 WB 1/100 IHC, ICC	Rabbit polyclonal from Abcam Proteinase K antigen retrieval
F4/80	102	1/100IHC	Rabbit polyclonal from Abcam. Proteinase K antigen retrieval, ABC protocol.
NIMP	~18	1/200 IHC	Rat monoclonal from Abcam. Proteinase K antigen retrieval, ABC protocol

OV-6	56	1/100 ICC	R & D biosciences, mouse monoclonal
Vimentin	57	1/2000WB	Rabbit monoclonal from chemicon

Table 2.2 – Antibodies. The name, predicted molecular weight of detected peptide, dilution details and description of antibodies used for Western blot (WB), immunohistochemistry (IHC) and immunocytochemistry (ICC).

2.11. Calculation of half maximal effective concentration (EC₅₀) and half maximal inhibitory concentration (IC₅₀)

Half maximal effective concentration (EC₅₀) and the equivalent value for antagonist relationships, half maximal inhibitory concentration (IC₅₀), are values which are often used to compare efficacy of different treatments in dose response experiments. When a dose response relationship forms a sigmoidal curve and the change in response to a treatment occurs rapidly over a limited number of concentrations, EC₅₀ (or IC₅₀) can be estimated graphically.

Using a non-computational method a semi-log plot is created from the dose response data, from this two different values can be obtained, Absolute EC₅₀ and relative EC₅₀. Absolute EC₅₀ describes 50% of the dynamic range of the assay system, whereas relative EC₅₀ describes 50% of the activity of the test substance based on the experimental data. Whilst this non computational method for calculation of EC₅₀ provides a good estimation, it may not provide a high level of accuracy as it is reliant upon construction of a sigmoidal curve and the EC₅₀ may fall between points on the log scale.

To gain a higher degree of accuracy, EC₅₀ can be calculated using statistical datafitting software which plots the data and by application of the hill coefficient to calculate the slope of the sigmoidal curve, calculates an EC₅₀ value.

The Hill coefficient, widely used in biochemistry, refers to a value calculated for the slope of a sigmoidal curve formed in a dose response experiment, via application of the Hill equation. The Hill equation was first devised by Archibald Vivian Hill in 1910 to calculate the cooperative binding of haemoglobin to O₂. Free software available online at www.changebioscience.com was used for data fitting and calculation of EC₅₀ and IC₅₀

3. Chapter 3 – Results

**3.1. Development of a screening system for transcriptional
estrogenic activity**

In order to identify xenobiotics that may estrogenic activity, a reliable screening method was developed. An *in vitro* system by which a relatively large number of compounds could be tested for transcriptional estrogenic activity accurately and efficiently was required. Using the estrogen responsive breast carcinoma cell line MCF-7, two separate methods were developed to measure estrogen receptor activation by xenobiotics. These were by luciferase reporter gene assay and by SYBR-Green qRT-PCR analysis of the expression of the known estrogen responsive gene, trefoil factor 1 (TFF1)⁹⁶.

3.1.1. Construction of an estrogen receptor luciferase reporter construct

3.1.1.1. pGL3-Promoter vector

The family of pGL3 luciferase reporter vectors provide a basis by which the regulation of mammalian gene expression can be quantitatively measured *in vitro*. The pGL3 vector contains a large number of common restriction sites, which allows it to be modified by inserting custom DNA fragments alongside its modified firefly luciferase gene. The pGL3-Promoter variant also has a SV40 promoter upstream of the luciferase gene.

3.1.1.2. Estrogen response element insert

A DNA fragment consisting of three repeats the consensus estrogen response element sequence (GGTCAnnnTGACC) was designed (3 x ERE), along with its complementary sequence. This fragment was flanked with sticky ends complementary to restriction sites of *SacI* and *XhoI*. These two restriction sites are found at positions 11 and 32 respectively of the pGL3-Promoter multiple cloning region, upstream of the SV40 promoter and luciferase gene, a schematic of the insert is shown in Fig 3.1A.

3.1.1.3. Construction of a (ERE)₃-Luciferase construct

The pGL3-Promoter vector was linearised by digestion with *SacI* and *XhoI*, the digestion was confirmed by agarose gel electrophoresis, using undigested plasmid as a control. The linearised plasmid was then separated from the small segment that lies between the two restriction sites, again by agarose gel electrophoresis, and purified. The 3xERE fragment was then ligated into the plasmid.

To select a correctly constructed recombinant plasmid, numerous clones were screened by restriction digest with *MluI*. The restriction site for this enzyme lies in the fragment of the cloning region which was removed, as it is not present in the (ERE)₃ insert, clones which potentially contained the correct insert were identified. From the colonies selected, it was established that 3 clones were missing the *MluI* restriction site, colonies #2, 5 and 7. Fig 3.1B

These 3 clones were sent for DNA sequencing to ensure that the exact sequence had been inserted, and that it was orientated correctly. The sequencing results revealed that both clones 5 and 7 were correctly assembled, but had a small number of differences in their sequence around the *SacI* and *XhoI* restriction sites Fig 3.1C.

3.1.2. (ERE)₃-Luciferase reporter construct is estrogen responsive

To confirm the correct functioning of the newly developed constructs and to ascertain which was the most responsive, they were tested in the estrogen responsive breast carcinoma cell line, MCF-7. In order to maximise reporter gene responsiveness to estrogens it is necessary to culture MCF-7 cells in medium supplemented with stripped serum to reduce the levels of estrogenic compounds within the culture (cell cultures which have undergone this process are termed 'withdrawn'⁹⁷). Expression of the ER was confirmed by RT-PCR and Western blot. Fig 3.2A demonstrates that the MCF-7 cell line expresses ER α mRNA under normal culture conditions and after 4 days of withdrawal. This was confirmed by Western blot, it was apparent that the level of ER α protein increased following culture with stripped serum, relative to β -actin loading control. (Fig 3.2B)

Purified plasmid DNA from both colonies 5 and 7 (termed ERLuc5 and ERLuc7 respectively) were transiently transfected into MCF-7 cells, which were then treated for 24 hours with 10 μ M E2. Fig 3.2C demonstrates that untransfected MCF-7 cells had no luciferase activity, whereas cells transfected with the unmodified pGL3-Promoter vector exhibit a basal amount of luciferase activity which is driven by the promoter region and was unaffected by treatment with E2. MCF-7 transfected with either ERLuc5 or ERLuc7 exhibited a significant increase in luciferase activity over untransfected cultures.

Luciferase activity of MCF-7 cells transfected with either modified plasmid was significantly increased following treatment with E2 relative to DMSO vehicle control group. It was determined that ERLuc5 was the most responsive version of the construct and so was chosen for use in future investigations.

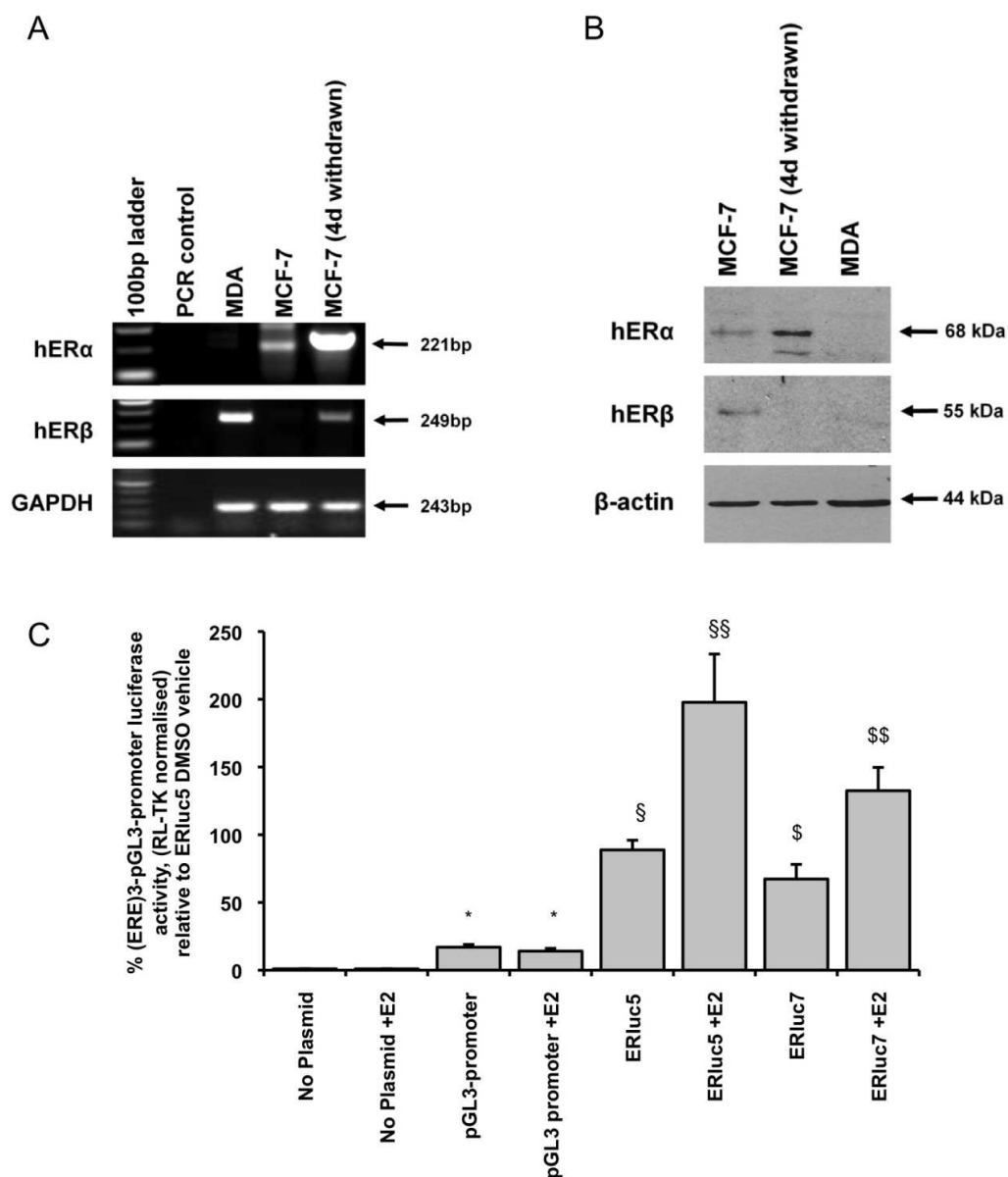


Figure 3.2 – MCF-7 dual luciferase assay. A. Confirmation of the expression of expression of hER in breast cancer cell lines by RT-PCR. Cells were cultured either in normal conditions or subjected to withdrawal for 4 days before isolation of RNA and RT-PCR using primer pairs specific for the human ER. PCR products were visualised by agarose gel electrophoresis and UV transillumination **B. Confirmation of the expression of expression of hER in breast cancer cell lines by Western Blot.** Cells were cultured either in normal conditions or subjected to withdrawal for 4 days before isolation of total protein and analysis by Western blot as described in chapter 2- materials and methods. 25 μ g of total protein/lane **C. (ERE)₃-pGL3-promoter luciferase plasmid is estrogen responsive.** MCF-7 cells were transiently transfected with (ERE)₃-pGL3-promoter-luciferase variants and *Renilla* luciferase constructs before treatment with 10 μ M E2 or DMSO vehicle for 24 hours before analysis by dual-luciferase assay, expressed relative to *Renilla* luciferase. (Mean and SD of n=3). *=Significant increase over untransfected control, §/§= significant increase over unmodified pGL3-promoter, §§/§§=significant increase over DMSO vehicle. (p<0.05, Students t-test, two tailed).

3.1.3. (ERE)₃-pGL3-Promoter construct (ERLuc5) is specific for estrogen receptors α and β

In order to determine whether the (ERE)₃-pGL3-promoter construct was specific for/preferentially transactivated by the ER, (ERE)₃-pGL3-promoter activation was assessed in the non estrogen responsive breast carcinoma cell line MDA-MB-231 (MDA) cell line.

The expression of the ER in MDA cells was examined by RT-PCR and Western blot. ER α was not detected at either mRNA or protein levels, ER β transcript was detected but no ER β protein was observed (Fig 3.2A,B).

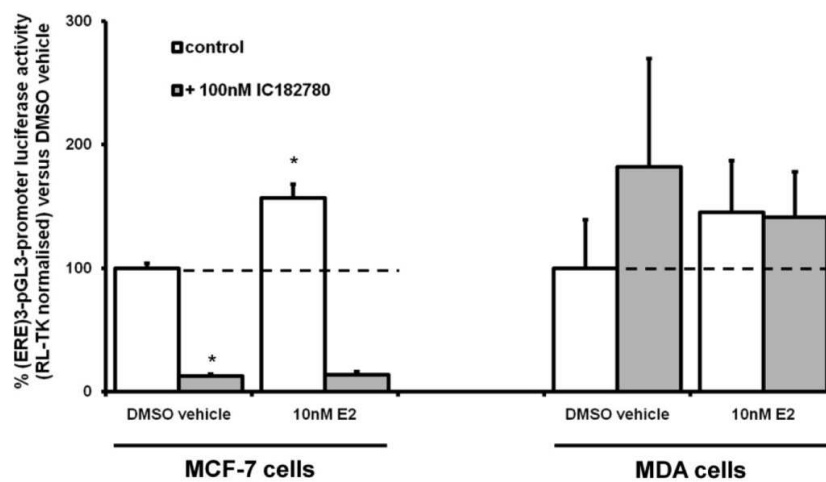
MDA cells were transiently transfected with (ERE)₃-pGL3-Promoter and pre treated with the pure estrogen receptor antagonist ICI182780. Figure 3.3A demonstrates that MDA cells transfected with (ERE)₃-pGL3-Promoter do not respond to either E2 or ICI182780, suggesting that (ERE)₃-pGL3-Promoter was not transactivated, this is shown alongside a comparable investigation using the estrogen responsive MCF-7 cells, highlighting the difference in response.

MDA cells were co-transfected with both (ERE)₃-pGL3-Promoter and a range of expression constructs coding for the expression of a variety of nuclear receptors, or one which results in the expression of a green fluorescent protein (pEGFP-N1 or GFP). pEGFP-N1 is unrelated to steroid hormone signaling and was used as a control to show that any effects observed were not as a result of protein over expression.

Fig 3.3B shows that over expression of ER α in MDA cells resulted in the activation of (ERE)₃-pGL3-Promoter by a significant increase in luciferase activity over the cells transfected with pEGFP-N1. Treatment with 10nM E2 resulted in a further increase in luciferase activity in cells expressing ER α or ER β . This shows that the (ERE)₃-pGL3-Promoter vector is activated by the human ER α and ER β and also that its luciferase expression is regulated in an estrogen dependent manner.

No increase in luciferase activity was observed, nor was there a difference in activity following treatment with 10nM E2 over DMSO vehicle in MDA cells transfected with constructs coding for the expression of other nuclear receptors (androgen receptor (AR), testosterone receptor (TR), progesterone receptor (PR), glucocorticoid receptor (GR) and vitamin D receptor (VDR)).

A



B

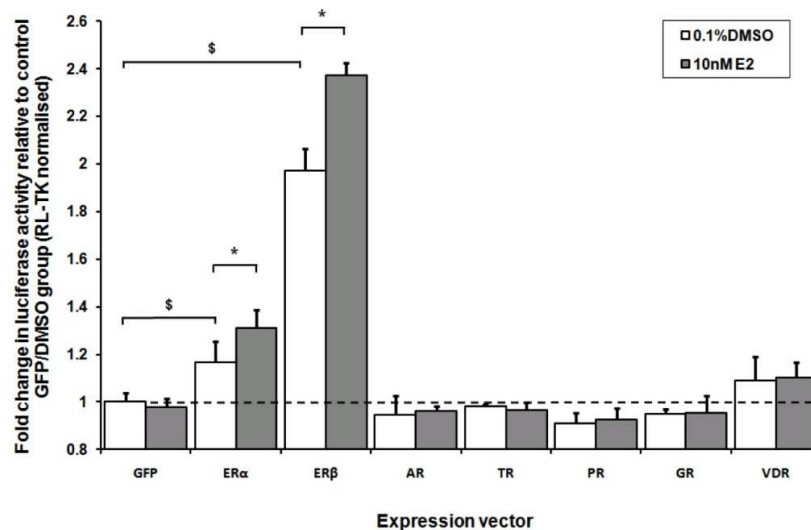


Figure 3.3 – Specificity of (ERE)₃-pGL3-promoter-luciferase **A. MDA cells are not estrogen responsive.** Cells were transiently transfected with (ERE)₃-pGL3-promoter-luciferase and *Renilla* luciferase constructs before treatment for 24 hours with 10nM E2 or DMSO vehicle (+/- ICI182780). Luciferase activity was assessed by dual luciferase reporter assay and expressed relative to *Renilla* luciferase. (Mean and SD of n=3). * = Significantly different (p<0.05) to relevant control group (Students t-test, two tailed) **B. (ERE)₃-pGL3-promoter-luciferase construct is specific for the ER.** MDA cells were transiently transfected with plasmids coding for the expression of a range of different nuclear receptors, (ERE)₃-pGL3-promoter-luciferase and *Renilla* luciferase constructs before treatment for 24 hours with 10nM E2 or DMSO vehicle. Luciferase activity was assessed by dual luciferase reporter assay and expressed relative to *Renilla* luciferase (Mean and SD of n=3). \$ = Significant increase over GFP control group, * = significant increase over DMSO vehicle control group. (p<0.05, Students t-test, two tailed).

3.1.4. Estrogen mediated expression of trefoil factor 1.

Trefoil factor 1 (TFF1) is a small cysteine-rich protein that is regulated by the ER in estrogen responsive breast carcinoma cell lines, but not in estrogen receptor negative breast cancer cells. TFF1 expression in breast carcinoma cell lines is regulated primarily by estrogen signalling, mediated by the binding of an estrogen receptor-ligand complex to the consensus ERE, located 400bp upstream of the TFF1 transcription start site⁹⁸. Because TFF1 expression in MCF-7 cells is consistently up regulated by transcriptional estrogenic activity⁹⁶, it was used to measure transcriptional estrogenic activity of estrogenic xenobiotics.

3.1.4.1. TFF1 mRNA is expressed in MCF-7 cells

Expression of TFF1 mRNA was confirmed in the cell lines MCF-7 and MDA by RT-PCR using primers designed to specifically amplify a section of the TFF1 gene. Fig 3.4 A shows that TFF1 mRNA was detectable in MCF-7 by RT-PCR.

3.1.4.2. Estrogen increases TFF1 expression is in MCF-7 but not MDA cell lines

MCF-7 cells were cultured in culture media supplemented with charcoal-dextran treated FBS for a minimum of 4 days, after which they were treated with either DMSO vehicle or 10nM E2, a working concentration based on previous work by May *et al*⁹⁶. Expression of TFF1 mRNA was assessed quantitatively by SYBR

Green qRT-PCR. Following treatment with 10nM E2 a 3-fold increase in TFF1 mRNA expression over DMSO vehicle was observed.

Treatment with the ER antagonist ICI182780 at a concentration of 100nM caused a significant reduction in TFF1 expression in both DMSO and E2 treatment groups, suggesting that even following a withdrawal process, estrogenic components persisted in the cell culture and an induced level of estrogenic activity remained in this MCF-7 cell model (Fig 3.4B).

MDA cells are widely regarded as a classical estrogen non-responsive cell line⁹⁹, and it is reported that non-estrogen responsive breast carcinoma cell lines do not express detectable TFF1 due to silencing by methylation of the non translated region -464 to +294 at the 5' end of the TFF1 gene¹⁰⁰. Fig 3.4A shows that in our hands a PCR product of the predicted size for TFF1 was detected in MDA cells, visualised at a lower intensity than in MCF-7. It is possible that at the point of RNA isolation TFF1 was expressed at a low level in our MDA cells. No change in TFF1 mRNA expression was observed following treatment with either 10nM E2 or 100nM ICI182780 (Fig 3.4B).

The expression of TFF1 following treatment was investigated by RT-PCR. Fig 3.4C confirms shows that a single PCR product at the predicted size for TFF1 was observed, which appears more abundant in the E2 treated cells.

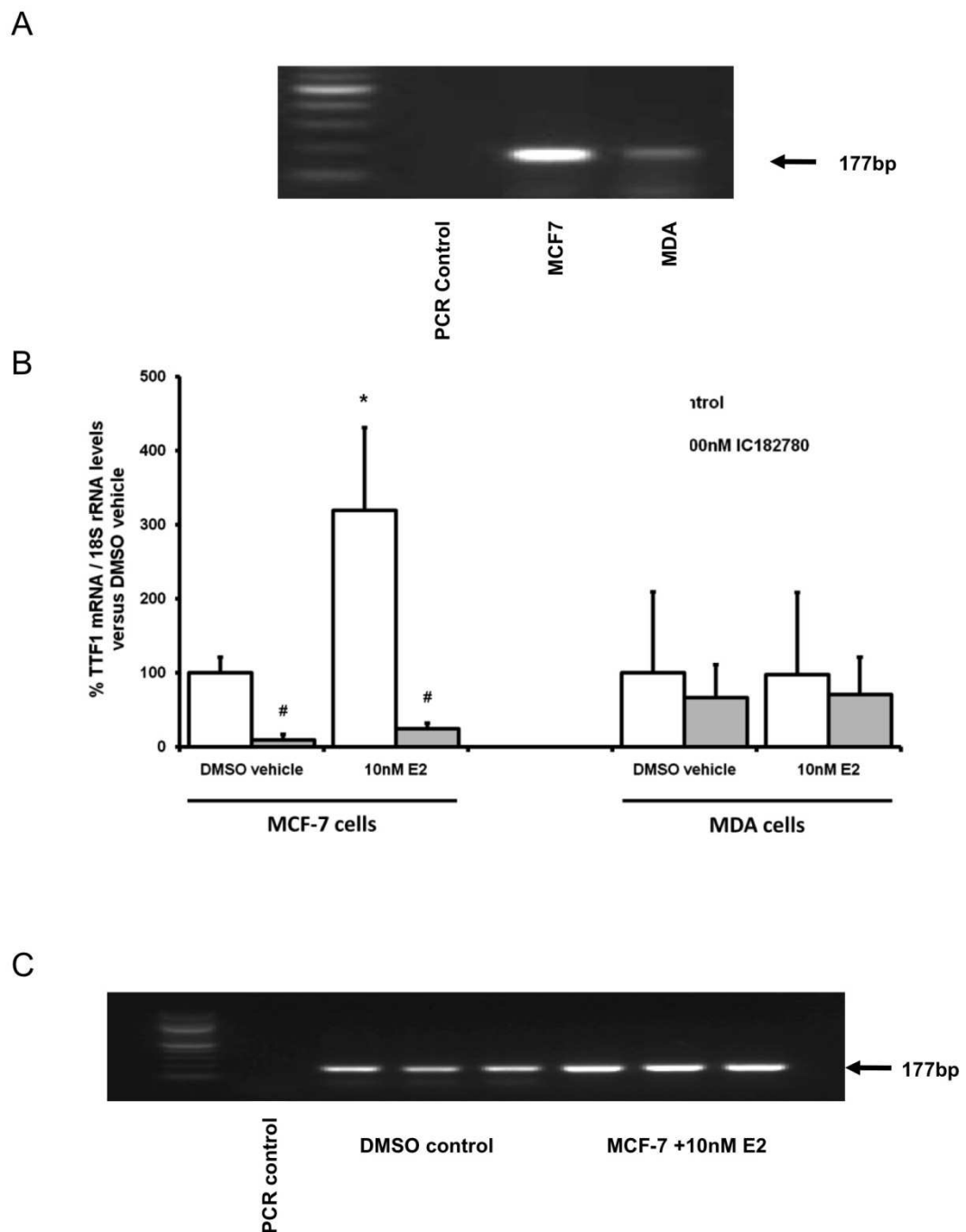


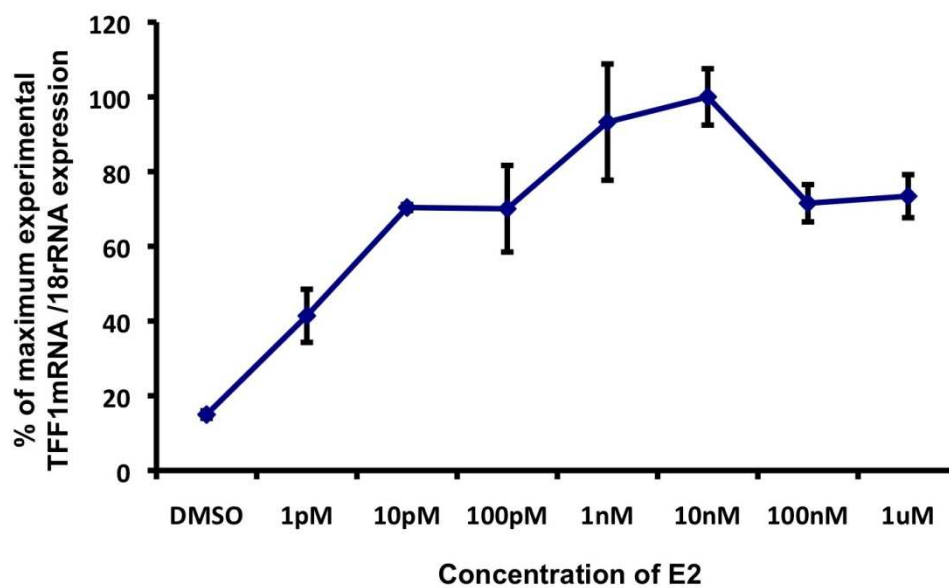
Figure 3.4 – TFF1 induction in MCF-7. A. Confirmation of expression of TFF1 in MCF-7 cells. Expression of TFF1 was confirmed by RT-PCR in MCF-7 and MDA cell lines using a primer pair designed to be specific for TFF1. PCR products were visualised by agarose gel electrophoresis and UV transillumination. **B. Quantitative analysis of TFF1 mRNA expression.** MCF-7 and MDA treated for 24 hours with 10nM E2 or DMSO +/- pre-treatment with ICI 182780 before analysis of TFF1 transcript levels by SYBR Green qRT-PCR (Mean and SD of n=3). *= significant increase over DMSO vehicle control group. #=significant decrease from no antagonist group. (p<0.05, Students t-test, two tailed). **C. Confirmation of TFF1 induction by E2 by RT-PCR.** RT-PCR for TFF1 in MCF-7 cells following treatment for 24 hours with 10nM E2 or DMSO vehicle. PCR products were visualised by agarose gel electrophoresis and UV transillumination.

A dose response curve of TFF1 gene induction in response to E2 at concentrations starting at 1pM, increasing sequentially by a factor of 10, up to a maximum of 1µM. A significant increase in TFF1 transcript over DMSO vehicle was observed at all concentrations, a peak response was identified at a concentration of 10nM (Fig 3.5A)

3.1.4.3. Treatment with the anti-estrogen, tamoxifen, inhibits TFF1 mRNA expression in MCF-7 cells

To ensure that the increase in TFF1 gene expression seen was response to estrogen treatment and via the classical estrogen signalling pathway, cultures of MCF-7 cells were treated with increasing concentrations of the anti-estrogenic drug, tamoxifen. A dose response experiment was performed using concentrations of tamoxifen from 1pM up to a maximum of 1µM. MCF-7 cell cultures were treated with tamoxifen for 24hr, after which they were retreated with and also administered 10nM E2. The expression of TFF1 mRNA, relative to DMSO vehicle was significantly decreased by administration of tamoxifen, with a maximal effect at a concentration of 100nM (Fig 3.5B).

A



B

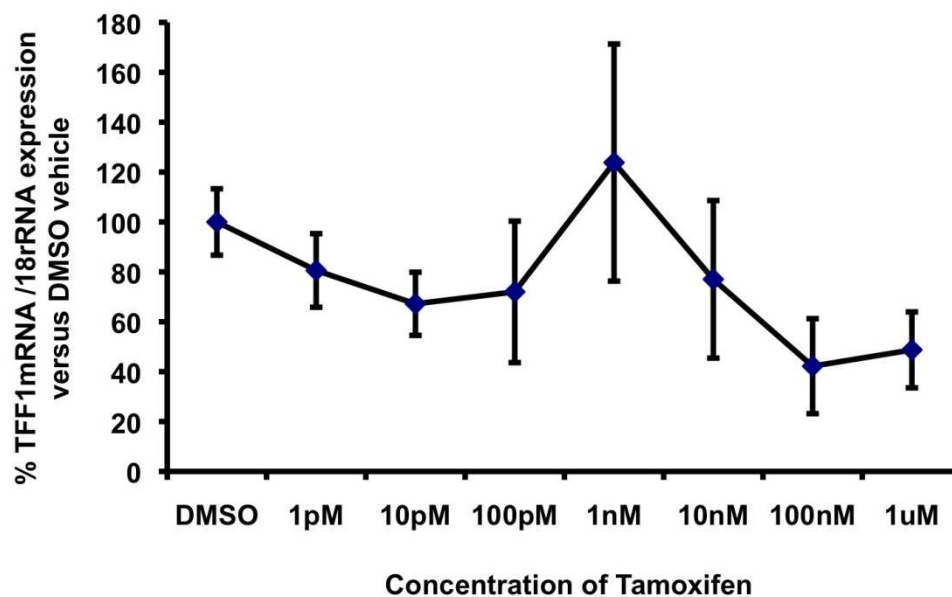


Figure 3.5 – TFF1 expression dose-response. **A. Dose-response curve of TFF1 expression in response to E2.** Expression of TFF1 in MCF-7 cells was quantified following treatment for 24 hours with increasing concentrations of E2 or DMSO before analysis of TFF1 transcript levels by SYBR Green qRT-PCR (Mean and SD of n=3). **B. Dose-response study of TFF1 inhibition by tamoxifen.** Expression of TFF1 in MCF-7 cells was quantified following treatment for 24 hours with increasing concentrations of tamoxifen or DMSO before analysis of TFF1 transcript levels by SYBR Green qRT-PCR (Mean and SD of n=3).

3.1.5. Chapter 3.1 discussion

A specific, accurate and reproducible means by which xenobiotics can be screened for transcriptional estrogenic activity was required. This was achieved by two means, a dual luciferase reporter system and by quantitative measurement of the well-known estrogen responsive gene, TFF1.

A unique estrogen responsive luciferase reporter construct was developed which consists of 3 repeats of the consensus ERE controlling the expression of the luciferase gene. The transient transfection of this vector into MCF7 cells was optimized and its functionality and specificity for the ER were confirmed. Using the ERE-Luc5 construct and by quantification of TFF1 mRNA expression in MCF cells human estrogenic transcriptional activity can be confidently assessed.

It was also determined that cell culture models have high levels of endogenous transcriptional estrogenic activity, which must be depleted in order to gain an accurate measurement of xenoestrogenic activity.

3.2. Screening for transcriptional estrogenic activity of xenobiotics

Using the construct and methodologies outlined in chapter 3.1, xenobiotics that have been proposed by others to be linked to the incidence of PBC were screened for transcriptional estrogenic activity. Examples include heavy metals and manufacturing by-products that may be found in industrial or mining areas and cosmetic/pharmaceutical preservatives and colouring agents.

3.2.1. Screening for transcriptional estrogenic activity by dual luciferase assay.

As described in chapter 3.1, a screening system for transcriptional estrogenic activity was developed using the estrogen responsive breast carcinoma cell line MCF-7 utilising a dual luciferase reporter assay system.

Initially MCF-7 cells that were transiently transfected with the 3xERE-luciferase reporter construct were treated for 24 hours with either DMSO vehicle control or 10 μ M of each compound.

Figure 3.6A shows a number of compounds which were screened for xenoestrogenic activity, and were chosen based upon their possible ability to substitute lipoic acid upon PDC-E2. 2-octynoic acid, a compound frequently found in cosmetic products has previously been shown to have the potential to substitute lipoic acid on PDC-E2¹⁰¹, so 2-octynoic acid and a range of structurally similar compounds were examined. The results show that although

some of these compounds may modulate ER α transcriptional activity, none of them acted as a direct ER α agonist and mainly inhibited reported gene activity.

Exposure to certain pesticides, such as organophosphates, have been previously linked to some autoimmune conditions, although the mechanisms and long term effects are not well understood. Considering that some pesticides have also been described as environmental xenoestrogens the group of compounds shown in fig 3.6B were considered potential candidates for initiating PBC. The results confirm the known estrogenic activity of methoxychlor, other compounds in this group either had no effect or were inhibitory upon reporter gene expression.

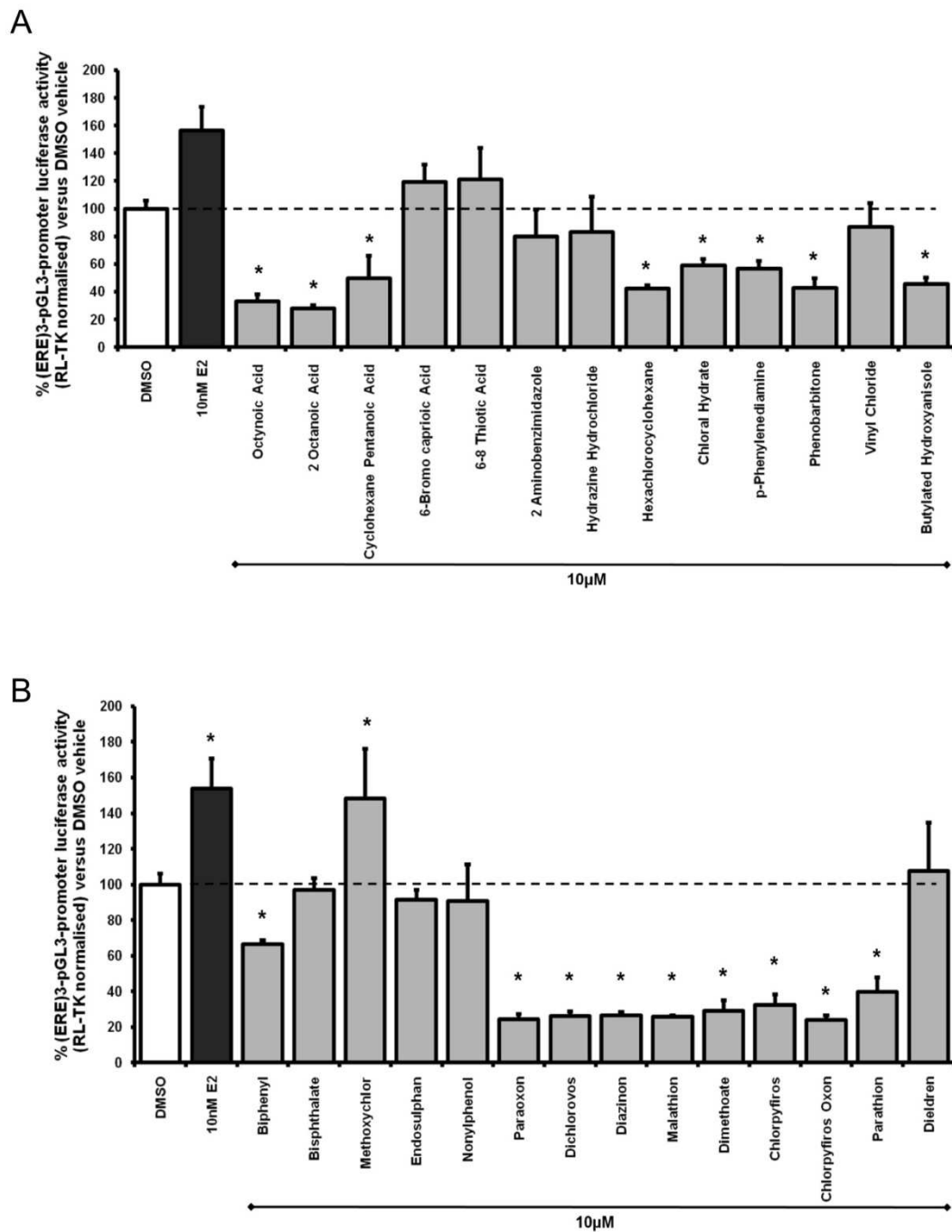


Figure 3.6 –Xenoestrogen screening 1. MCF-7 cells were transiently transfected with (ERE)₃-pGL3-promoter-luciferase and *Renilla* luciferase constructs before treatment for 24 hours with 10nM E2 or 10µM of a selected xenobiotic. Luciferase activity was assessed by dual luciferase reporter assay and expressed relative to *Renilla* luciferase. (Mean and SD of n=3). * = Significantly different (p<0.05) to DMSO control group (Students t-test, two tailed).

A selection of heavy metals, representing those which may be found contaminating the environment in industrial or mining areas were tested, the results are shown in fig 3.7A. None of these were found to increase ER α mediated gene expression, all of which were apparently inhibitory.

Epidemiological studies have previously associated frequent use of certain cosmetic products with such as nail polish and hair colouring products with an increased incidence of PBC¹⁰². Fig 3.7B shows that some compounds which are commonly found in cosmetic products are human ER α agonists. Both butyl and propyl paraben which are both used as preservative agents in cosmetics, were transcriptional ER α agonists confirming the findings of Routledge *et al*¹⁰³. In addition the cosmetic and food colouring agents sunset yellow (E110) and tartrazine (E102) were shown to increase ER α mediated reporter gene expression.

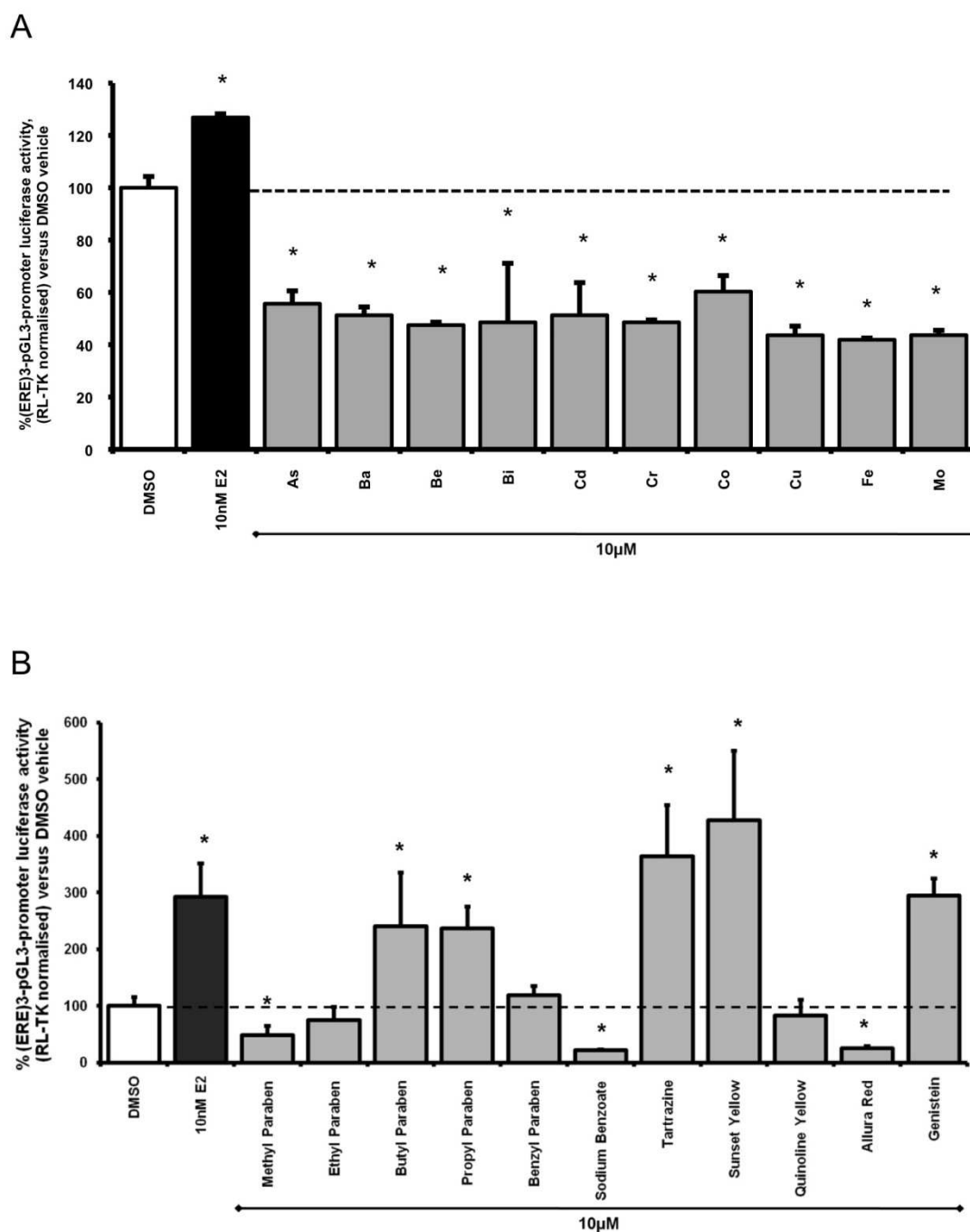


Figure 3.7 –Xenoestrogen screening 2. MCF-7 cells were transiently transfected with (ERE)₃-pGL3-promoter-luciferase and *Renilla* luciferase constructs before treatment for 24 hours with 10nM E2 or 10µM of a selected xenobiotic. Luciferase activity was assessed by dual luciferase reporter assay and expressed relative to *Renilla* luciferase. (Mean and SD of n=3). *= Significantly different (p<0.05) to DMSO control group (Students t-test, two tailed). Metal compounds were delved into acid vehicle then diluted into cell culture media, an appropriate DMSO/metal vehicle combination was used as a control.

3.2.2. Xenobiotic mediated increase in luciferase activity is inhibited by ICI182780.

Following the initial screening process, compounds that tested positive for ER α mediated transcriptional activity were repeated. In this investigation the MCF-7 cells were also pre-treated with the pure estrogen receptor antagonist ICI182780 or vehicle control. This was performed to ensure the activity observed was mediated by ER α and not another transactivating nuclear receptor with affinity for the ERE. Fig 3.8 illustrates how the 3xERE-luciferase mediated gene activity induced by sunset yellow, tartrazine, parabens and other compounds which initially tested positive was inhibited by the presence of ICI182780.

Steroid hormones, other than estrogen, were also screened for estrogenic activity in our assay system. When administered at a concentration of 10 μ M many of these hormones increased ER α mediated gene transcription. Having already confirmed that the 3xERE-luciferase reporter construct is not activated by any other steroid hormone receptors, this result suggests that at high concentrations these other hormones can activate the ER α .

Interestingly, the increase in ER mediated luciferase activity of some other forms of estrogen, ethinyl estradiol, estriol, estrone and equilin, and certain other steroid hormones was not decreased by ICI182780 in this investigation suggesting that this compound functions as a competitive agonist.

To examine this effect further, the same investigation was repeated at a lower and much more physiologically realistic treatment concentration of 10nM. In this study the increase in ER α mediated gene expression by the same set of steroid hormones was still observed, but the ER α mediated gene induction activity was comprehensively decreased by ICI182780 pre treatment (Fig 3.9).

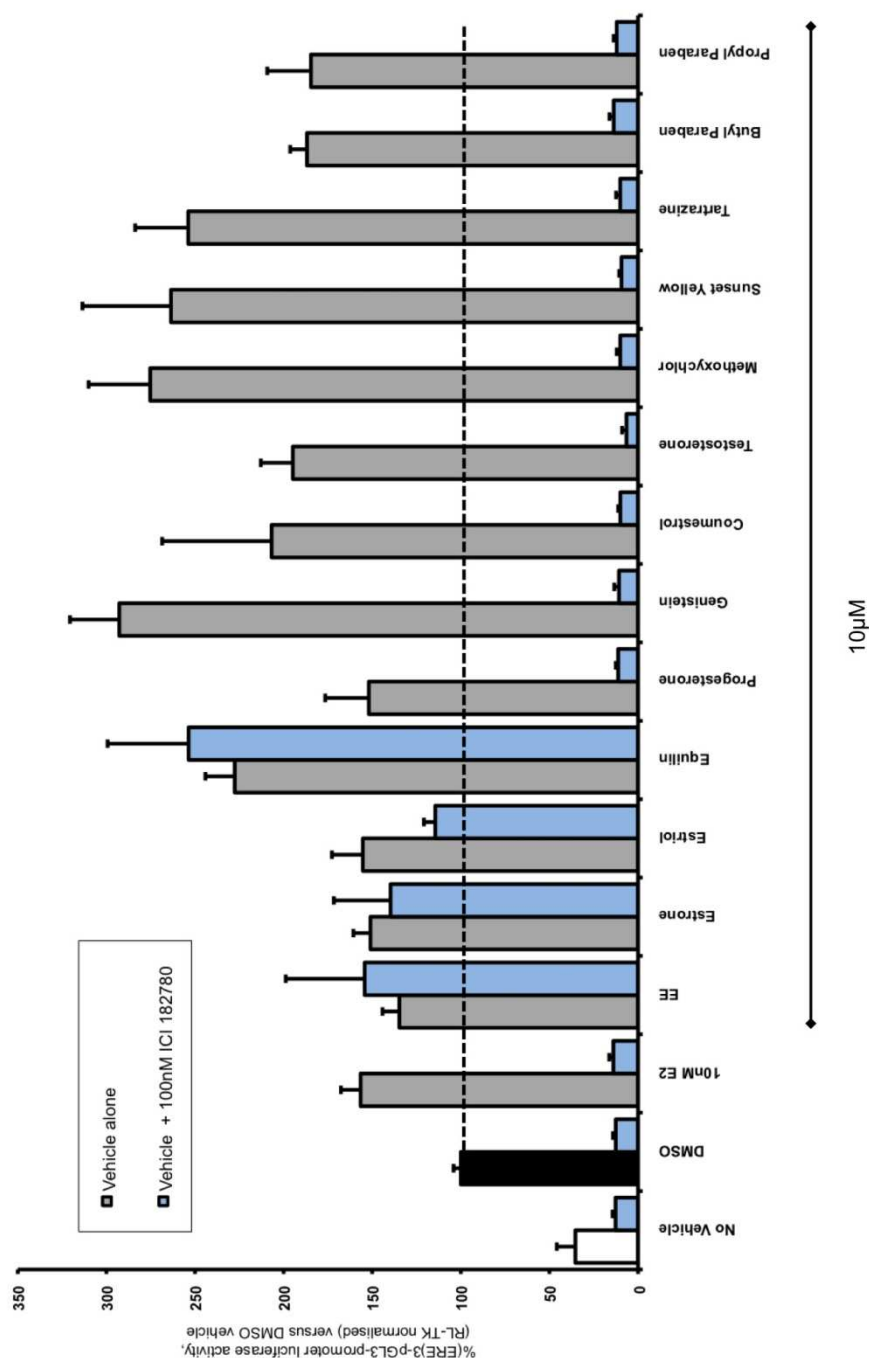


Figure 3.8 –Antagonism of xenoestrogenic activity by ICI182780. MCF-7 cells were transiently transfected with $(ERE)_3$ -pGL3-promoter-luciferase and *Renilla* luciferase constructs before treatment for 24 hours with 10nM E2 or 10µM of a selected xenobiotic (+/- 100nM ICI182780). Luciferase activity was assessed by dual luciferase reporter assay and expressed relative to *Renilla* luciferase. (Mean and SD of n=3). * = Significantly different ($p < 0.05$) to DMSO control group (Students t-test, two tailed).

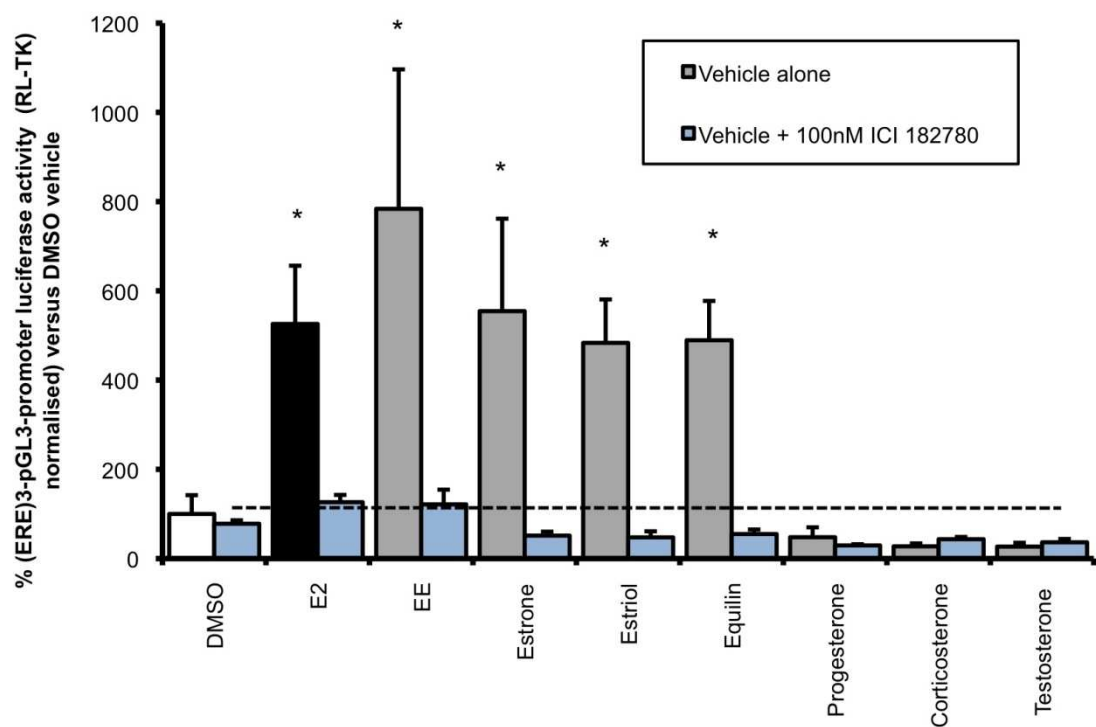


Figure 3.9 – Estrogenic activity of 10nM concentration of steroid hormones. MCF-7 cells were transiently transfected with (ERE)₃-pGL3-promoter-luciferase and *Renilla* luciferase constructs before treatment for 24 hours with 10nM concentration of various steroid hormones (+/- 100nM ICI182780). Luciferase activity was assessed by dual luciferase reporter assay and expressed relative to *Renilla* luciferase. (Mean and SD of n=3). * = Significantly different (p<0.05) to DMSO control group (Students t-test, two tailed).

3.2.3. Dose-response study of xenobiotic mediated transcriptional estrogenic activity.

To investigate the potency of the xenoestrogens which were identified by the initial screening process, and to compare this activity to that of E2, dose response curves were constructed for the compounds of interest in the MCF-7/3xERE-luciferase reporter assay.

Typical dose-response curves for E2, tartrazine, sunset yellow, butyl paraben, propyl paraben and methoxychlor in MCF-7 cells are described in figs 3.10, 3.11, 3.12. In addition a typical dose response for the ER antagonist, ICI182780 is also shown. From these curves EC_{50} and IC_{50} values were calculated for the agonists and antagonist respectively (table 3.1).

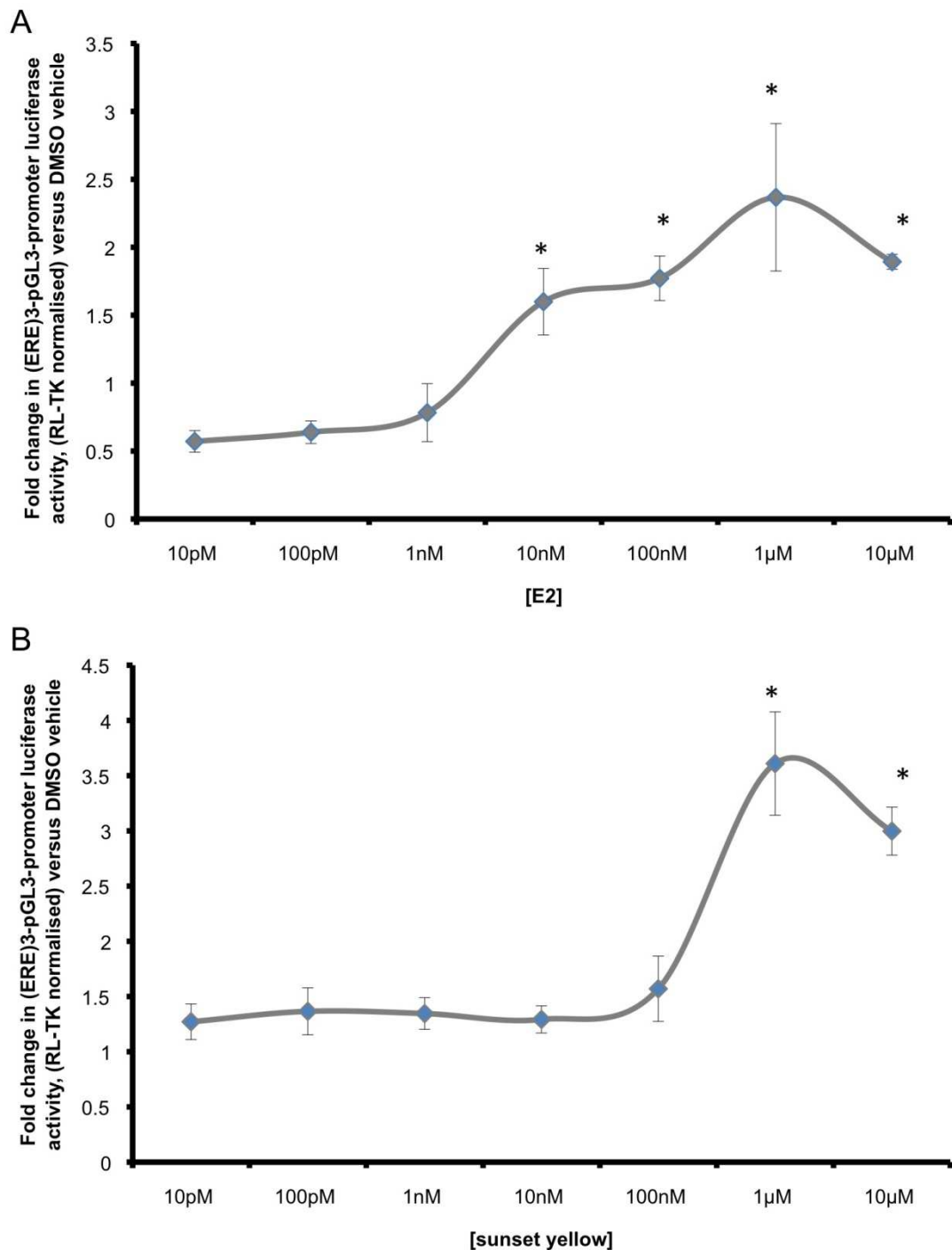


Figure 3.10 - Dose response studies of xenoestrogen activity. A. E2. MCF-7 cells were transiently transfected with (ERE)₃-pGL3-promoter-luciferase and *Renilla* luciferase constructs before treatment for 24 hours with increasing concentrations of E2. Luciferase activity was assessed by dual luciferase reporter assay and expressed relative to *Renilla* luciferase. (Mean and SD of n=3). * Denotes significant difference from lowest treatment concentration (p<0.05) (Tukey post hoc analysis) **B. Sunset yellow.** MCF-7 cells were transiently transfected with (ERE)₃-pGL3-promoter-luciferase and *Renilla* luciferase constructs before treatment for 24 hours with increasing concentrations of sunset yellow. Luciferase activity was assessed by dual luciferase reporter assay and expressed relative to *Renilla* luciferase. (Mean and SD of n=3). * Denotes significant difference from lowest treatment concentration (p<0.05) (Tukey post hoc analysis)

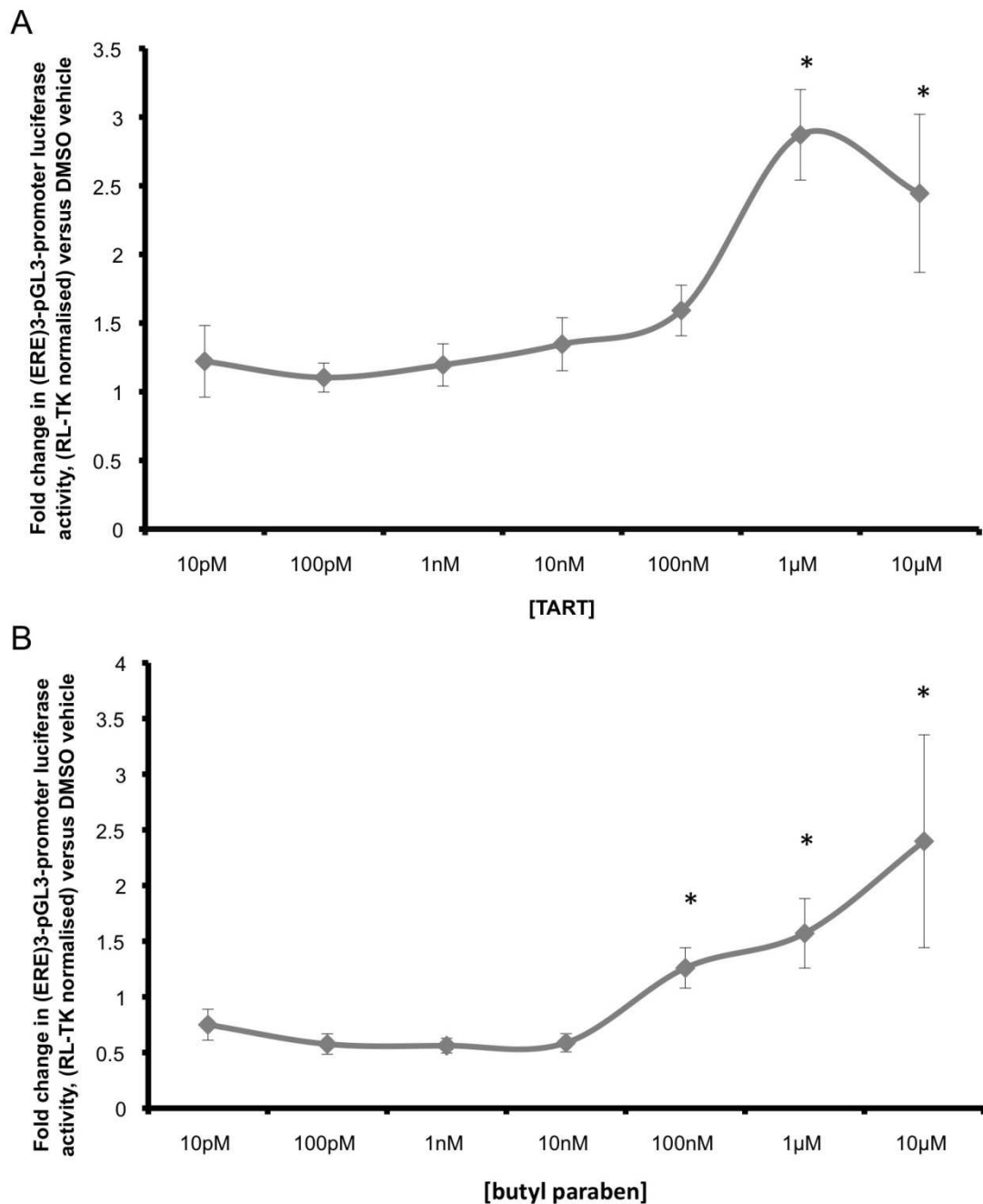


Figure 3.11 - Dose response studies of xenoestrogen activity. A. Tartrazine. MCF-7 cells were transiently transfected with (ERE)₃-pGL3-promoter-luciferase and *Renilla* luciferase constructs before treatment for 24 hours with increasing concentrations of Tartrazine. Luciferase activity was assessed by dual luciferase reporter assay and expressed relative to *Renilla* luciferase. (Mean and SD of n=3). * Denotes significant difference from lowest treatment concentration (p<0.05) (Tukey post hoc analysis) **B. Butyl paraben.** MCF-7 cells were transiently transfected with (ERE)₃-pGL3-promoter-luciferase and *Renilla* luciferase constructs before treatment for 24 hours with increasing concentrations of butyl paraben. Luciferase activity was assessed by dual luciferase reporter assay and expressed relative to *Renilla* luciferase. (Mean and SD of n=3). * Denotes significant difference from lowest treatment concentration (p<0.05) (Tukey post hoc analysis)

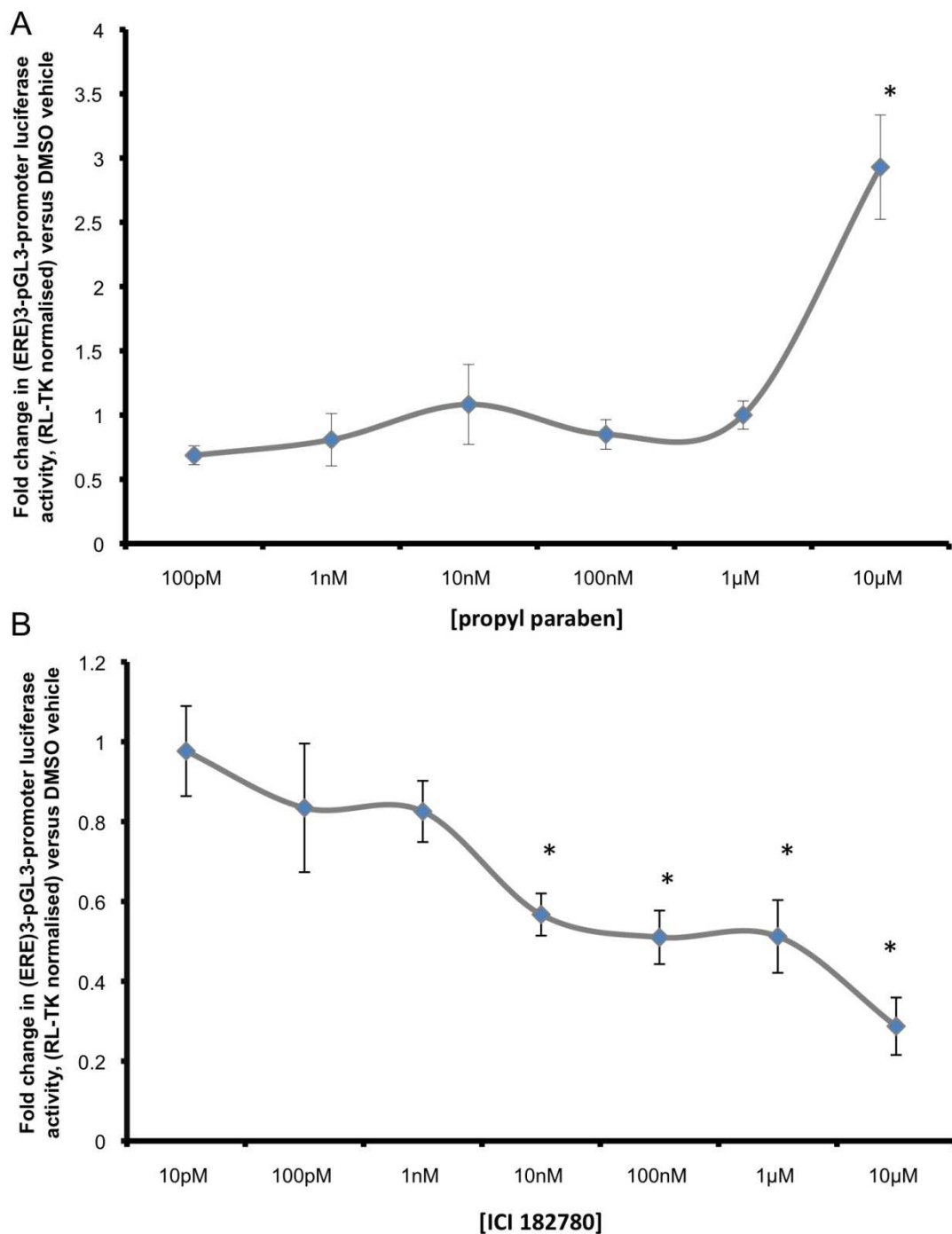


Figure 3.12 - Dose response studies of xenoestrogen activity. A. Propyl paraben. MCF-7 cells were transiently transfected with (ERE)₃-pGL3-promoter-luciferase and *Renilla luciferase* constructs before treatment for 24 hours with increasing concentrations of propyl paraben. Luciferase activity was assessed by dual luciferase reporter assay and expressed relative to *Renilla luciferase*. (Mean and SD of n=3) * Denotes significant difference from lowest treatment concentration (p<0.05) (Tukey post hoc analysis)**B. ICI 182780.** MCF-7 cells were transiently transfected with (ERE)₃-pGL3-promoter-luciferase and *Renilla luciferase* constructs before treatment for 24 hours with increasing concentrations of ICI182780. Luciferase activity was assessed by dual luciferase reporter assay and expressed relative to *Renilla luciferase*. (Mean and SD of n=3). * Denotes significant difference from lowest treatment concentration (p<0.05) (Tukey post hoc analysis)

ER effectors	EC _{50%} [*] (+/- SEM) (nM)
E2	5.3 ± 1.27
Tartrazine	160 ± 39.2
Sunset yellow	220 ± 87.3
Butyl paraben	620 ± 138
Propyl paraben	5000 ± 3570
	IC _{50%} [†] (+/- SEM) (nM)
IC182780	4.7 ± 0.465

Table 3.1 – Xenoestrogen EC50 values. Calculated EC₅₀/IC₅₀ values from dose response experiments, figs 3.10, 3.11, 3.12.

These data suggest that the food and cosmetic colouring agents tartrazine and sunset yellow are in the region of 50 times less effective at activating the human ER than E2, whilst the parabens and methoxychlor were less potent still. This implies that a much higher concentration or level of exposure to these compounds would be required to produce a similar level of transcriptional activity to that of E2.

3.2.4. Screening for transcriptional estrogenic activity by measurement of TFF1 expression in MCF-7 cells

The effects upon ER mediated transcription observed by dual luciferase assay were confirmed using an alternative measurement of estrogenic activity in the same cell line. The relative induction in expression of TFF1 mRNA in MCF-7 cells was measured (as described in the previous chapter) in response to treatment with the xenoestrogens which were identified through their effects upon 3xERE-pGL3 reporter activity. The investigation was again conducted +/- ICI182780 pre-treatment. In this assay the same compounds which had induced 3xERE-pGL3 reporter gene activity also significantly increased the level of TFF1 transcription over that of the vehicle control. The action of the ER antagonist ICI182780 was also parallel to the previous investigation, inhibiting increased TFF1 expression in a similar manner (Fig 3.13).

The effects of high concentrations (10 μ M) of certain steroid hormones namely progesterone, testosterone and other forms of estrogen were concordant with the findings of the dual luciferase reporter assay screen. 10 μ M concentrations of both testosterone and progesterone significantly increased TFF1 mRNA expression over vehicle controls. Equally pre treatment with ICI182780 did not significantly reduce the TFF1 gene induction caused by administration of high concentration of the estrogen analogues estrone, ethinyl estradiol and estriol.

As before, the investigation was repeated at a more physiologically realistic concentration of 10nM, Fig 3.14 details the findings of this study. In line with the

data obtained by luciferase reporter assay, only estrogens increased TFF1 mRNA expression at 10nM concentrations, and in all cases TFF1 induction was inhibited by pre treatment with ICI182780.

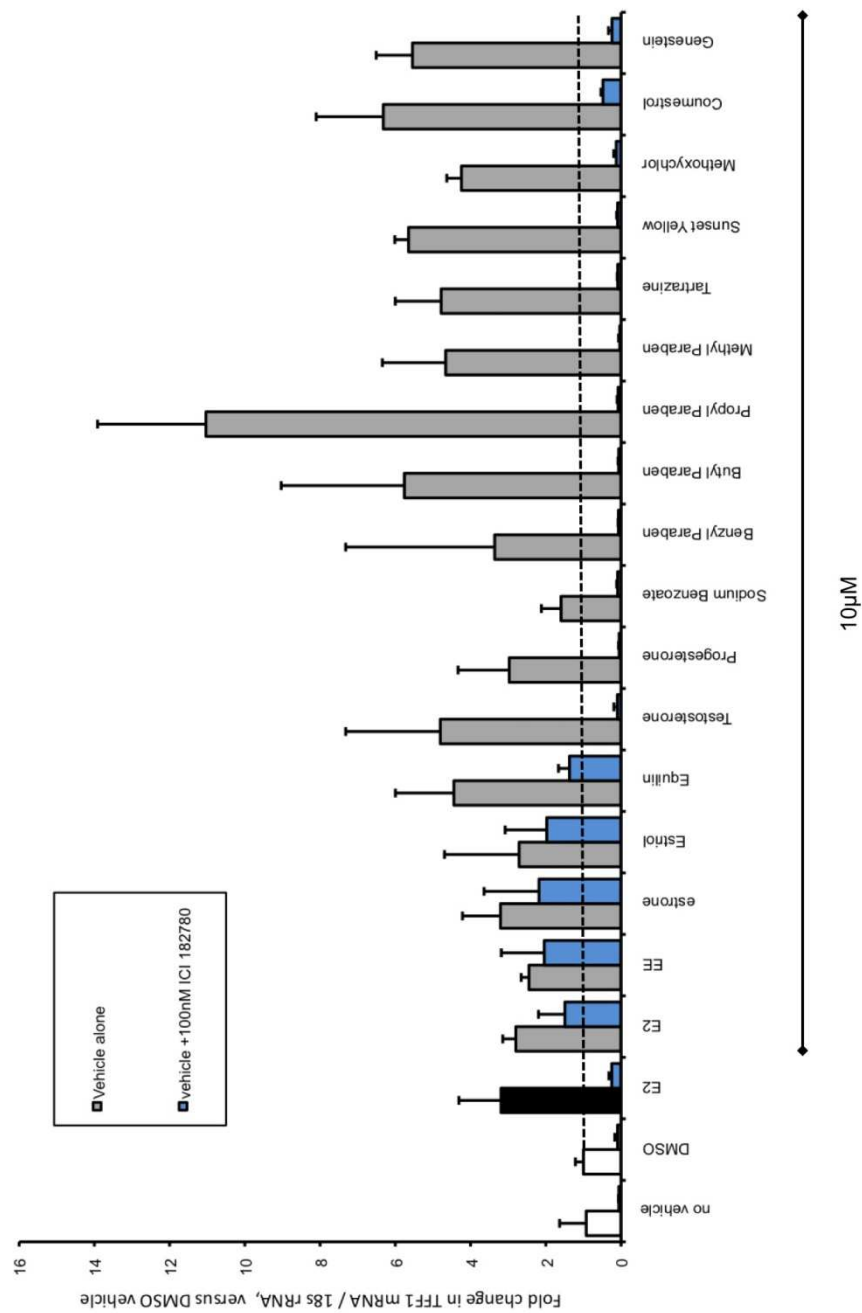


Figure 3.13 – Xenoestrogen mediated TFF1 induction. Expression of TFF1 in MCF-7 cells was quantified by SYBR Green qRT-PCR following treatment for 24 hours with 10nM E2, 10µM xenobiotics or DMSO vehicle (+/- pre-treatment with 100nM ICI182790) before analysis of TFF1 transcript levels by SYBR Green qRT-PCR *= significant increase over DMSO vehicle control group (p<0.05) (Students t-test, two tailed) Data are mean and SD of n=3.

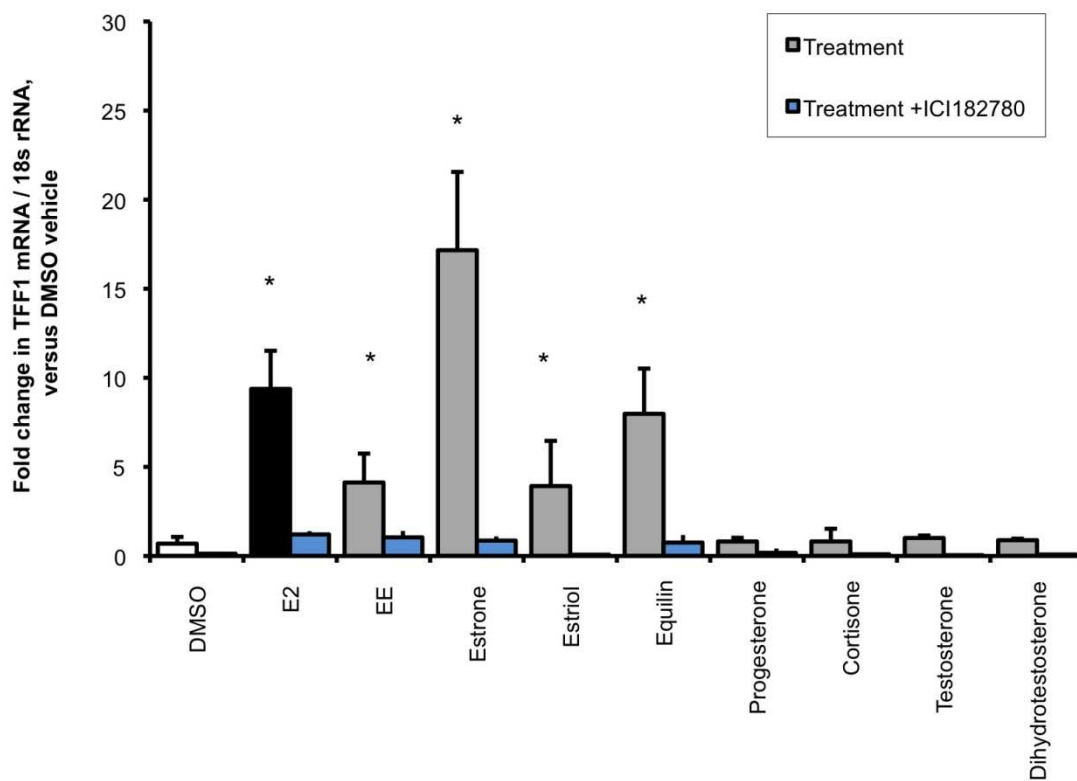


Figure 3.14 – Expression of TFF1 following treatment with 10nM steroid hormones. Expression of TFF1 in MCF-7 cells was quantified by SYBR Green qRT-PCR following treatment for 24 hours with increasing 10nM concentration of various steroid hormones or DMSO vehicle (+/- pre-treatment with 100nM ICI182790). TFF1 transcript levels were quantified by SYBR Green qRT-PCR. * = significant increase over DMSO vehicle control group ($p < 0.05$) (Students t-test, two tailed) Data are mean and SD of $n=3$.

3.2.5. Screening for transcriptional xenoestrogenic activity in primary rat hepatocytes by dual luciferase reporter assay.

Since we are interested in the potential estrogenic effects of xenobiotics on the liver the estrogenic activity of a range of xenobiotics was examined in cultures of primary rat hepatocytes.

Expression of both ER α and ER β mRNA was examined by RT-PCR. ER α transcript was detectable in whole liver (very low expression) and in hepatocytes at t=0, 48 and 72 hours. ER α was detected in quiescent and activated hepatic stellate cell cultures and also in the pancreatic progenitor cell line b13 in both its normal state and in its hepatocyte like phenotype termed b13/h¹⁰⁴. ER β mRNA was detected in all of the samples, with the exception of activated hepatic stellate cells. These results were confirmed by Western blotting. (Fig3.15)

Compounds were chosen as before, based on their presence in products or specific localized environments that have been linked to PBC through previous epidemiological studies. Individual or groups of compounds which were inhibitory in the MCF-7 model were omitted from this process.

Cultures of primary rat hepatocytes were transfected with 3xERE-luciferase reporter construct as previously described and treated with 10 μ M concentration of the chosen compounds for a period of 24 hours. The luciferase activity was

normalised to *Renilla* luciferase and expressed as a percentage of DMSO vehicle control, the results are shown in fig 3.16.

In rat hepatocytes neither 10nM or 10µM E2 significantly increased ER mediated luciferase activity over DMSO vehicle. In contrast ethinyl estradiol (EE) significantly increased luciferase activity in this assay. Of the xenobiotics examined, methyl, propyl and benzyl paraben, sodium benzoate, sunset yellow, and tartrazine all tested positive for increased ER mediated transcriptional luciferase activity. In addition genistein, a known phytoestrogen increased ER mediated transcriptional luciferase activity over the control group.

2-octynoic acid, a common cosmetic and food additive did not cause any increase in luciferase activity, nor did any other structurally similar compounds.

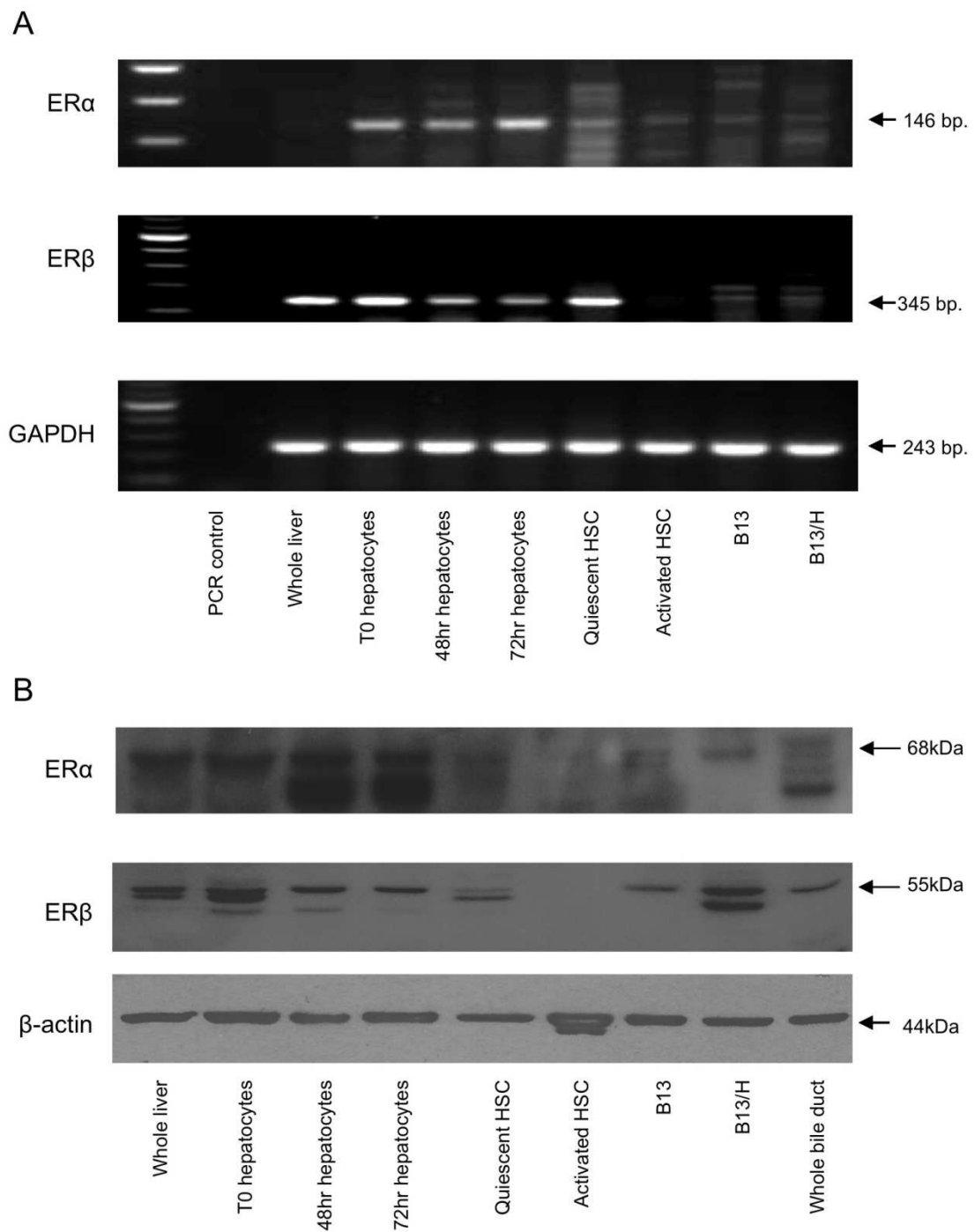


Figure 3.15 – Expression of the rat ER. A. Confirmation of the expression of the ER in rat liver cells by RT-PCR. Cells were cultured under normal conditions before isolation of RNA and RT-PCR using primers specific for the rat ER. PCR products were visualised by agarose gel electrophoresis and UV transillumination **B. Confirmation of the expression of the ER in rat liver cells by Western blot.** Cells were cultured under normal conditions days before isolation of total protein and analysis by Western blot as described in materials and methods. 25 μ g of total protein/lane.

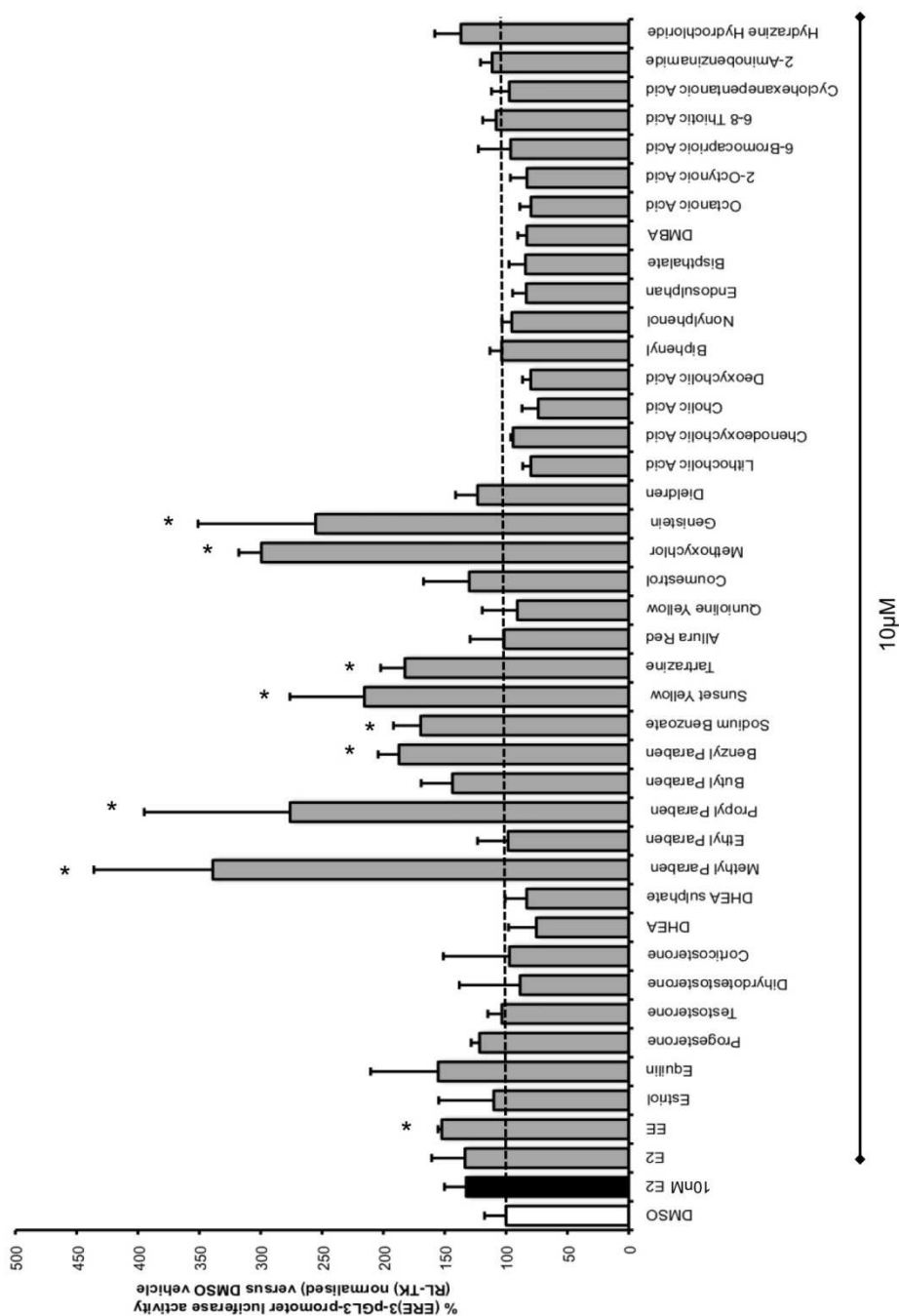


Figure 3.16 –Xenoestrogen screening in primary rat hepatocytes. Primary rat hepatocytes were transiently transfected with (ERE)₃-pGL3-promoter-luciferase and *Renilla* constructs before treatment for 24 hours with 10nM E2 or 10μM of a selected xenobiotic. Luciferase activity was assessed by dual luciferase reporter assay and expressed relative to *Renilla* luciferase. (Mean and SD of n=3). *= Significantly different (p<0.05) to DMSO control group (Students t-test, two tailed).

3.2.6. (ERE)₃-pGL3-Promoter is responsive to both ER α and ER β .

Since there are two different known ER genes, ER α and ER β , 2 ER null cell lines, MDA and the human cholangiocyte cell line H69, were used to establish whether (ERE)₃pGL3-Promoter is responsive to both ER types.

Cultures of MDA cells were transfected with a plasmid directing the expression of human ER α , along with (ERE)₃-pGL3-promoter and RL-TK before treatment with previously identified xenoestrogens. Fig 3.17A shows that treatment with both tartrazine and methoxychlor caused a significant increase in ER α mediated luciferase expression. Sunset yellow did not cause a change in ER α transcriptional activity in this model. In all cases pre treatment with the estrogen receptor antagonist ICI 182780 resulted in a significant decrease in ERE-luciferase activity.

A parallel investigation was performed, replacing the ER α expression vector with one coding for ER β . In this study, both sunset yellow and tartrazine caused a significant increase in reporter gene activity, similar to that of 10nM E2. Again, in all cases this activity was attenuated by administration of ICI 182780. Fig 3.17B

The H69 cell line is a stabilised human cholangiocyte cell line that does not express either a functional ER α or ER β . This cell line was transfected with plasmids directing either ER α or ER β , in a similar investigation to the previous study performed using the MDA model. Fig 3.18 demonstrates that in the H69

cell line 10nM E2 caused a significant increase in reporter gene expression, through activation of both ER α and ER β . Treatment with 10 μ M tartrazine also activated both estrogen receptor variants, but showed a much greater affinity for ER β subtype. Concordant with the findings in the MDA cell model, sunset yellow did not activate ER α in H69, but did significantly increase ER β mediated reporter gene activity, albeit with seeming low potency in comparison to E2 and tartrazine.

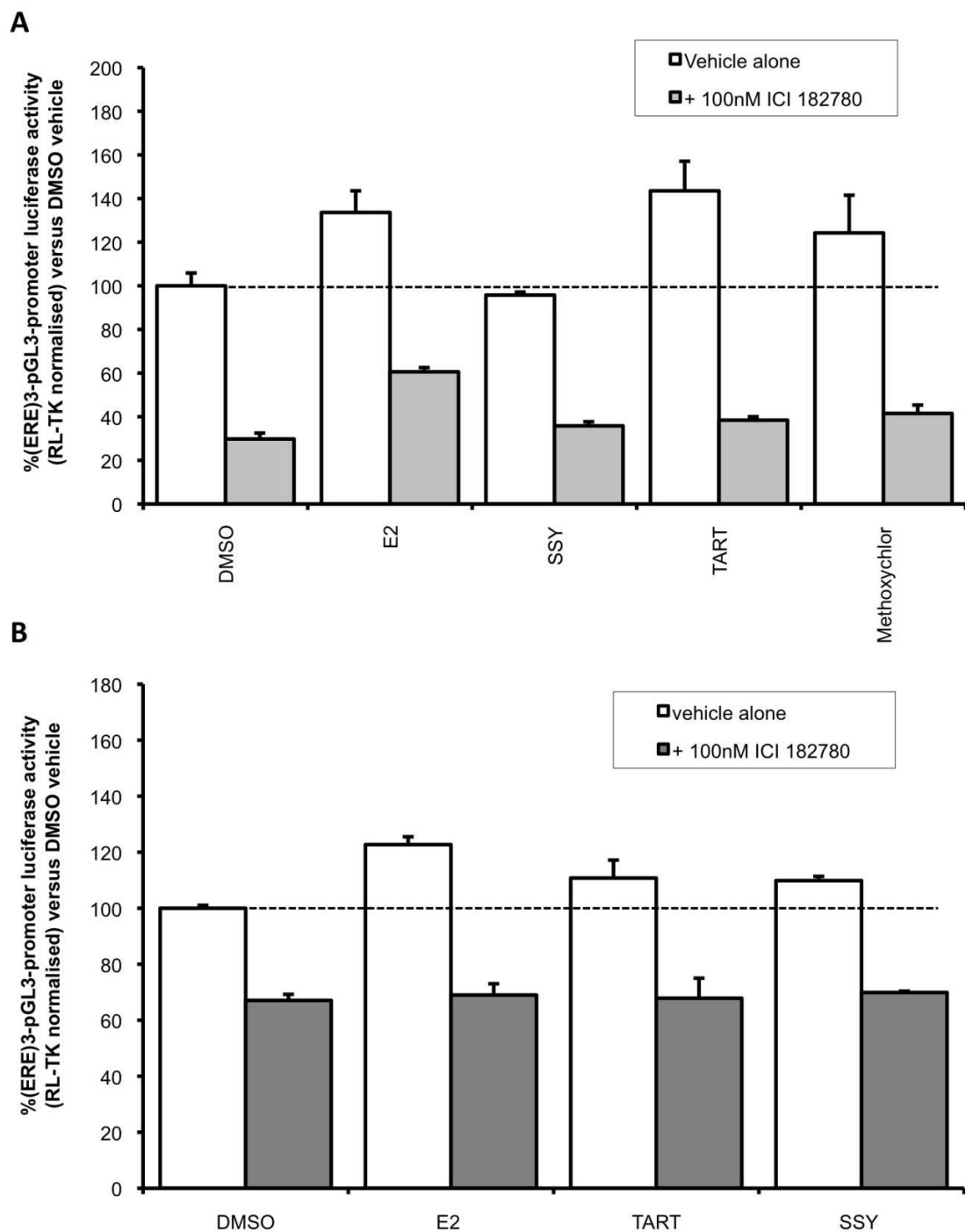


Figure 3.17 – Ectopic expression and activation of the hER in MDA cells . A. ER α . Non estrogen responsive MDA cells were transiently transfected with a plasmid coding for **A. ER α** or **B. ER β** , (ERE)₃-pGL3-promoter-luciferase and *Renilla* constructs before treatment for 24 hours with 10nM E2 or 10 μ M selected xenobiotic (+/- 100nM ICI182780). Luciferase activity was assessed by dual luciferase reporter assay and expressed relative to *Renilla* luciferase. (Mean and SD of n=3). *= Significantly different to DMSO control group, **=significantly decrease over no antagonist group (p<0.05) (Students t-test, two tailed).

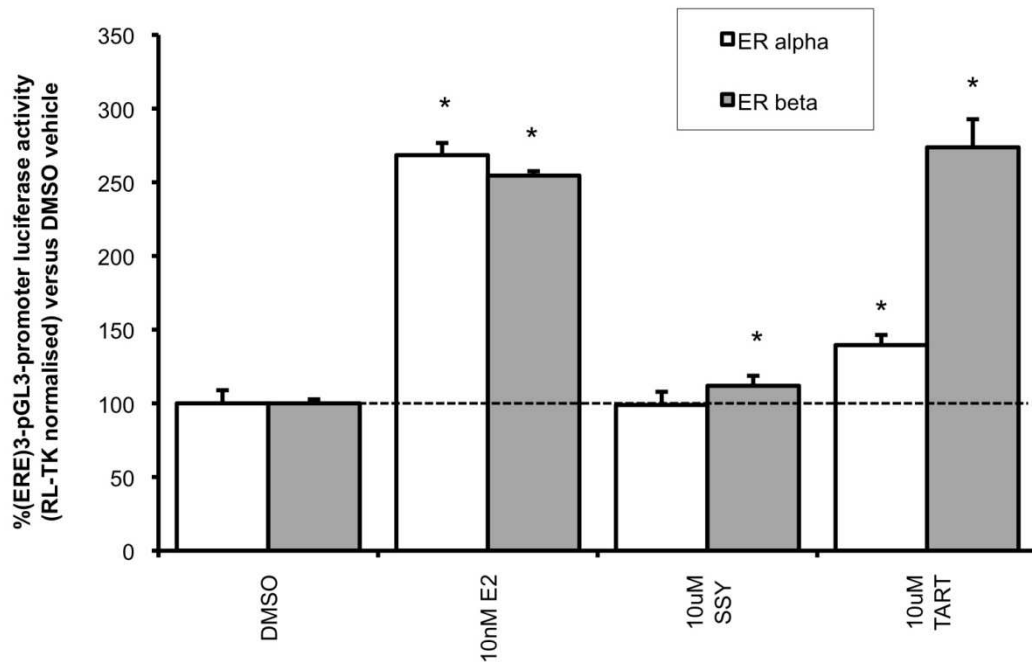


Figure 3.18 – Ectopic expression and activation of the hER in H69 cells . Non estrogen responsive H69 cells were transiently transfected with a plasmid coding for ER α or ER β , (ERE)₃-pGL3-promoter-luciferase construct and *Renilla* before treatment for 24 hours with 10nM E2 or 10 μ M selected xenobiotic. Luciferase activity was assessed by dual luciferase reporter assay and expressed relative to *Renilla* luciferase. (Mean and SD of n=3). *= Significantly different (p<0.05) to DMSO control group (Students t-test, two tailed).

3.2.7. Chapter 3.2 discussion

The specific aim of this series of investigations was to confirm that identified xenobiotics have transcriptional estrogenic activity. Compounds were initially screened for estrogenic activity utilizing the luciferase reporter assay developed in chapter 3.1 and by measuring TFF1 mRNA expression in the estrogen responsive breast carcinoma cell line MCF-7. Using these methods a variety of xenoestrogens were identified, most notably butyl paraben, propyl paraben, sunset yellow and tartrazine.

When this assay system was applied to primary rat hepatocytes the results were similar to those in the MCF-7 model, there were however, a few prominent differences. In hepatocytes E2 did not significantly increase activity, possibly due to the metabolic activity of hepatocytes rapidly deactivating E2. This is supported by the increase in luciferase reporter activity following treatment with EE, an estrogen variant which is known to be more resistant to hepatic metabolism^{85, 86}. Similarly, some forms of the group of parabens compounds which were active in MCF-7 were not active in hepatocyte cultures and vice versa.

3.3. Effect of xenoestrogen exposure on mitochondrial function and polarisation

The potential for a xenoestrogen exposure to be a initiating or risk factor for the development of PBC may be dependant upon it also being toxic to liver cells, potentially via interaction with mitochondria. This may be either through conjugation to PDC enzyme subunits or through another mechanism(s). These effects may result in loss of mitochondrial function or polarisation and development of AMA.

This chapter describes the ways in which previously identified xenoestrogens were screened for mitochondrial toxicity.

3.3.1. Mitochondrial reductase activity in primary rat hepatocytes in response to xenoestrogen exposure.

Cultures of primary rat hepatocytes were treated for 24 hours with a range of compounds which were selected based on their estrogenic activity identified in the previous chapter. Figure 3.19 shows that at a concentration of 10 μ M, none of the xenoestrogenic compounds selected caused a significant decrease in mitochondrial reductase enzyme activity. In contrast, the vitamin K precursor, menadione, known for its effects on mitochondrial function and polarisation through interference with mitochondrial Calcium homeostasis¹⁰⁵, significantly decreased MTS reduction in rat hepatocytes at a final treatment concentration of 200 μ M. Treatment with both 10 μ M E2 and EE resulted in a significant increase in mitochondrial reductase activity over DMSO vehicle group.

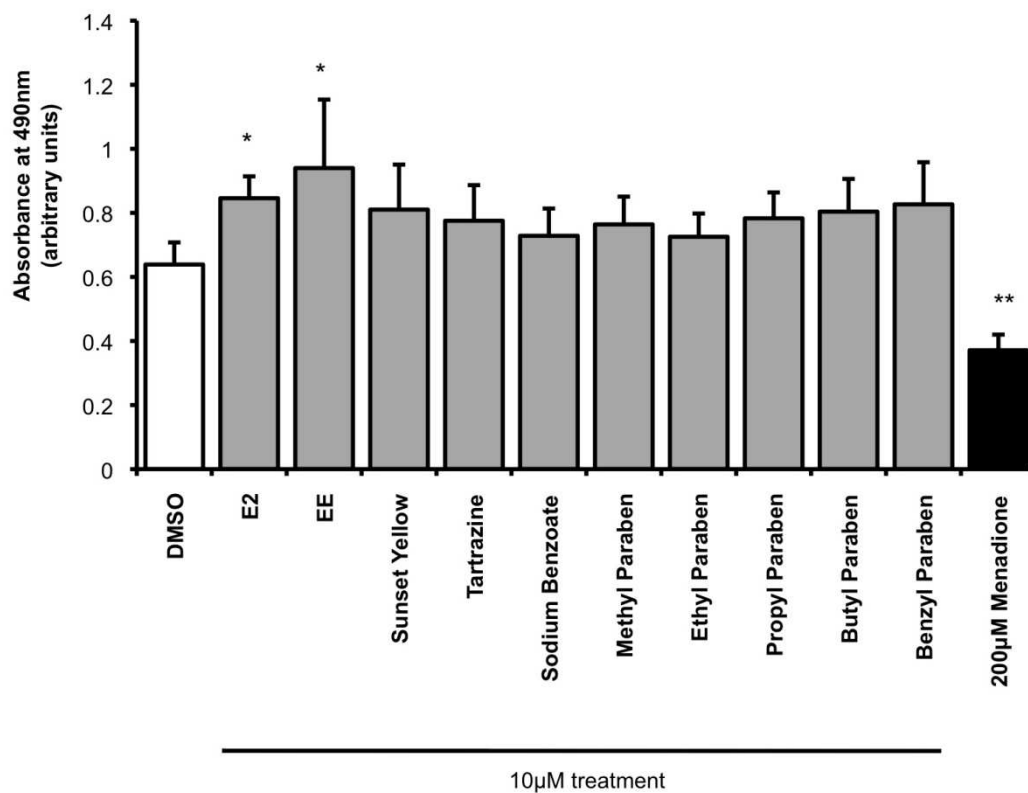


Figure 3.19 –MTS activity in primary rat hepatocytes following xenoestrogen exposure
 Cultures of primary rat hepatocytes were treated for 24 hours with selected compounds at a concentration of 10µM or 200µM menadione as a positive control .Mitochondrial reductase activity was assessed by MTS assay (Mean and SD of n=8). *= Significant increase, **=significant decrease, over DMSO control. (p<0.05) (Students t-test, two tailed).

Menadione is commonly used to model mitochondrial depolarisation at a final treatment concentration of 200 μ M, it is possible that high concentrations of xenobiotics may be required to produce similar effects in an *in vitro* model. To investigate this, dose-studies were performed for the food and cosmetic colouring agents tartrazine and sunset yellow.

Fig 3.20 shows that after 24 hours treatment, reduction of MTS by mitochondrial reductase enzymes in primary rat hepatocytes was significantly decreased by sunset yellow at concentrations of 1mM and 100 μ M, suggesting that under these conditions the concentration of sunset yellow required to produce a negative effect on mitochondrial reductase activity lies between 100 and 10 μ M. After 48 hours treatment, 1mM sunset yellow resulted in a significant decrease in mitochondrial reductase function, suggesting that there is either a degree of recovery from the sunset yellow insult, or that the metabolic activity of primary hepatocytes results in breakdown and detoxification of the sunset yellow compound.

The MTS reduction by primary rat hepatocytes treated with varying concentrations of tartrazine after 48 hours is shown in Fig 3.21. In this investigation, none of the treatment concentrations of tartrazine resulted in any significant decrease in MTS reduction, relative to DMSO vehicle control.

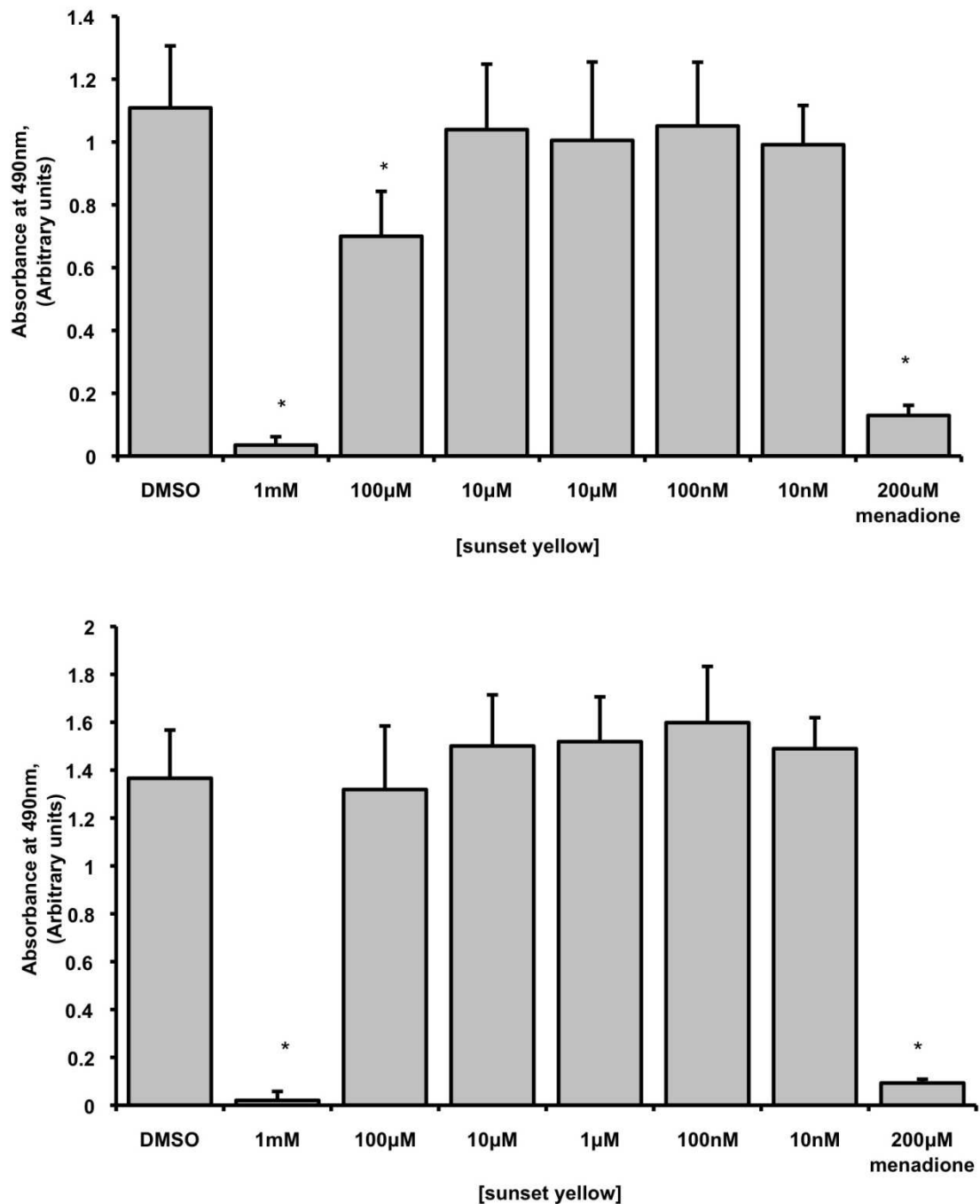


Figure 3.20 –Dose response study of MTS reduction in primary rat hepatocytes treated with sunset yellow **A.** Cultures of primary rat hepatocytes were treated for 24 hours with increasing concentrations of sunset yellow or 200µM menadione as a positive control. Mitochondrial reductase activity was assessed by MTS assay (Mean and SD of n=12). *= Significantly different to DMSO control. (p<0.05) (Students t-test, two tailed). **B.** Cultures of primary rat hepatocytes were treated for 48 hours with increasing concentrations of sunset yellow or 200µM menadione as a positive control. Mitochondrial reductase activity was assessed by MTS assay (Mean and SD of n=12). *= Significantly different to DMSO control. (p<0.05) (Students t-test, two tailed).

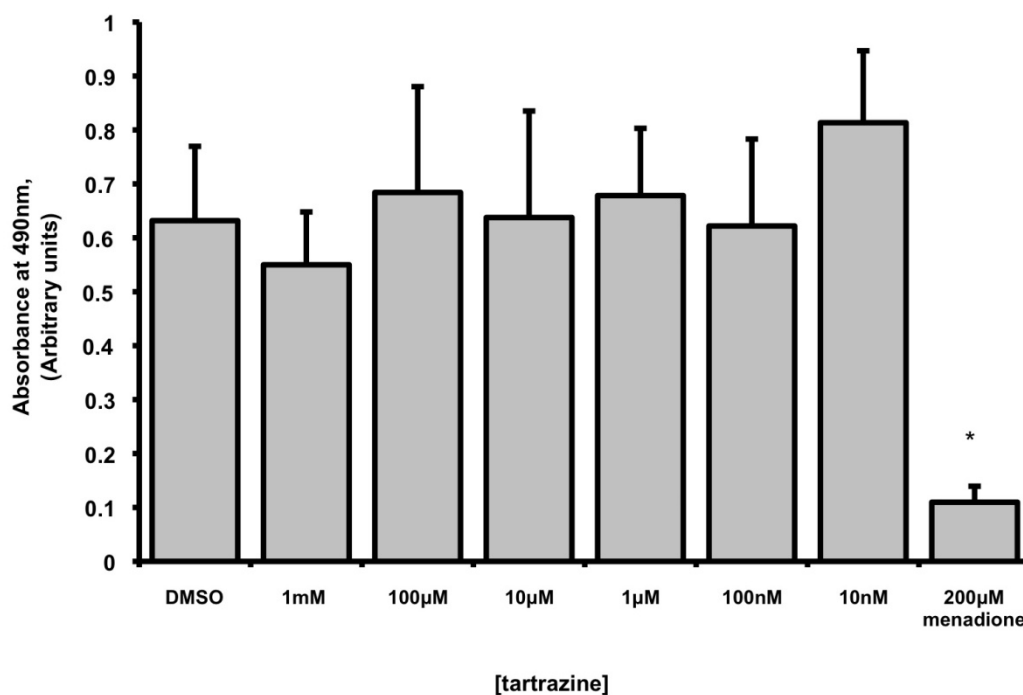


Figure 3.21 –Dose response study of MTS reduction in primary rat hepatocytes treated with tartrazine. Cultures of primary rat hepatocytes were treated for 24 hours with increasing concentrations of tartrazine or 200µM menadione as a positive control. Mitochondrial reductase activity was assessed by MTS assay. (Mean and SD of n=12). *= Significantly different to DMSO control. ($p < 0.05$) (Students t-test, two tailed).

In an attempt to identify the mechanism by which sunset yellow causes loss of mitochondrial reductase enzyme activity in rat hepatocytes. Cultures of primary hepatocytes were treated with 200 μ M sunset yellow, alongside a variety of different compounds which are known to influence mitochondrial functionality and also a selection of caspase inhibitors.

Fig 3.22 demonstrates that 200 μ M sunset yellow results in a significant decrease in MTS reduction in primary rat hepatocytes as described previously. Treatment of hepatocytes with 2 μ M bongkrelic acid also resulted in a reduction in MTS reduction. Administration of caspase 3, 4 and 9 inhibitors all resulted in a significant increase in MTS reduction over DMSO vehicle control. This may be a result of increased viability of deteriorating primary hepatocyte cultures by inhibition of apoptosis by selected caspase inhibitors.

Co-treatment of hepatocyte cultures with 200 μ M sunset yellow 1 μ M and the reducing agent dithiothreitol (DTT) or bongkrelic acid caused an exacerbation of the effect of treatment with sunset yellow alone. Caspase 3 and 4 inhibitors again caused an increase in MTS reduction, but the positive effect of caspase 9 inhibitor was lost. Treatment of rat hepatocytes with high concentration D-glucose caused a reduction in the loss of mitochondrial reductase activity produced by sunset yellow.

In this investigation a reduction in enzyme activity was observed, it may be that this is caused by a reduction in mitochondrial viability, but it may also be accounted to a reduction in cell number and therefore the number of

mitochondria present, caused by either cell death or reduced proliferation.
Without performing a corresponding protein assay this is difficult to determine.

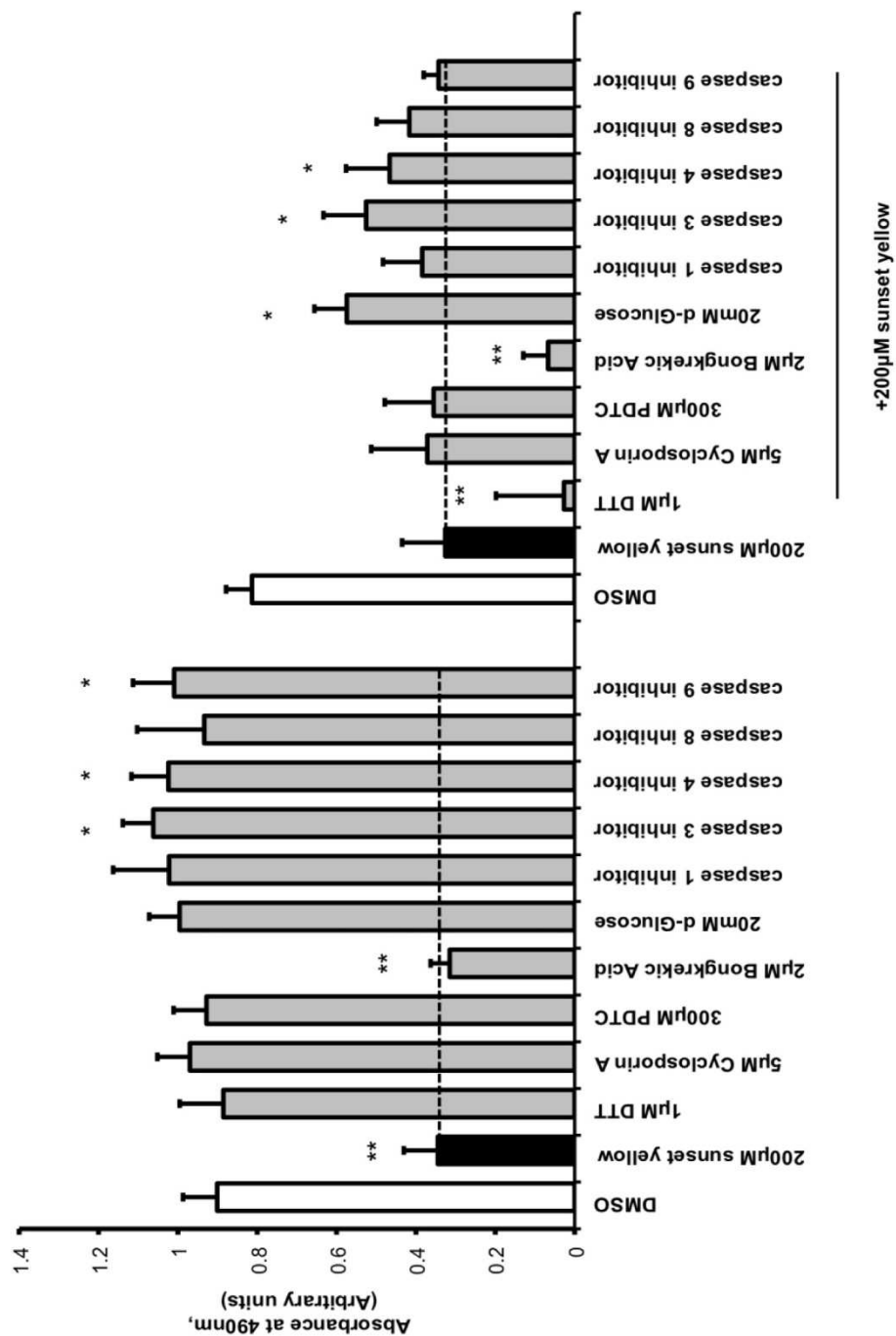


Figure 3.22 – Effects of modulators of mitochondrial function on MTS reduction in primary rat hepatocytes following treatment with sunset yellow. Cultures of primary rat hepatocytes were treated for 24 hours a variety of compounds known to affect mitochondrial function, +/- 200µM sunset yellow. 200µM menadione was used as a positive control Mitochondrial reductase activity was assessed by MTS assay. (Mean and SD of n=8). *= Significantly increase, **=significant decrease over DMSO control (p<0.05) (Students t-test, two tailed).

3.3.2. Measurement of mitochondrial polarisation in rat hepatocytes by live TMRM localisation following exposure to xenoestrogens

Mitochondrial functionality and viability in response to treatment with xenoestrogens was also assed by live imaging of TMRM localisation in primary rat hepatocytes. TMRM is sequestered within mitochondria relative to the potential across the mitochondrial membrane.

Cultures of primary hepatocytes were pre loaded with TMRM before treatment with xenoestrogens or controls. Fig 3.23 details the mean intensity of fluorescence at the emission wavelength of TMRM (574nm) per field of view, following treatment. Intensity of fluorescence was measured at 40 time points of 15-minute intervals. It shows that some compounds, sodium benzoate, tartrazine and sunset yellow cause a loss of mitochondrial membrane potential, similar to the effect of menadione.

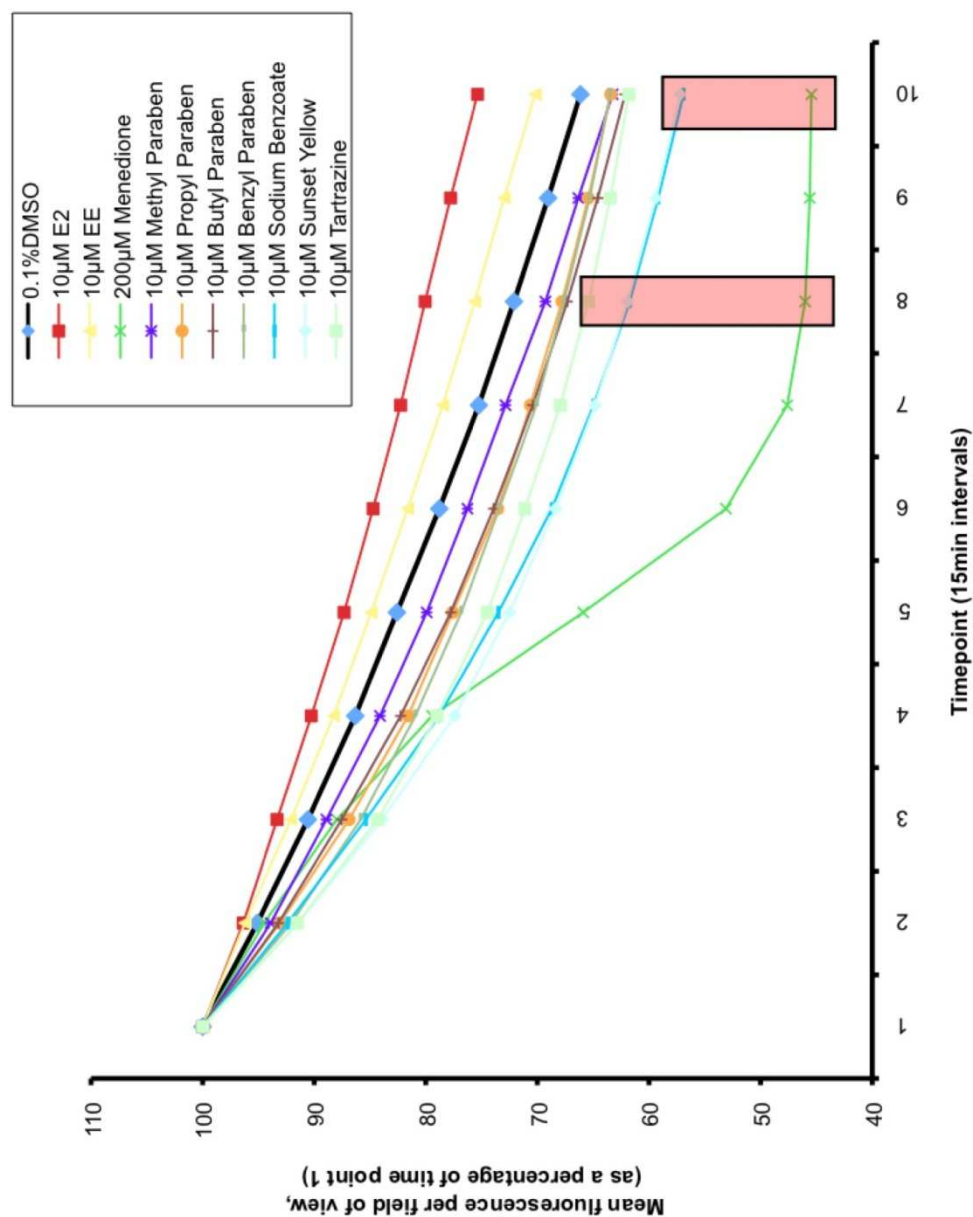


Figure 3.23 –TMRM intensity in primary rat hepatocytes following treatment with xenobiotics. Cultures of primary rat hepatocytes were loaded with 250µM TMRM before treatment with 10µM xenoestrogens or 200µM menadione as a positive control. Mean fluorescence was assessed by imaging on the Attovision Pathway (BD Biosciences) every 15min. Measurement of mean intensity per field of view was performed using Velocity image analysis software. (Mean and SD of n=8). Red box = significant decrease in intensity from DMSO control ($p < 0.05$) (Students t-test, two tailed).

3.3.3. Chapter 3.3 discussion.

The aim of this section was to identify which, if any, of the previously discovered xenoestrogens have an effect on hepatocyte mitochondrial function, viability or polarisation. Compounds were screened by both MTS assay as a measure of mitochondrial reductase enzyme functionality, and by live imaging of TMRM localisation to measure mitochondrial membrane potential.

The MTS assay revealed that treatment with sunset yellow caused a decrease in mitochondrial reductase activity in primary rat hepatocytes. This effect of sunset yellow was exaggerated upon administration of DTT and decreased by treatment with high concentration D-glucose. This may imply that the effects of sunset yellow are upon, or intrinsically linked, with components of the electron transport chain or another aspect of mitochondrial energetics. It may also suggest that either sunset yellow is a more potent mitochondrial toxin upon being reduced by DTT. Sunset yellow is known to be susceptible to reduction, and its major route of metabolism is reduction via intestinal bacteria, an action which is known to be inhibited by high glucose concentrations^{106, 107}

The screening system developed to measure changes in mitochondrial polarisation by imaging of TMRM localisation revealed that sodium benzoate, tartrazine and sunset yellow all caused a reduction in membrane potential after 2 hours of treatment.

These results intimate that the food and cosmetic additives sunset yellow and tartrazine, both of which were also shown to activate the human estrogen receptor, may have damaging effects on mitochondrial function. However, without performing corresponding assays to determine cell number, it is not possible to say whether these effects may be attributed to loss of cell viability or reduced proliferation following treatment.

3.4. *in vivo* exposure to xenoestrogens

The effects of exposure to estrogen, and xenoestrogens identified in the previous chapters, upon the liver were investigated using a variety of *in vivo* models.

The effect of estrogen exposure upon liver has previously been documented; it is known that administration of estrogen to the mouse results in a cholestatic condition, and altered expression of bile salt transport proteins, the two factors possibly being intrinsically linked¹⁰⁸.

The aims of this component of the project were to investigate further these effects of estrogen, and compare them to the effects of the xenoestrogens identified through the screening process described in chapters 3.2 and 3.3.

A further aim was to determine whether treatment with any of these compounds could produce a response which would indicate that it had the potential to be an initiating factor in the development of PBC.

3.4.1. Expression of estrogen receptors *in vivo*

The expression of ER α and ER β in the mouse were studied by RT-PCR. Tissue samples from both male and female C57Bl/6 mice were analysed using primers specific for either estrogen receptor isoform using standard RT-PCR protocols. Fig 3.24A shows that ER α was detectable in female liver, lung, brain and

uterus, and also in male liver, lung, brain and testis. Expression of ER β was confirmed in lung brain and uterus/testis of the animals, but was not detectable in the liver by this method.

3.4.2. Acute exposure to estrogen causes portal tract inflammation in the mouse

As part of a series of pilot studies, the effect of acute exposure to estrogen on portal tract inflammation (PTI) in the mouse was initially examined. Male C57Bl/6 mice were administered either E2, EE or vehicle control by i.p. injection on three consecutive days, following which the degree of portal tract inflammation was assessed and compared to that of a mouse subjected to ligation of the common bile duct (cBDL, a standard model of cholestatic liver disease). Fig 3.24B shows that after treatment with E2 there was a significant increase in PTI over the vehicle control group, similar to that observed following cBDL. Treatment with EE did not result in any significant change in this study.

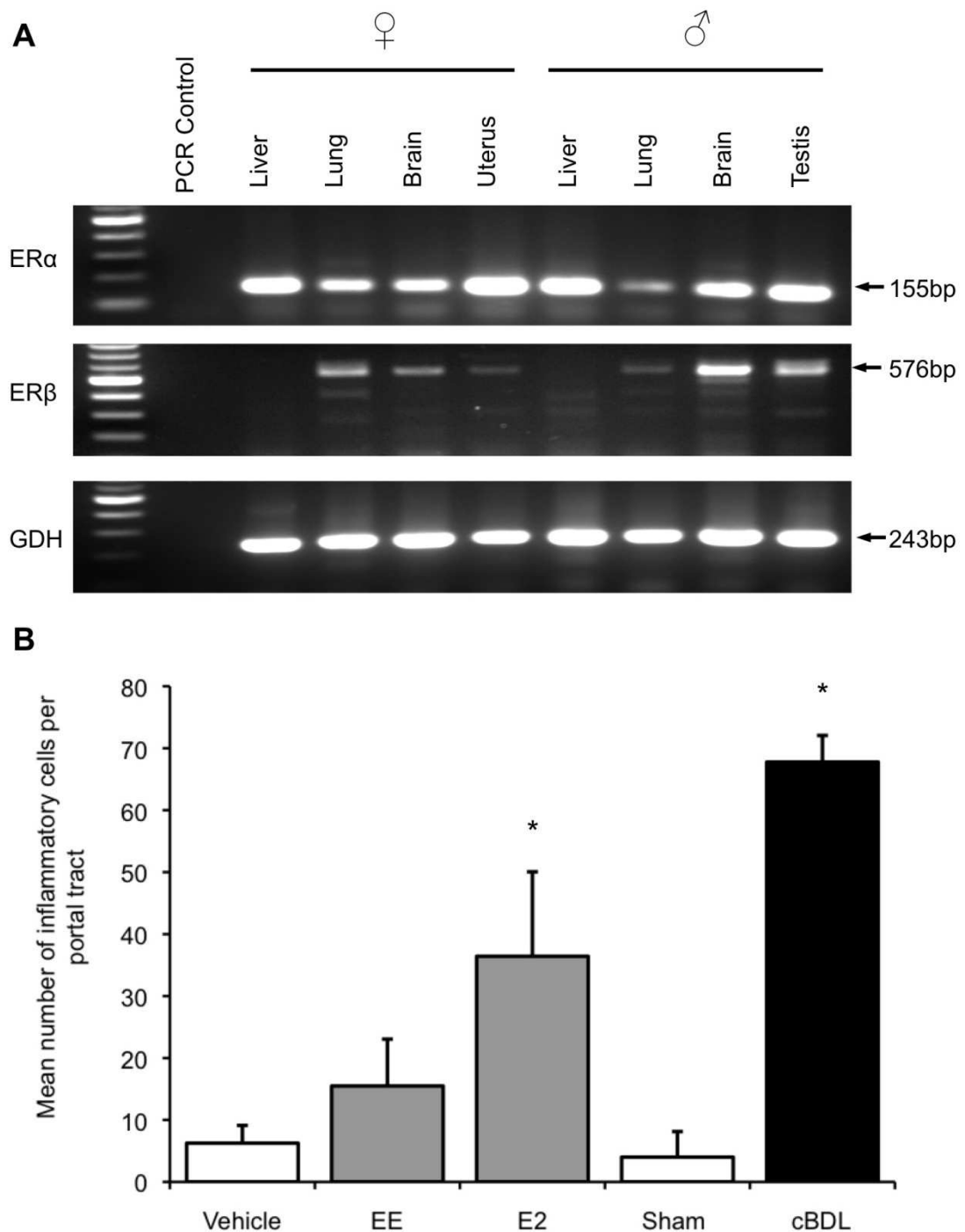


Figure 3.24 – A. Confirmation of the expression of the ER in the mouse by RT-PCR. Organs were harvested from adult male and female C56Bl/6 mice before isolation of RNA and subsequent RT-PCR using primers specific for the mouse ER. PCR products were visualised by agarose gel electrophoresis and UV transillumination **B. Quantification of PTI in the mouse liver following treatment with estrogen.** Adult male C57Bl/6 mice were treated with 0.5mg/kg EE/E2 or vehicle control by single daily *i.p.* injection on 3 consecutive days before termination by schedule I method. Mean number of inflammatory cells per portal tracts were calculated. Animals subjected to cBDL or sham were used as a positive control for cholestatic liver injury. Data are mean and SD of 3 portal tracts per animal, n=4. *= Significant increase in PTI over relevant control ($p < 0.05$) (Students t-test, two tailed).

The expression of the estrogen receptor in the mouse following treatment with E2 was examined by IHC, fig 3.25 shows that ER α is detectable at low levels in the hepatocytes in the normal mouse liver, and following treatment with E2. Positive ER α staining was observed to increase following common bile duct ligation (cBDL), a model for cholestatic liver disease. Whilst ER β was not detectable in the liver by RT-PCR, positive staining for ER β in the cholangiocytes and hepatocyte nuclei was observed in both control and E2 treated animals in a model of acute estrogen exposure, following cBDL the expression of ER β was observed not only in the cholangiocytes but throughout the hepatocytes, Fig 3.26. It is possible that ER β is not detectable by RT-PCR as the expression is very low in the normal or mildly cholestatic mouse liver. This supports work previously documented by Alvaro *et al* who report that ER β was not detectable in the normal human liver but in cholestatic liver conditions such as PBC, ER β expression is up regulated⁹².

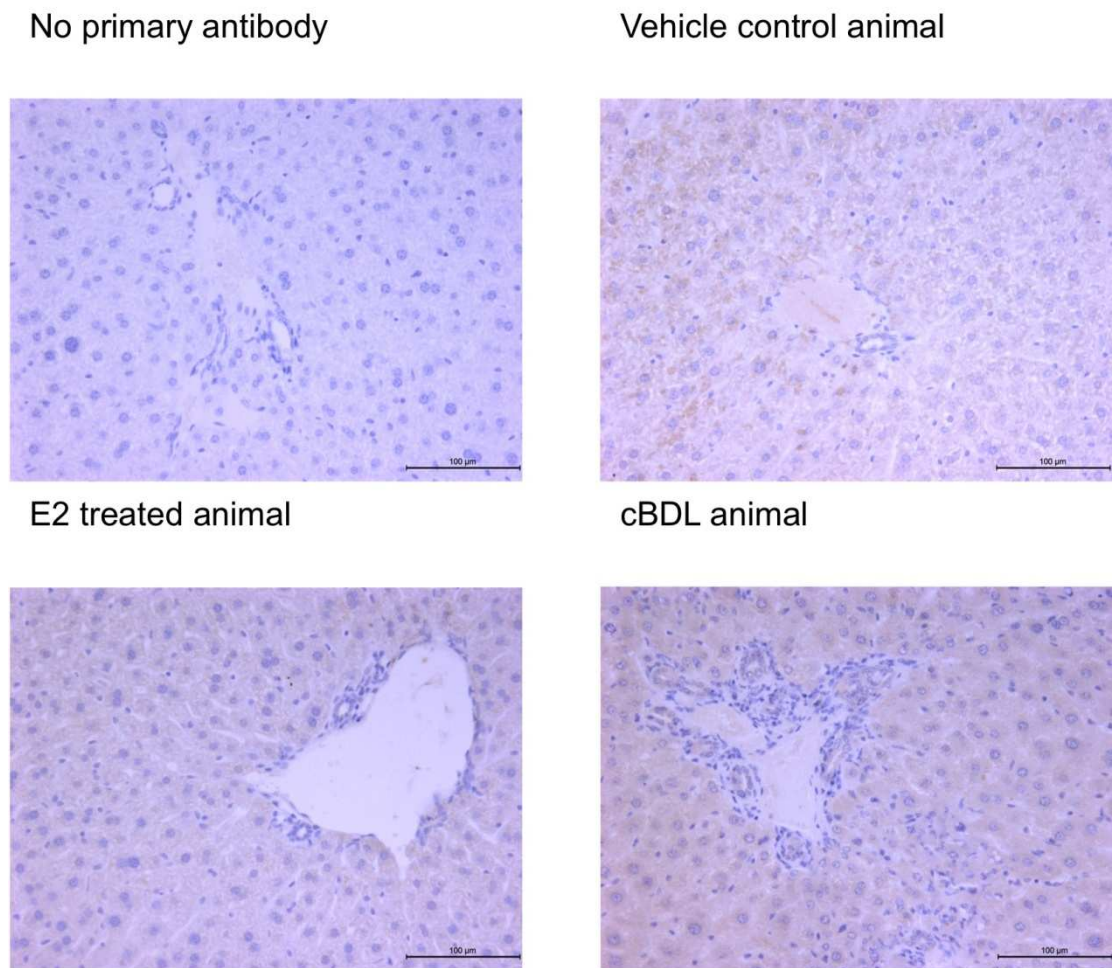


Figure 3.25 –Expression of ER α in the mouse liver by IHC. 5 μ m sections of formalin fixed and paraffin embedded mouse liver were stained with a primary antibody specific for ER α and HRP-conjugated secondary antibody, as described in chapter 2 – materials and methods. Sections were counterstained with haematoxylin. No primary antibody controls were included and stained as outlined, with the substituting ER α primary antibody with antibody diluent.

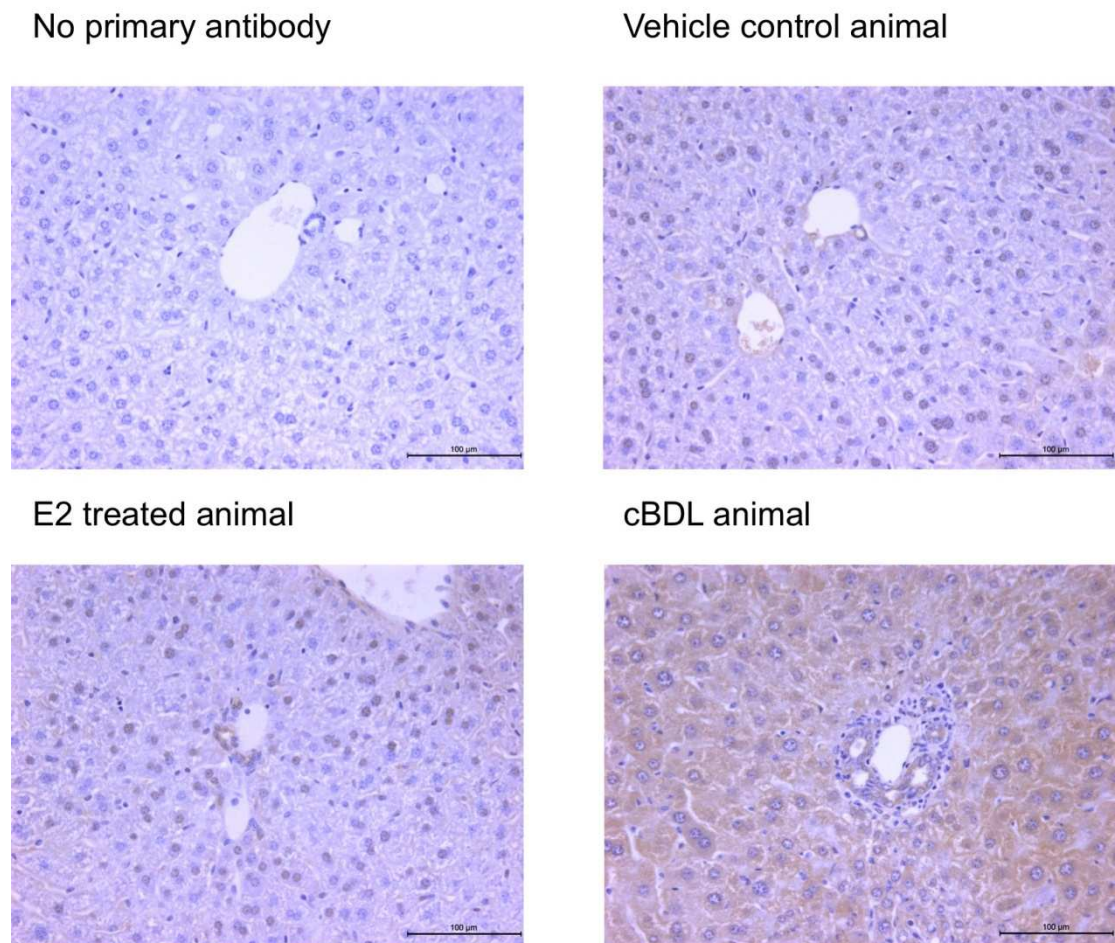


Figure 3.26 – Expression of ER β in the mouse liver by IHC. 5 μ m sections of formalin fixed and paraffin embedded mouse liver were stained with a primary antibody specific for ER β and HRP-conjugated secondary antibody, as described in chapter 2 – materials and methods. Sections were counterstained with haematoxylin. No primary antibody controls were included and stained as outlined, substituting ER β primary antibody with antibody diluent.

3.4.2.1. Inflammatory infiltrate around the portal tract are of a mixed population which contain some NIMP positive cells

The nature of the inflammation seen around the portal tracts in cholestasis is often poorly defined. In an attempt to identify which cell types were present around the portal tracts following acute administration of estrogen, sections of mouse liver were stained by IHC for markers specific for different types of inflammatory cells.

Fig 3.27 is a typical result of staining with an antibody specific for the NIMP antigen, the expression of which is specific to neutrophils. Fig 3.26B shows a cluster of NIMP positive cells in the liver, this is often observed and is possibly a localised immune response, it is used here as a positive control. Fig 3.27C shows a typical portal tract subject to a small amount of inflammatory infiltrate following treatment with E2, some of the inflammatory cells were positive for the NIMP antigen suggesting that neutrophils make up some of the inflammatory cells in E2 induced PTI.

The antigen F4/80 is an extracellular membrane protein found on mature macrophages, Fig 3.28B shows the detection of Kupffer cells, the resident liver macrophage, by F4/80 specific antibody. No F4/80 positive cells were found in the portal tract inflammation of E2 treated mice, Fig 3.28C.

CD3 refers to cluster of differentiation complex; it is a group of peptides that form part of the T-cell receptor complex found on mature T-lymphocytes. Fig

3.29B shows the detection of CD3 positive cells in the mouse thymus. No CD3 positive cells were found in the PTI of E2 treated animals, Fig 3.29C.

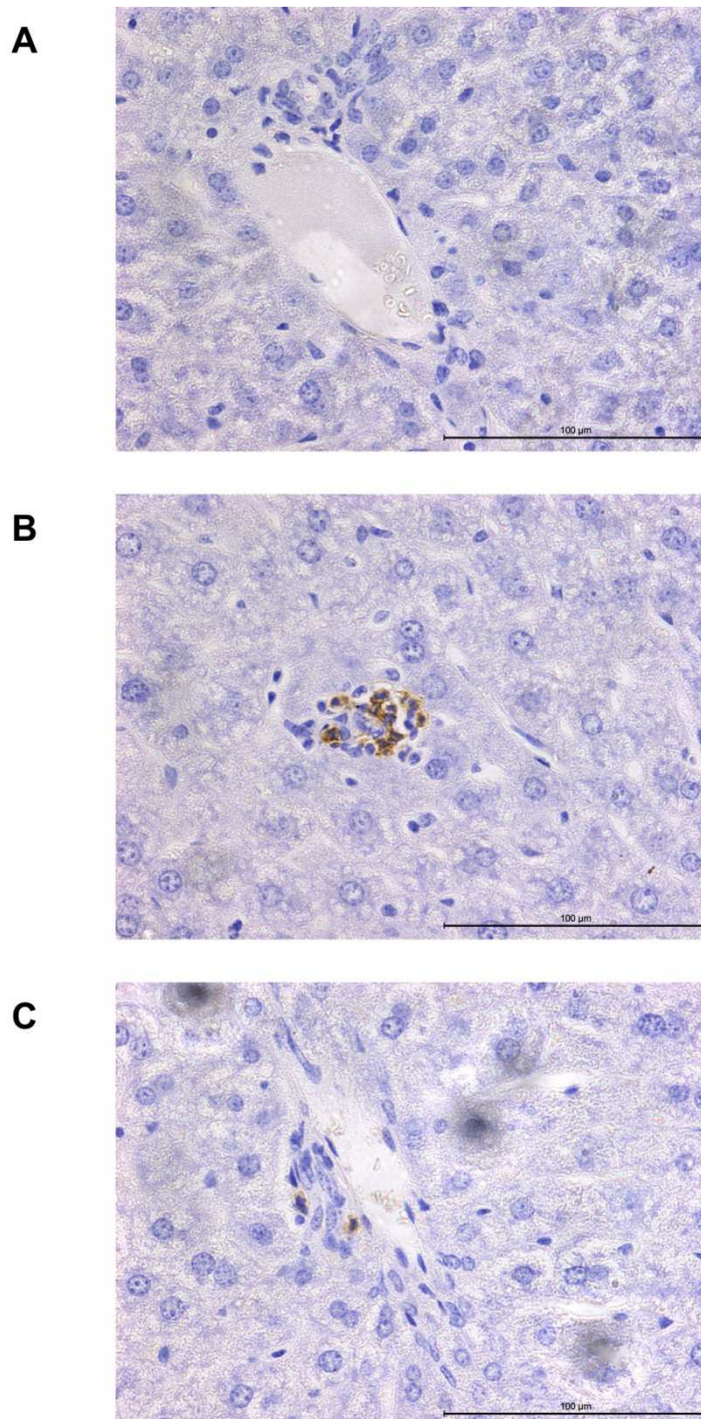


Figure 3.27 – Detection of cells expressing the NIMP antigen in PTI in the mouse liver. 5µm sections of formalin fixed and paraffin embedded mouse liver were stained with a primary antibody specific for the NIMP antigen and HRP-conjugated secondary antibody, as described in chapter 2 – materials and methods. Sections were counterstained with haematoxylin, no primary antibody controls were included and stained as outlined, with the substituting NIMP primary antibody with antibody diluent. **A;** No primary antibody control. **B** positive control, **C;** portal tract of E2 treated animal

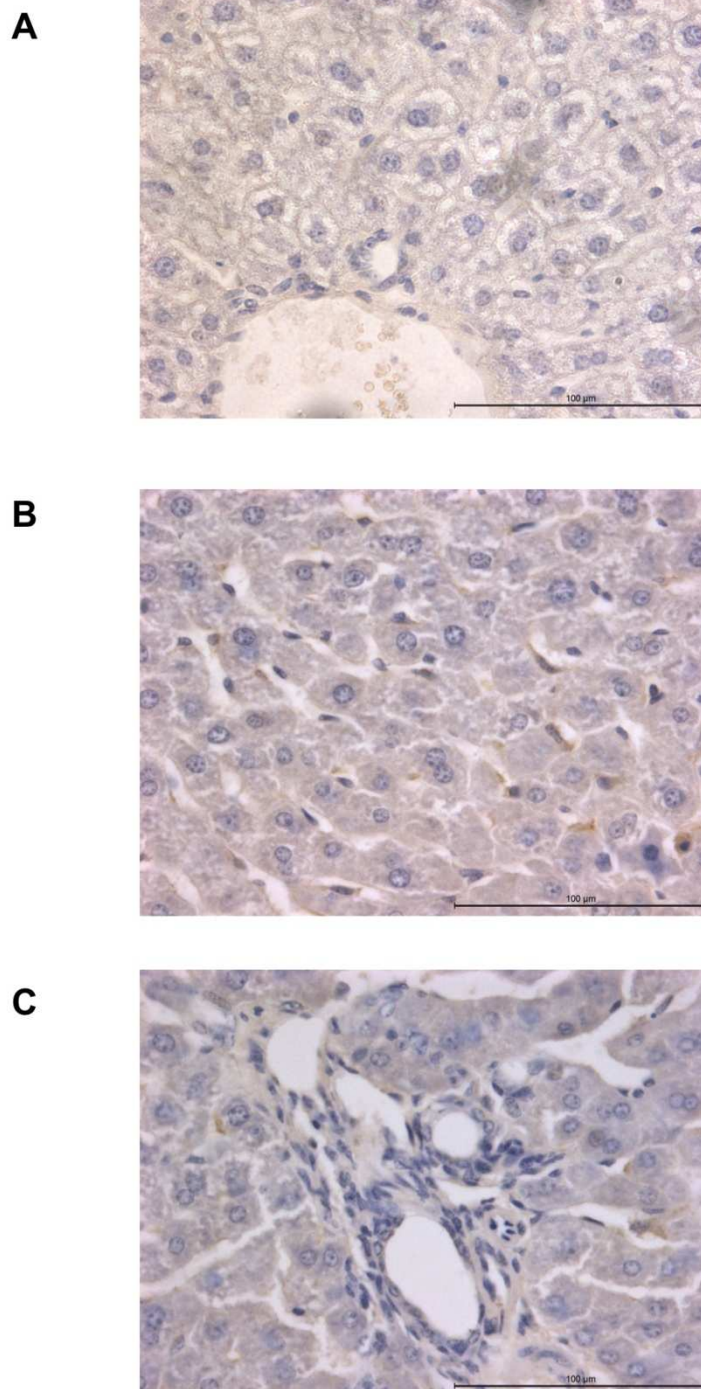


Figure 3.28 – No cells expressing the F4/80 antigen were detected in PTI in the mouse liver. 5µm sections of formalin fixed and paraffin embedded mouse liver were stained with a primary antibody specific for the F4/80 antigen and HRP-conjugated secondary antibody, as described in chapter 2 – materials and methods. Sections were counterstained with haematoxylin. No primary antibody controls were included and stained as outlined, with the substitution F4/80 primary antibody with antibody diluent. **A**; No primary antibody control. **B** positive control, **C**; portal tract of E2 treated animal

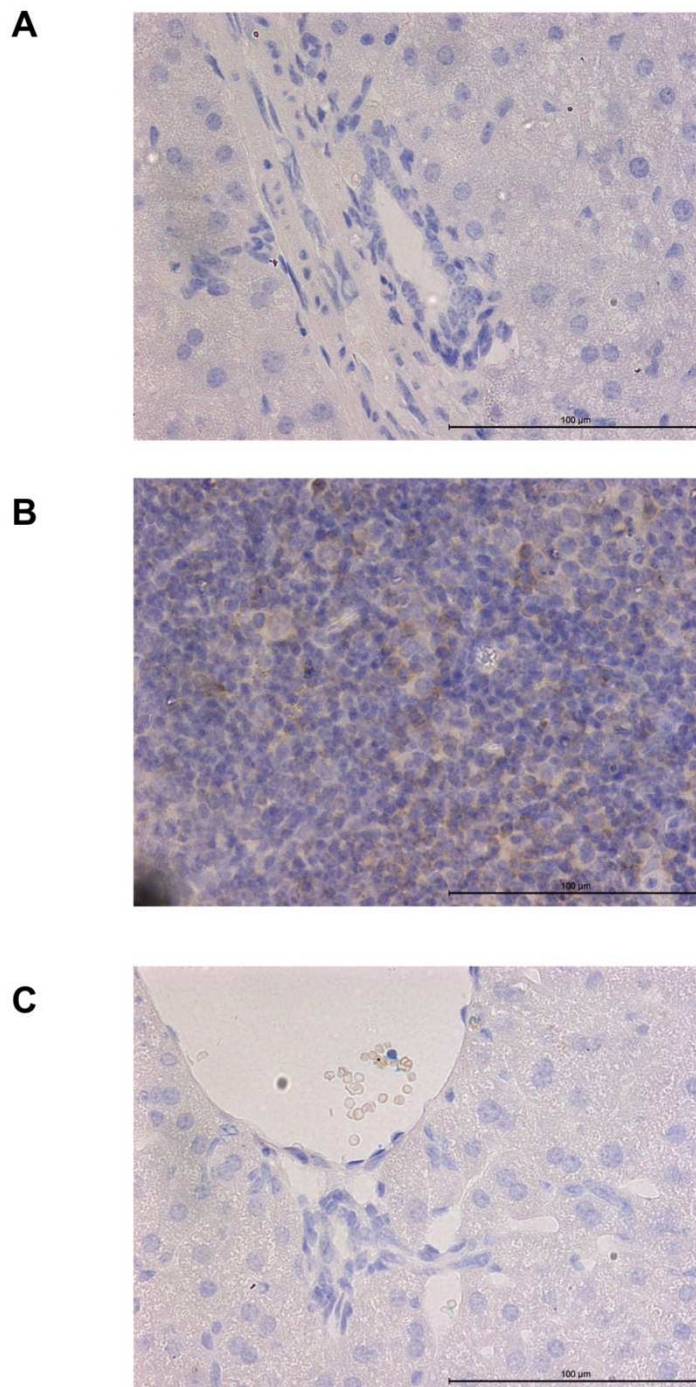


Figure 3.29 – No cells expressing the CD3 antigen were detected in PTI in the mouse liver. 5µm sections of formalin fixed and paraffin embedded mouse liver were stained with a primary antibody specific for the CD3 antigen and HRP-conjugated secondary antibody, as described in chapter 2 – materials and methods. Sections were counterstained with haematoxylin. No primary antibody controls were included and stained as outlined, with the substituting CD3 primary antibody with antibody diluent. **A**; No primary antibody control. **B** positive control, **C**; portal tract of E2 treated animal

3.4.3. Tartrazine and sunset yellow do not test positive for estrogenic activity by mouse uterine bioassay

In the *in vitro* screening systems previously described, a number of compounds were found to have transcriptional estrogenic activity in human cell line models. The estrogenic effects of these compounds were examined *in vivo*.

The mouse uterine bioassay is a classical method by which estrogenic activity can be assessed *in vivo*. In this system, pre-pubescent mice (19 d.o.) are administered potentially estrogenic compounds for 4 consecutive days by i.p injection. The effect of estrogen or other estrogenic compounds is an increase in uterine weight over the relative vehicle control group.

Fig 3.30A describes the effect of treatment with sunset yellow, tartrazine, butyl paraben and methoxychlor on uterine development, relative to vehicle and E2 controls. Treatment of pre-pubescent mice with methoxychlor, a known xenoestrogen, resulted in a significant increase in wet uterine mass relative to total body mass. Administration of butyl paraben, which has previously been described to have estrogenic activity in this model, produced an increase in uterine weight which was approaching significance. Treatment with sunset yellow or tartrazine did not produce any significant change in uterine weight. Examples of uteri from this study are shown in fig 3.30B, this clearly demonstrates the effect of E2 on uterine size.

3.4.4. In vivo model of xenoestrogen exposure on liver function in the mouse

The effect of administration of the human ER activators, sunset yellow and tartrazine, alongside E2, on liver function were investigated *in vivo*. Adult male C57Bl/6 mice were administered either E2, sunset yellow, tartrazine or relevant vehicle control (PBS or olive oil (OO)) 10 times in 14 days by i.p injection. Treatment concentrations were chosen based on the standard dose of E2 for inducing physiological estrogenic effects and the relative EC₅₀ values calculated for the xenobiotics *in vitro* in the ERE-luciferase reporter gene assay described in chapters 3.1 and 3.2. Whilst PBC predominantly affects females, male mice were chosen for this model as the mouse menstrual cycle is short relative to the time of the study. It was reasoned that males would have a lower, and more consistent, level of circulating estrogen, and therefore would be a more accurate system.

After treatment, animals were sacrificed and tested for a variety of different indicators which would link treatment with these any of these compounds to a risk of developing cholestatic liver disease or PBC.

3.4.4.1. Administration of E2 and tartrazine both cause elevated serum ALP activity in the mouse

Elevated serum alkaline phosphatase (ALP) levels are used as a clinical indicator of cholestatic liver disease. Serum taken from mice treated with

sunset yellow, tartrazine or E2 was tested for serum ALP levels. Fig 3.31 shows that treatment with both E2 and tartrazine resulted in an increase in serum ALP over the relevant vehicle control. Whilst it is already understood that elevated estrogen levels can cause cholestasis, this data suggests that tartrazine may produce a similar cholestatic effect.

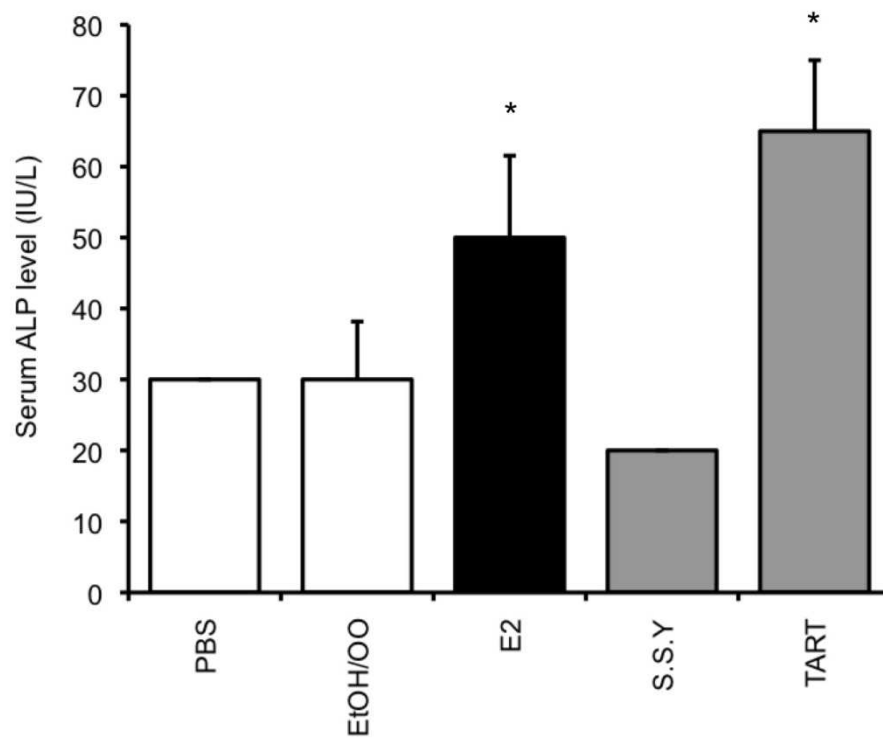


Figure 3.31 – Treatment with E2 and tartrazine cause elevated serum ALP activity in the mouse. Serum ALP activity following treatment 10 times in 14 days I.P. with 1mg/kg E2 (n=4), 500mg/kg tartrazine (n=4), PBS (tartrazine vehicle, n=3) or 1:20 EtOH:OO (E2 vehicle, n=4). *=Significantly different ($P < 0.05$) versus relevant vehicle control group, Student's T-test (two tailed)

3.4.4.2. E2 and Tartrazine both cause increased PTI in the mouse

The degree of PTI in this model was assessed using the same technique as in the model of acute estrogen exposure that was described at the beginning of this chapter. Fig 3.32 shows images of typical portal tracts following treatment with E2, sunset yellow, tartrazine or vehicle controls. It is clear that there is an increase in PTI following treatment with both E2 and tartrazine (highlighted by black arrow). This PTI was quantified, shown by fig 3.34A, both E2 and tartrazine resulted in a significant increase in PTI over the corresponding vehicle control group.

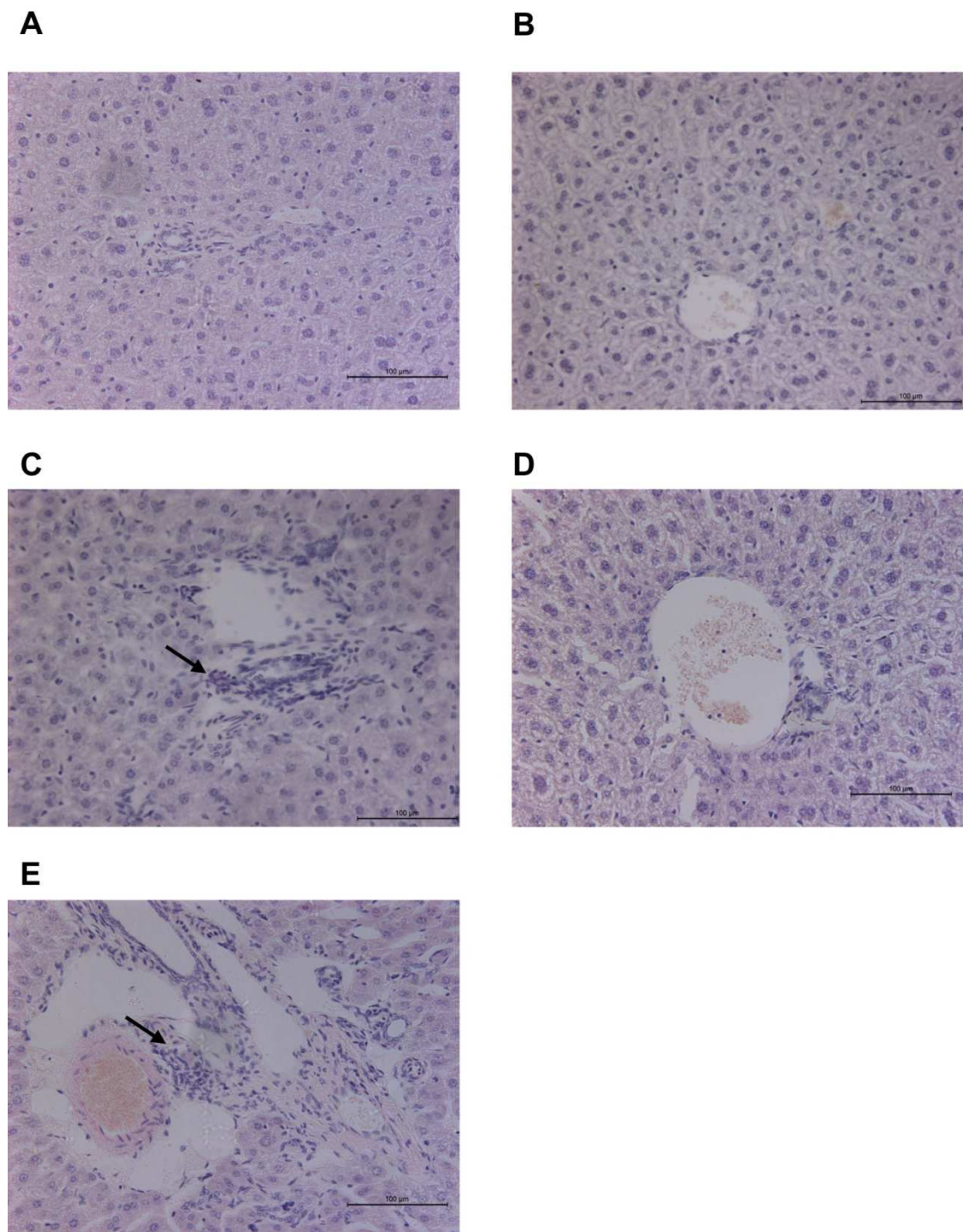


Figure 3.32 – Typical PTI in the mouse liver following treatment with E2 and tartrazine
5µm sections of formalin fixed and paraffin embedded mouse liver were stained with haematoxylin and eosin as outlined in chapter 2, following treatment 10 times in 14 days by single *i.p.* injection with **A.** PBS vehicle (sunset yellow/tartrazine vehicle). **B.** 1:20 EtOH:olive oil vehicle (E2 vehicle), **C.** 1mg/kg E2. **D.** 500mg/kg sunset yellow. **E.** 500mg/kg tartrazine.

3.4.4.3. Treatment with E2 and tartrazine both cause increased collagen deposition around the portal tracts of the mouse liver.

Collagen deposition is synonymous with fibrosis, typically in cholestatic liver disease and in PBC, an increase in collagen deposition is observed around the portal tracts. The degree of collagen deposition following treatment with xenoestrogens was examined by quantitative analysis of Sirius red staining around the portal tracts. Fig 3.33 shows images of typical portal tract areas following treatment and reveals that there is an increase in collagen deposition (highlighted by black arrow) following treatment with both E2 and tartrazine relative to vehicle controls. The degree of positive Sirius red staining was quantified and is shown in Fig 3.34B, treatment of mice with both E2 and tartrazine caused a significant increase in positive staining.

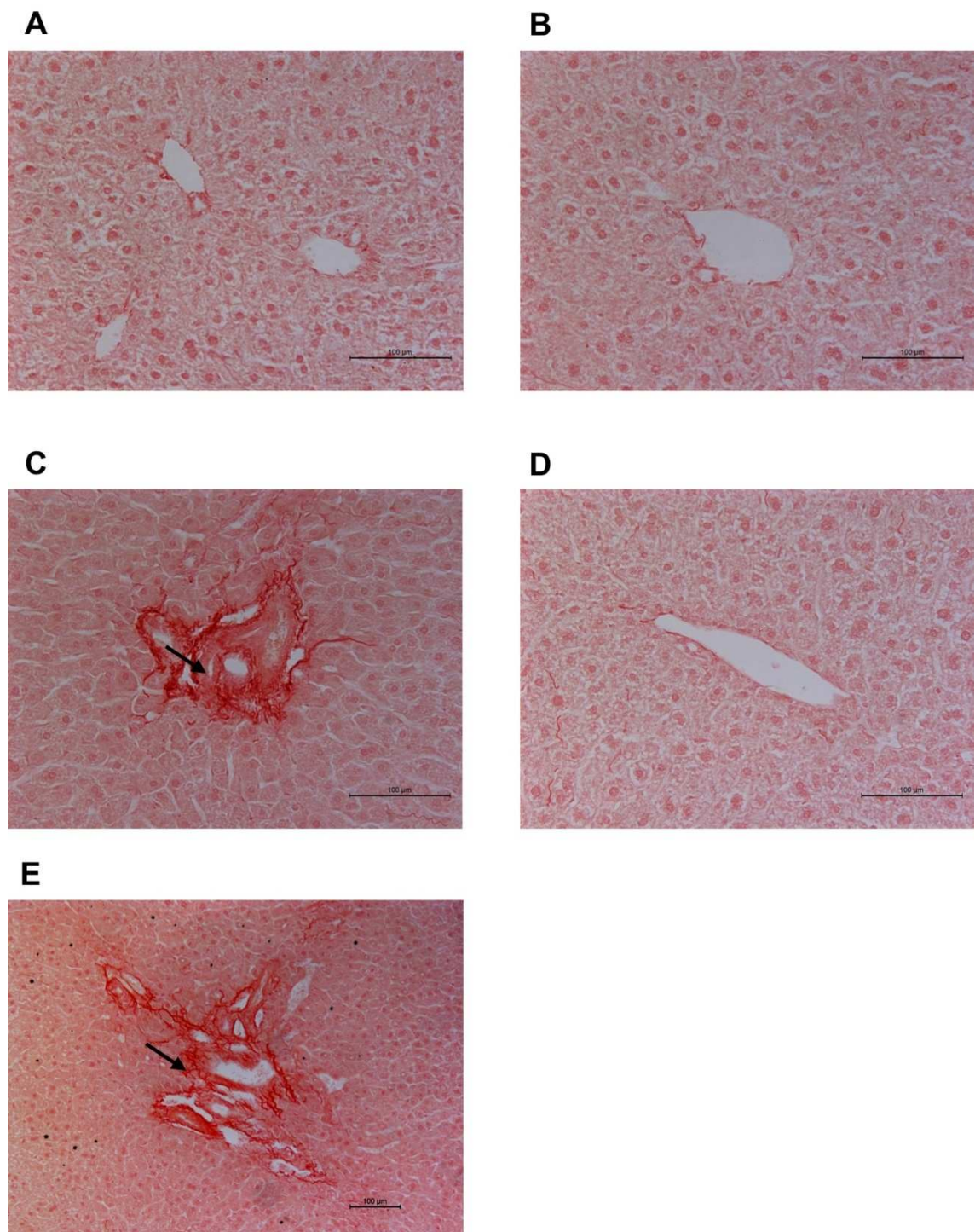


Figure 3.33 – Typical Sirius red staining in the mouse liver following treatment with E2 and tartrazine 5µm sections of formalin fixed and paraffin embedded mouse liver were stained with Sirius red for collagen as outlined in chapter 2, following treatment 10 times in 14 days by single *i.p.* injection with **A.** PBS vehicle. **B.** 1:20 EtOH:Olive oil vehicle, **C.** 1mg/kg E2. **D.** 500mg/kg sunset yellow. **E.** 500mg/kg tartrazine.

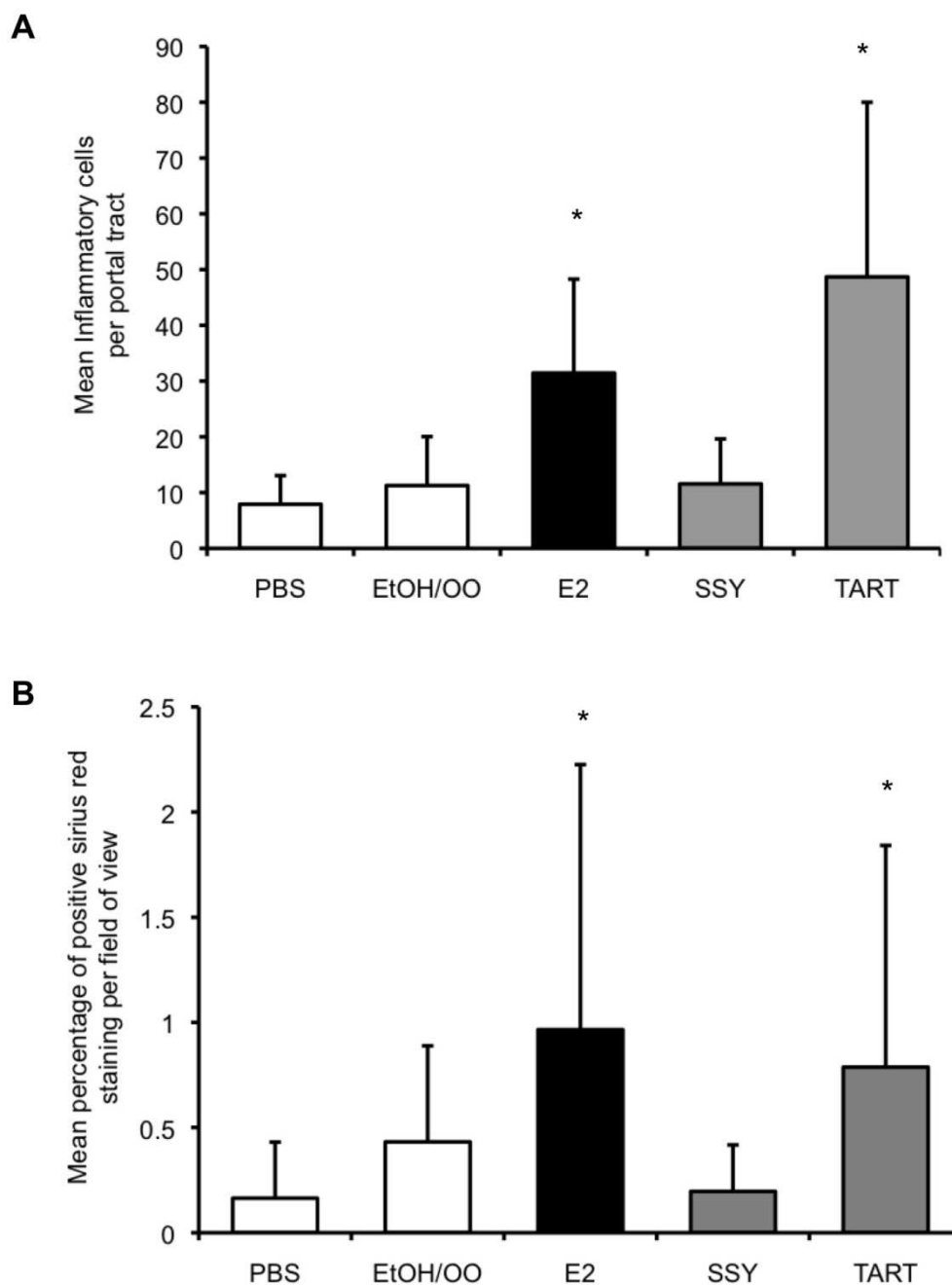


Figure 3.34 Analysis of portal tract injury following treatment with xenoestrogens A – Treatment with E2 and tartrazine causes a significant increase in PTI in the mouse liver 5 μ m sections of formalin fixed and paraffin embedded mouse liver were stained with haematoxylin and eosin as outlined in chapter 2, following treatment 10 times in 14 days by single *i.p.* injection with either 1mg/kg E2 (n=4), 500mg/kg sunset yellow (n=4) 500mg/kg tartrazine (n=4), PBS (sunset yellow/tartrazine vehicle, n=3) or 1:20 EtOH:OO (E2 vehicle, n=4). Mean number of inflammatory cells were counted for 8 portal tracts per animal. **B. Treatment with E2 and tartrazine causes a significant increase in collagen deposition in the mouse liver.** 5 μ m sections of formalin fixed and paraffin embedded mouse liver were stained with Sirius red as outlined in chapter 2, following treatment 10 times in 14 days by single *i.p.* injection with either 1mg/kg E2 (n=4), 500mg/kg sunset yellow (n=4) 500mg/kg tartrazine (n=4), PBS (sunset yellow/tartrazine vehicle, n=3) or 1:20 EtOH:OO (E2 vehicle, n=4). Mean amount of positive staining was quantified for 8 different fields of view per animal. *= Significant increase control group ($p < 0.05$) (Students t-test, two tailed).

3.4.4.4. Estrogen and xenoestrogen exposure causes altered bile/drug transport protein expression in the mouse liver

The relative expression of a range of transporter proteins which are involved in uptake/ efflux of bile acids were analysed by SYBR green qRT-PCR following treatment with estrogen or the ER activating compounds sunset yellow and tartrazine.

Elevated exposure to estrogen has previously been described to cause changes in expression of certain transporter proteins in the rat and the mouse^{108, 109}, this provides a potential mechanism for the cholestasis sometimes seen in response to elevated serum estrogen levels. The expression genes encoding known or potential bile acid transporters was assessed in this mouse model of xenoestrogen exposure.

The Abcc family of genes encode a number of membrane transport proteins in the super family of ATP binding cassette (ABC) transporters. Abcc1-6 encode multidrug resistance associated proteins 1-6 (MRP1-6) respectively, all of which are expressed in the normal liver at varying levels¹¹⁰. The expression of Abcc1-6 in the mouse liver was examined by quantitative PCR following treatment with E2, sunset yellow and tartrazine.

Fig 3.35 shows that expression of Abcc1 was unchanged following treatment, in contrast, administration of E2 caused a significant decrease in expression of Abcc2 relative to vehicle control, sunset yellow and tartrazine had no significant

effect on level of Abcc2. MRP3 is reported to be the most highly expressed of this family of proteins in the liver, the expression of Abcc3, which codes for this protein was significantly down regulated by both E2 and tartrazine in the mouse. Bile salts are known to be good substrates for MRP3¹¹¹. No significant changes in Abcc4 levels were observed, though this gene was found to be variable in its expression in the mouse, supporting evidence for its variable expression profile describe in the human reported previously ¹¹². Abcc5 has been reported to be expressed at moderate levels in the mouse liver relative to other members in this family, Abcc5 gene was significantly up regulated by tartrazine in this model. A trend towards a decrease in Abcc6 expression was observed following treatment with both E2 and tartrazine, although this was not statistically significant probably due to variability of Abcc6 expression.

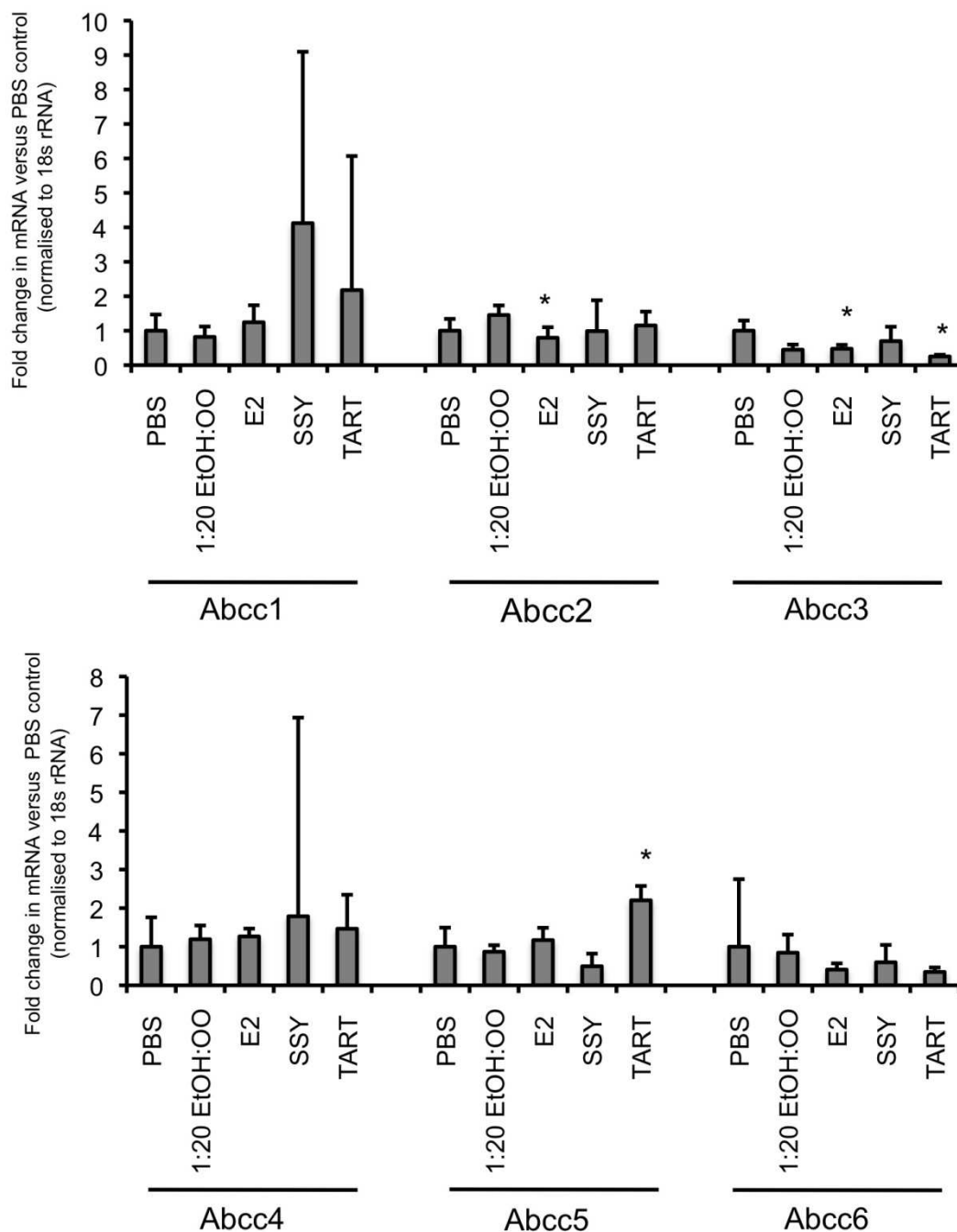


Figure 3.35 –Expression of Abcc family of transport proteins in the mouse liver following treatment with xenoestrogens. Expression of Abcc1-6 in the mouse liver was quantified by SYBR Green qRT-PCR following treatment 10 times in 14 days by single *i.p.* injection with either 1mg/kg E2 (n=4), 500mg/kg sunset yellow (n=4) 500mg/kg tartrazine (n=4), PBS (sunset yellow/tartrazine vehicle, n=3) or 1:20 EtOH:OO (E2 vehicle, n=4) *= significantly different to vehicle control group (p<0.05) (Students t-test, two tailed).

It has previously been reported that expression of the gene *Abcb11*, which encodes the bile salt export pump (BSEP) is down regulated following estrogen exposure in the rat¹⁰⁹. In this study, a trend towards a decrease in BSEP expression was observed, but this effect was not statistically significant due to outlying results.

The gene *Slc10a1* encodes the sodium (Na⁺) taurocholate co-transporting polypeptide (NTCP), a bile salt transport protein expressed on the hepatic sinusoid¹¹³. Expression of this gene was significantly down regulated in the mouse following treatment with sunset yellow.

Permeability glycoprotein (p-gp), encoded by *Abcb1b*, is a well-characterised transporter belonging to the ABC super family. It is expressed on the canalicular membrane of hepatocytes and is associated with xenobiotic clearance and drug resistance¹¹⁴. Treatment with tartrazine was found to significantly increase *Abcb1b* expression in the mouse liver.

The inflammatory cytokine Interleukin-1- β (IL1 β) has previously been shown to be induced in the mouse liver following treatment with estrogen. The expression of IL1 β was examined in the model of xenoestrogen exposure, it was found that IL1 β was elevated by treatment with E2, but whilst this result was approaching statistical significance, once again variability between the animals was evident.

The expression of both ER α and ER β were also studied by SYBR green qRT-PCR. The expression of ER α in this model was not altered following treatment with E2, sunset yellow or tartrazine.

As described previously, ER β expression was not detectable by standard RT-PCR methods and agarose gel electrophoresis in the mouse liver. But by qPCR methods a single product was detected, possibly due to the sensitivity of this system. Treatment of mice with sunset yellow caused a large decrease in expression of ER β at the mRNA level, no effects relating to the expression of ER β following treatment with E2 or tartrazine were seen. This may imply that the level of cholestasis necessary to cause a significant increase in ER β mRNA was not reached in this model. (Fig 3.36)

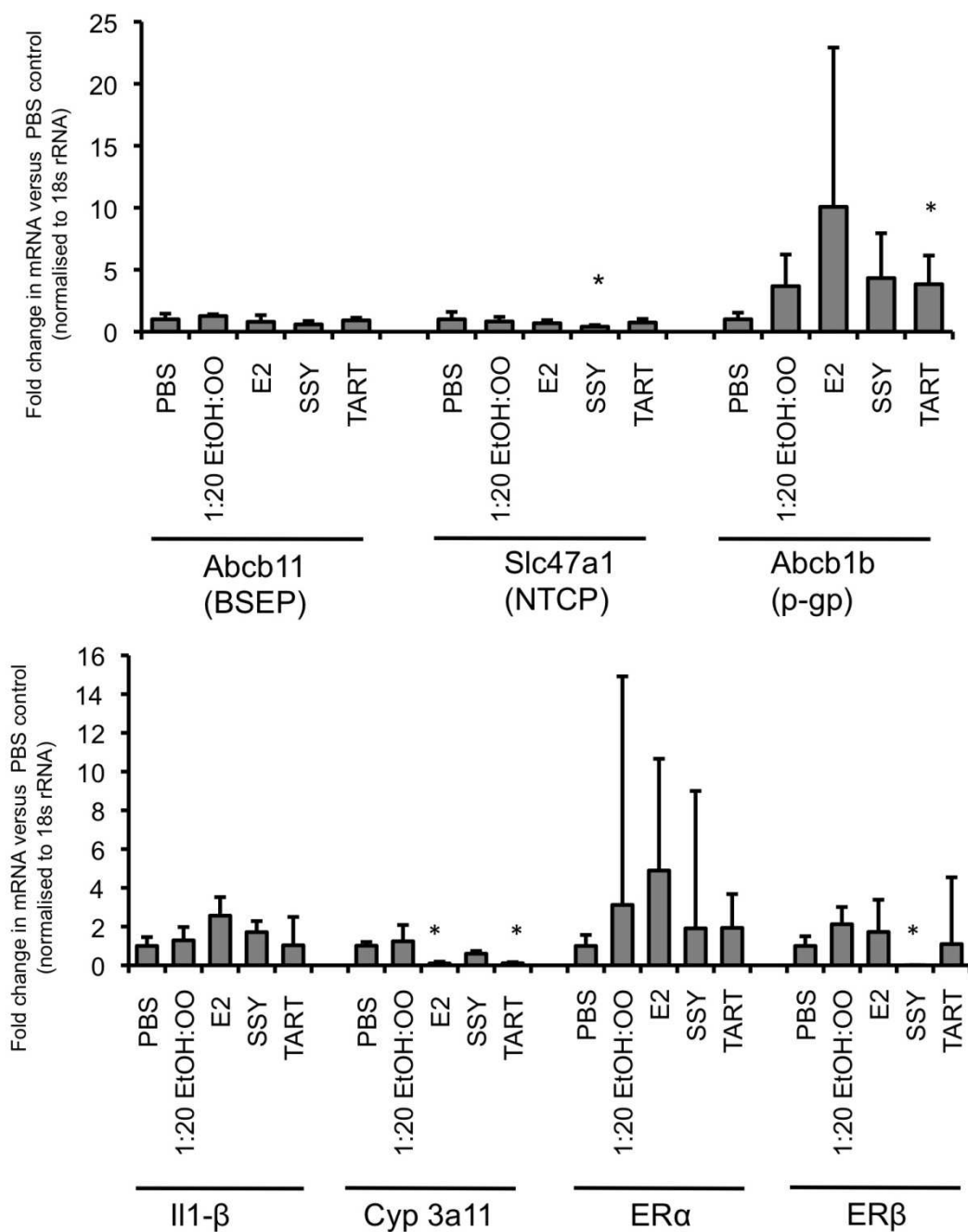


Figure 3.36 –SYBR green qRT-PCR analysis of gene expression in the mouse liver following treatment with xenoestrogens. Expression of selected genes in the mouse liver was quantified by SYBR Green qRT-PCR following treatment 10 times in 14 days by single *i.p.* injection with either 1mg/kg E2 (n=4), 500mg/kg sunset yellow (n=4) 500mg/kg tartrazine (n=4), PBS (sunset yellow/tartrazine vehicle, n=3) or 1:20 EtOH:OO (E2 vehicle, n=4) *= significantly different to vehicle control group. (p<0.05) (Students t-test, two tailed).

3.4.4.5. Exposure to estrogen causes increased serum AMA titre in the mouse

The presence of antimitochondrial antibodies (AMA) in PBC patient sera is observed in around 95% of cases, and is normally considered the defining hallmark of PBC. Indeed serum AMA titre is used clinically as a marker of PBC¹⁰¹.

An established ELISA system of measuring AMA titre in the mouse was used to measure serum AMA levels in the mouse model of xenoestrogen exposure⁹⁵. Fig 3.37A shows that treatment of mice with E2 resulted in a significant increase in serum AMA titre over vehicle control group. Treatment with tartrazine did increase AMA titre over the PBS control group, but variability between animals resulted in a loss of statistical significance.

Differences in the level of in the response of animals in this study to tartrazine was something that was noticed in both the PTI and Sirius red quantification performed previously. It was for this reason that the AMA titre was compared to the level of PTI for each animal. Fig 3.38 describes the result of plotting AMA titre against the PTI score for each animal, it is evident that there is a correlation between the level of AMA titre and PTI, suggesting that the AMA levels in response to treatment with E2 or tartrazine are dependent on the degree of liver insult. Vehicle control groups and sunset yellow, which had no effect on any other markers of damage or cholestasis, lay in the lower values of both measurements.

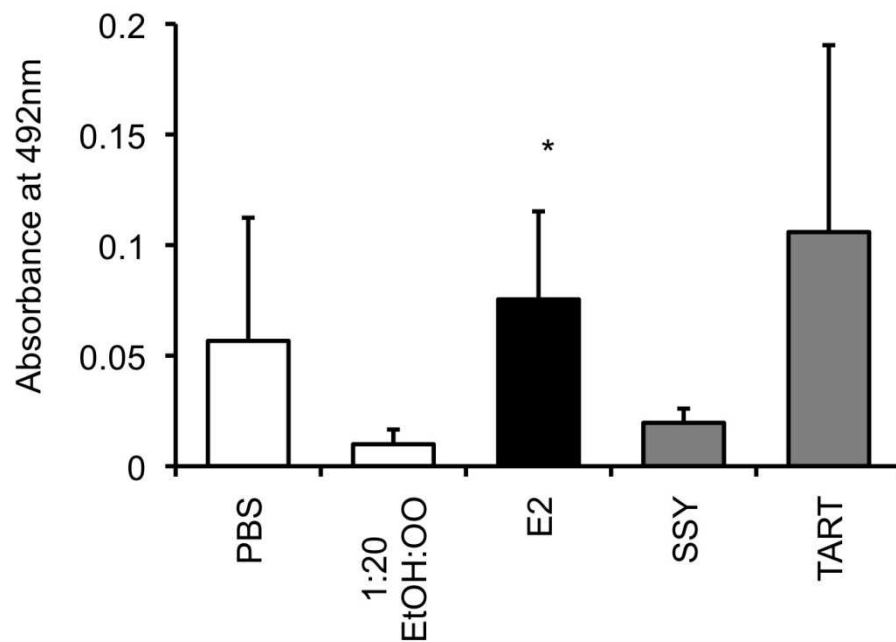
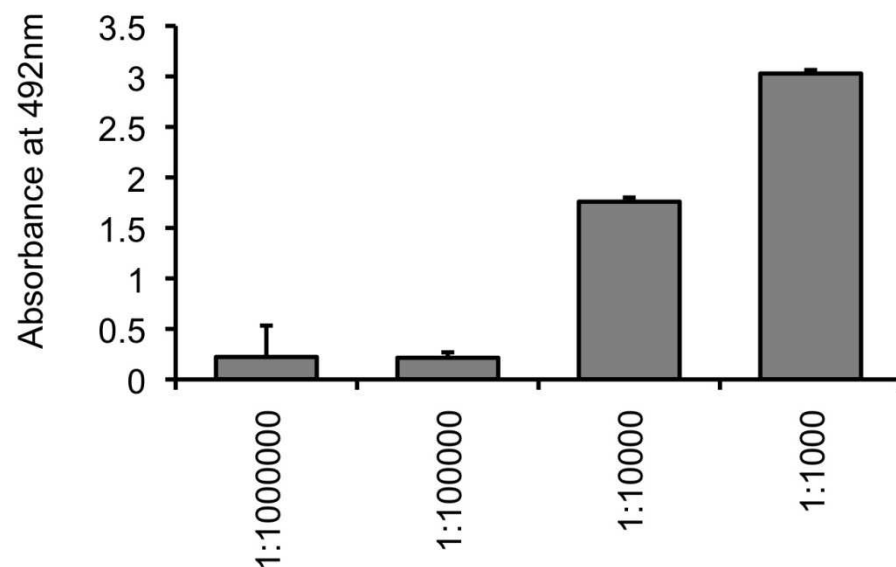
A**B**

Figure 3.37 –Serum AMA activity in the mouse following treatment with xenoestrogens. **A.** Mouse serum AMA activity against murine PDC-E2 was analysed by ELISA following treatment 10 times in 14 days by single *i.p.* injection with either 1mg/kg E2 (n=4), 500mg/kg sunset yellow (n=4) 500mg/kg tartrazine (n=4), PBS (sunset yellow/tartrazine vehicle, n=3) or 1:20 EtOH:OO (E2 vehicle, n=4) *= significantly different to vehicle control group. (p<0.05) (Students t-test, two tailed). **B.** Serum AMA activity against murine PDC-E2 of positive control sera from mice immunised with foreign PDC-E2.

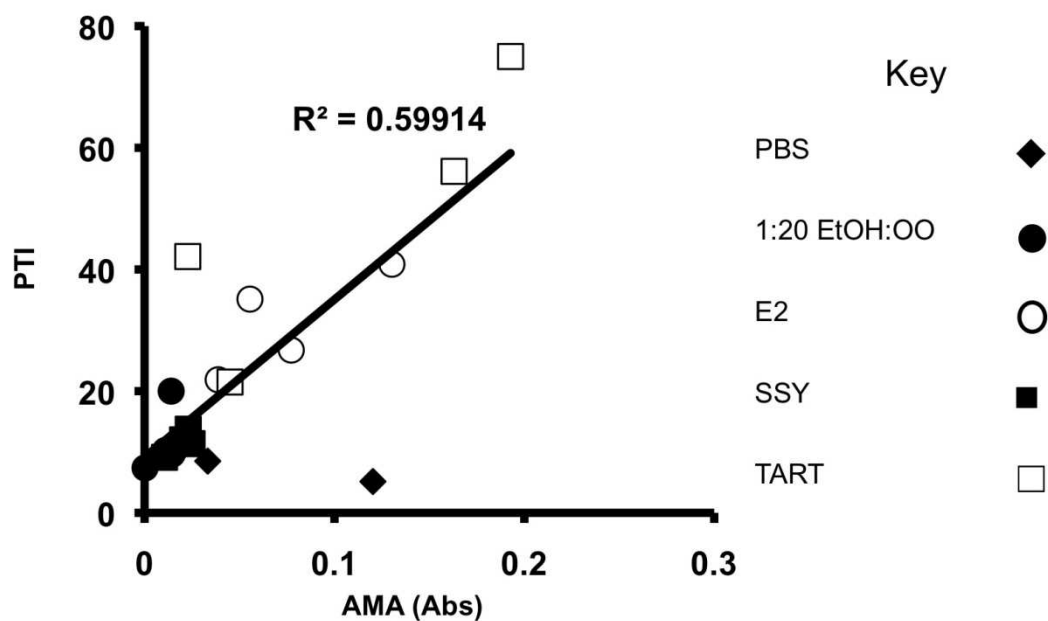


Figure 3.38 – Correlation between serum AMA activity and severity of cholestatic liver injury. Plot of serum AMA activity against PTI count in a mouse model of xenoestrogen exposure. Mice were treated 10 times in 14 days by single *i.p.* injection with 1mg/kg E2 (open circle)(n=4), 500mg/kg tartrazine (open square) (n=4), 500mg/kg sunset yellow (filled square)(n=4), PBS (filled diamond)(tartrazine/sunset yellow vehicle, n=3), or 1:20 EtOH:OO (filled circle)(E2 vehicle, n=4).

3.4.5. Chapter 3.4 discussion

In this chapter the effects of exposure to estrogen as human ER activators in chapter 3.2 were studied *in vivo*.

The expression of both ER α and ER β was determined in the mouse by RT-PCR and immunohistochemistry. Expression of ER α was found to be widespread throughout the hepatocytes, whilst ER β was undetectable by RT-PCR, but was observed at the protein level in cholangiocytes (accounting for only around 5% of liver cells) by IHC.

An acute study of estrogen exposure in male mice showed that 3 days of treatment with E2 resulted in a significant increase in portal tract inflammation. The nature of this PTI was examined and was found to be of a mixed cell type, consisting of at least some NIMP positive cells, suggesting the presence of neutrophils.

Utilising the classical mouse uterine bioassay, the human ER activators sunset yellow and tartrazine were found to have no uterotrophic effects.

In a 2 week study of estrogen/xenoestrogen exposure in the mice, both E2, as before, and the food and cosmetic colouring agent, tartrazine, were found to significantly increase PTI in the mouse. Both of these compounds also caused a significant increase in positive Sirius red staining in the liver and also an elevation in serum ALP levels, synonymous with cholestasis.

The expression of bile salt transport proteins and efflux pumps was examined by SYBR green qRT-PCR. The expression of some of these genes was found to be altered following treatment with E2, sunset yellow or tartrazine, in concordance with previous work which suggest that estrogen induced cholestasis is in some part linked with altered expression profile of membrane transport proteins. It is worth mentioning that a lot of variability between animals was observed in this study, which had relatively small group numbers. This may have masked positive results or statistical significance.

The expression of CYP 3a11, a well described PXR dependent gene in the mouse was comprehensively down regulated by both E2 and tartrazine. PXR activation has previously been shown to be protective against liver injury, and also has been reported to drive the expression of the MRP family of ABC transporters¹¹⁵. This may be caused by PXR antagonism by both E2 and tartrazine, resulting in altered transporter expression, cholestasis and also a reduced capacity for liver recovery.

The expression of ER α was found to be unaffected following treatment with any of the selected compounds, but sunset yellow comprehensively down regulated ER β mRNA levels.

The presence of AMA in mouse sera was studied following exposure to the same set of compounds. E2 exposure was found to increase serum AMA activity over controls, tartrazine did appear to increase titre but fell short of statistical significance due to variability, but a correlation was discovered between the degree of PTI and serum AMA titre, suggesting that appearance of AMA may be proportional to the severity of estrogen induced cholestatic liver injury.

3.5. Isolation, characterisation and proliferation of cells isolated from the intrahepatic biliary structure.

The intrahepatic biliary structure describes the network of bile duct which form a 'tree' like structure running throughout the liver. This network of bile ducts and smaller ductules is comprised primarily of cholangiocytes, but is also thought to be the location of resident hepatocyte and cholangiocyte progenitor cells^{116, 117}. It is possible to separate the entire biliary tree from the rat liver by collagenase digestion. From this structure cultures of cells were prepared and characterised to determine which cell types were present. The effect of estrogen upon the proliferation and differentiation of these cell cultures was examined.

3.5.1. Isolation of cell cultures from the intrahepatic biliary structure.

After collagenase perfusion and digestion of the rat liver, the whole biliary structure was retained, digested and filtered before culturing the resulting cells. Whilst the initial aim of producing primary cell cultures of cholangiocytes to simulate the population of the bile duct *in vitro* was apparently unsuccessful, it was evident that the actual product of these preparations may be much more significant.

Limited amounts of small (>10x smaller than an average primary hepatocyte), round cells, either individual or in clusters of no more than 5, were produced. Upon seeding these cells in standard tissue culture dishes and 2 days of culture, they formed tight clusters of cells as a 3 dimensional mass as shown in Fig 3.39A. After 5 days of culture, these original clusters of cells remained, but radiating from them were two distinctly different cell types, evident in figs 3.39

B,C,D. It was also discovered that these cultures would often form circular structures at the boundary of the original cell masses such as the one shown in Fig 3.39E. After passage, the original structures of cells were no longer present and only one cell type was observed in the cultures. Fig. 3.39F.

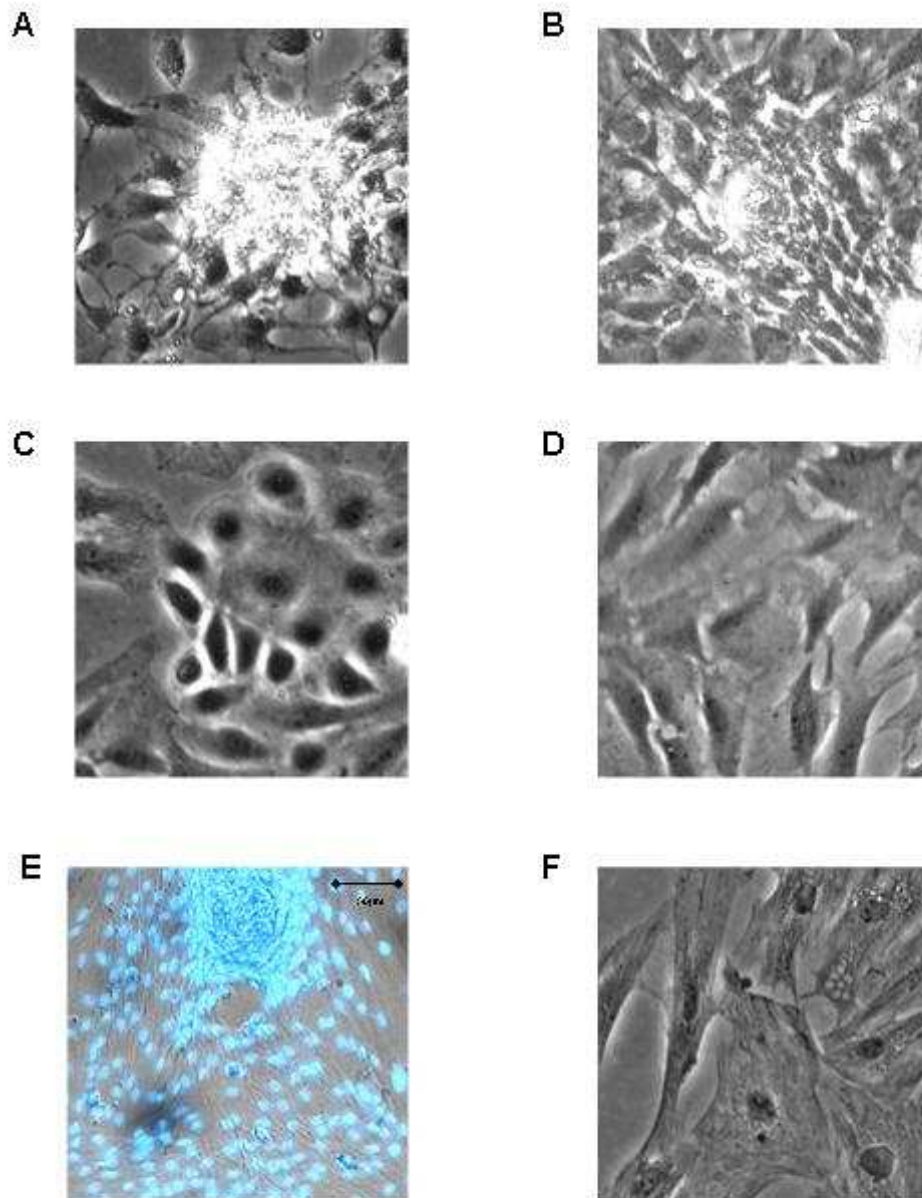


Figure 3.39 –Mixed cell cultures of cells isolated from the rat biliary structure. Bright field imaging of mixed cell cultures isolated from the intrahepatic biliary structure of the rat liver, **A.** t=48 hours, **B.** t=5 days. **C.** t=5days, **D.** t=5days. **E.** t=5 days. **F.** Passage 1.

3.5.2. Cell cultures isolated from the intrahepatic biliary structure contained an OV-6 positive progenitor, giving rise to cholangiocytes and fibroblasts

The cell types within the cultures were characterised by immunocytochemistry, fixed cell cultures were stained for a variety of different antigens, including OV-6, cytokeratin 19 (CK19), vimentin and albumin, the results are shown in Fig 3.40. Cells positive for the OV-6 antigen, deemed to be a marker of the resident liver progenitor cell, the oval cell, were observed only at the centre of the initial cell clusters¹¹⁸. Of the proliferating cells, one cell type was positive for CK19, whilst the other cell type was positive for vimentin. This suggests that the cells produced were a mixture of CK19 positive cholangiocytes and vimentin positive fibroblasts. Vimentin was also detected in the original cell clusters, this is concordant with previous findings that cultured stem cells often form a fibroblastic niche around themselves *in vitro*. In these areas both CK19 and albumin (a marker of hepatocytes, which has also been detected in both immature hepatocytes and precursor cells of the intrahepatic bile duct.)¹¹⁹

The expression of CK19 and vimentin was profiled throughout time in culture by RT-PCR using primers specific to each gene. Fig 3.41 shows that CK19 was detected in freshly isolated cells, and up to 3 days of culture after which CK19 mRNA was undetectable. The expression of vimentin mRNA was detectable at all of the time points examined, including after passage. This confirms that CK19 positive cholangiocytes were present in culture for up to 3 days after isolation, whereas fibroblasts were present throughout culture. This suggests

that either the cholangiocytes present in the earlier stages of culture either differentiate/ de-differentiate to fibroblasts over time, or undergo cell death leaving the fibroblasts to take over the culture. Albumin was detectable only at $t=0$.

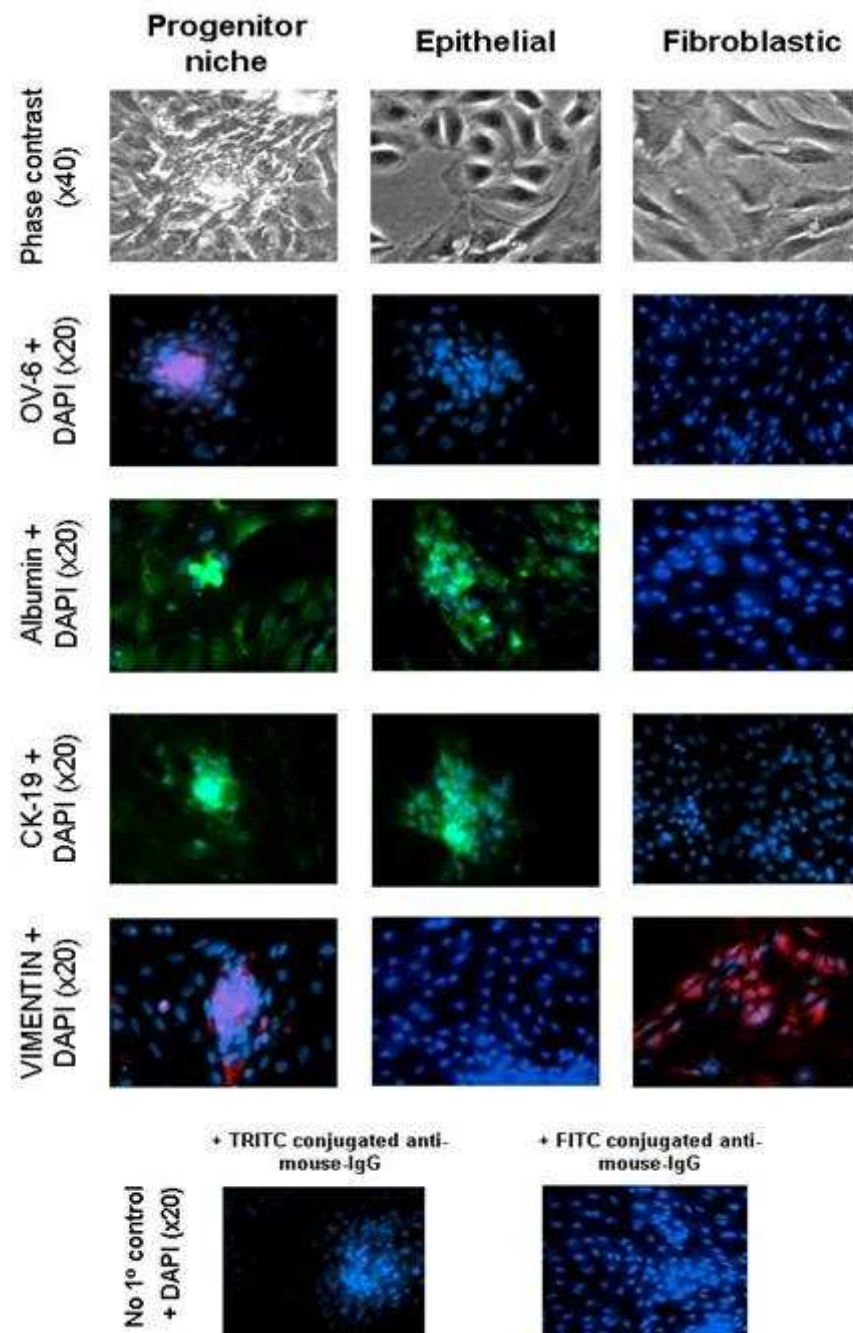


Figure 3.40 –ICC study of mixed cell cultures isolated from the rat intrahepatic biliary structure. Rat biliary cell preparations were formalin fixed *in situ* after 3 days of culture. Cells were incubated with the indicated primary antibody and corresponding fluorescent secondary. And counter staining with DAPI before imaging by fluorescence microscopy. Relevant no-primary controls included where primary antibody was substituted for antibody diluent. antibody diluent

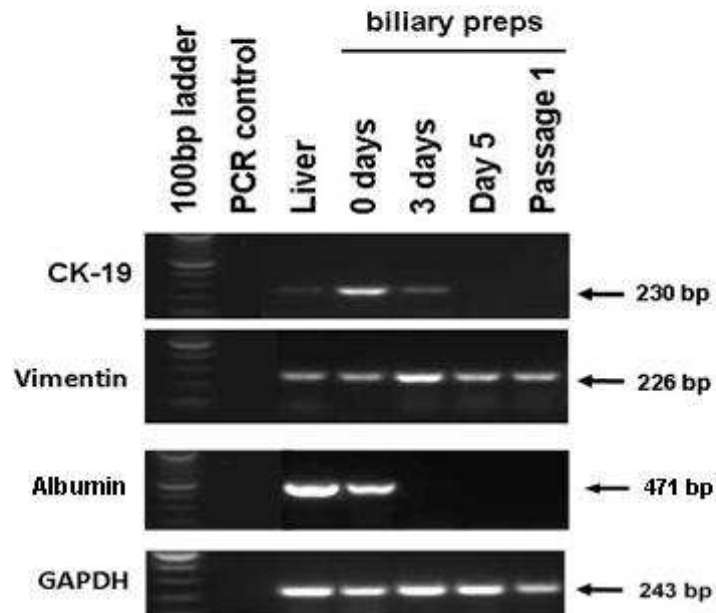


Figure 3.41 – Profile of CK-19, albumin and vimentin expression in biliary cell preparations throughout culture. Biliary cells were cultured for the indicated number of days before RNA isolation and RT-PCR with primers specific for CK19, albumin or vimentin as described in chapter 2 – materials and methods. Visualisation was performed by agarose gel electrophoresis and UV transillumination.

3.5.3. Cell cultures isolated from the intrahepatic biliary structure of the rat express common pluripotency/progenitor factors

Based upon the identification of both OV-6 and albumin antigens within the cultures prepared from the intrahepatic biliary structure by immunocytochemistry, the expression of various genes synonymous with progenitor cells and pluripotency were profiled throughout time in culture, by RT-PCR.

The expression of sox17, a gene linked with endodermal development and cell fate that may commonly be expressed in progenitor cells of epithelium of the respiratory and gastrointestinal tracts, along with the liver, lung and pancreas was detectable in biliary cell cultures at 0 and 3 days in culture, after which expression was not detectable¹²⁰.

The pluripotency factor Sox2, the expression of which is regarded as essential for maintenance of undifferentiated stem cells, was detectable at t=0, but not at any other point. Expression of two other pluripotency factors considered good indicators of stem cell like capacity, Klf4 and c-Myc^{121, 122}, were detected at all stages of culture of the primary biliary cell preps, however, expression was lost after passage. Expression of Oct4, a fourth transcription factor regarded as essential in induction and regulation of pluripotency, was not detected in the cultures^{121, 122} (Fig 3.42).

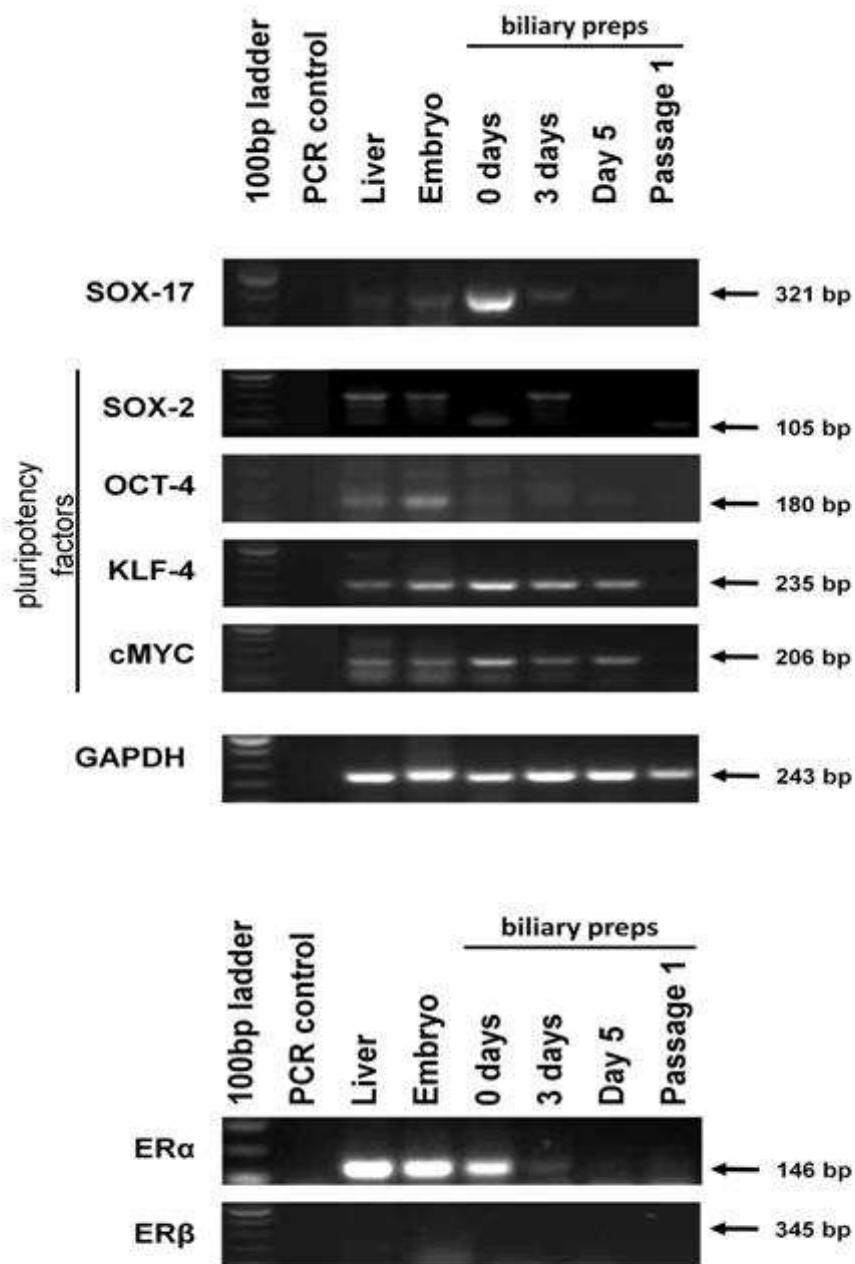


Figure 3.42 – Profile of the expression of pluripotency factors and the ER in biliary cell preparations . Biliary cells were cultured for the indicated number of days before RNA isolation and RT-PCR with primers specific for the described genes as described in chapter 2 – materials and methods. Visualisation was performed by agarose gel electrophoresis and UV transillumination.

3.5.4. Estrogen causes increased proliferation of biliary cell cultures

As previously described, PBC is characterised by proliferation of the intrahepatic bile ducts, accompanied by portal and periportal fibrosis. The cultures of cells which were isolated from the intrahepatic biliary network of the rat liver and characterised in the previous section provide a good model in which to examine the effects of estrogen treatment upon the bile ducts.

Cultures of biliary cells were treated with either 0.1% DMSO vehicle, 10nM/10 μ M E2 or 10 μ M EE (all +/- 100nM ICI 182780). Cells were treated for 5 days before analysis. Fig 3.43A shows images of typical fields of view of both the DMSO vehicle and 10 μ M E2 groups. The numbers of cells of 5 such fields of view, selected at random, in three separate studies were counted, shown by fig 3.43B. These results show that treatment with 10 μ M E2 significantly increased the number of cells present relative to the DMSO vehicle group. In all cases, treatment with 100nM ICI 182780 significantly reduced the number of cells present, compared to the relevant treatment group.

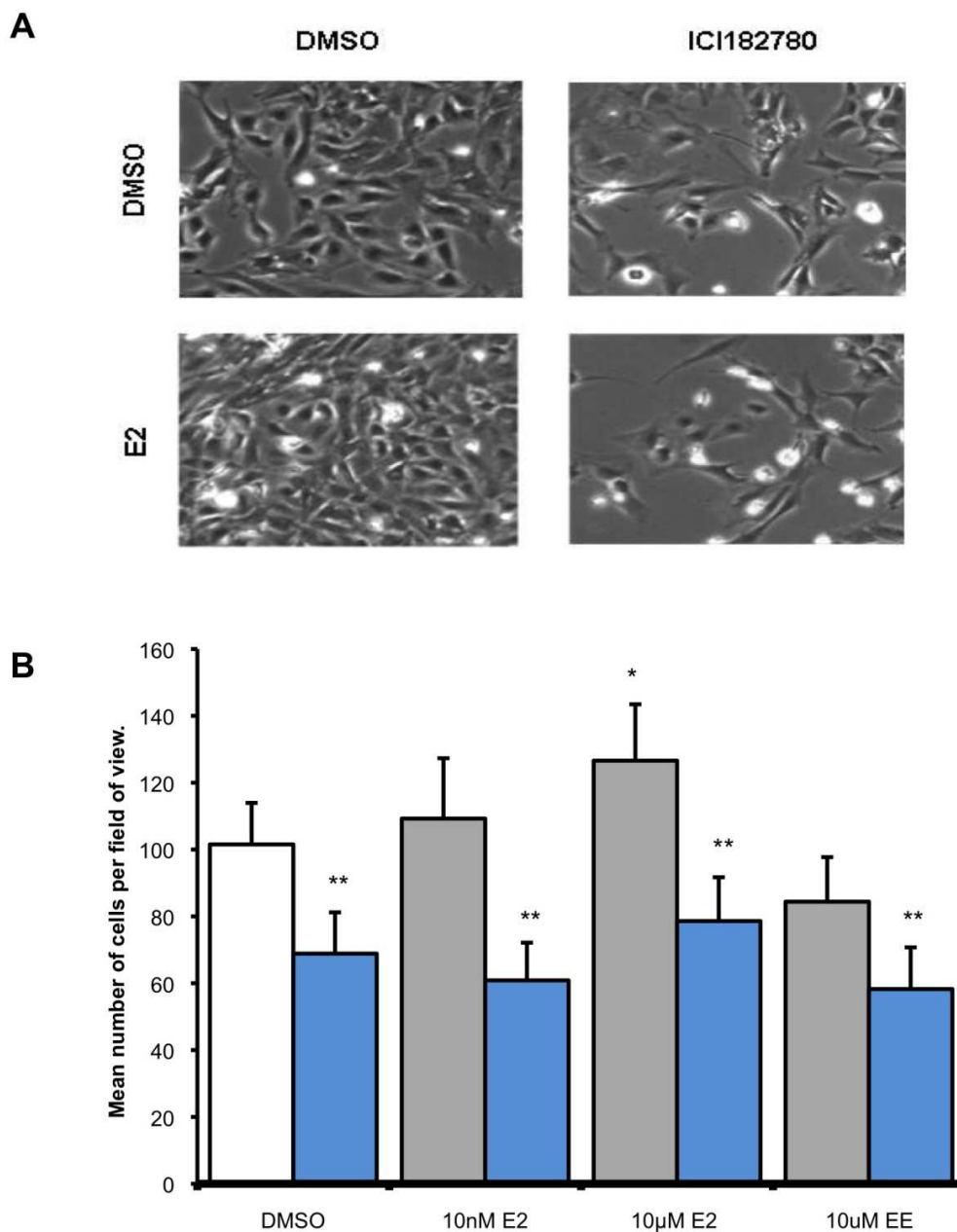


Figure 3.43 – Effect of E2 on the proliferation of biliary cell cultures. **A.** Typical images of biliary cell preparations following treatment with 10µM E2 or DMSO vehicle, +/- 100nM ICI 182780, for 5 days. Cell cultures were the formalin fixed *in situ* before imaging by bright field microscopy at 20x magnification. **B.** Quantification of mean number of cells per field of view from images of biliary cell preparations following treatment with 10nM/10µM E2 or DMSO vehicle, +/- 100nM ICI 182780, for 5 days. Cell cultures were the formalin fixed *in situ* before imaging by bright field microscopy. Data are mean and SD of n=3. *= Significantly increase, over DMSO vehicle**=significant decrease over no antagonist group. (p<0.05) (Students t-test, two tailed)

The effects of treatment on cell proliferation were also analysed by quantification of total protein by actin western blot. This method of analysis did not confirm an increase in total protein per well following treatment with E2, but did show that the estrogen receptor antagonist, ICI 182780, significantly decreased total protein, concordant with findings from the cell counts (Fig 3.44 A,B).

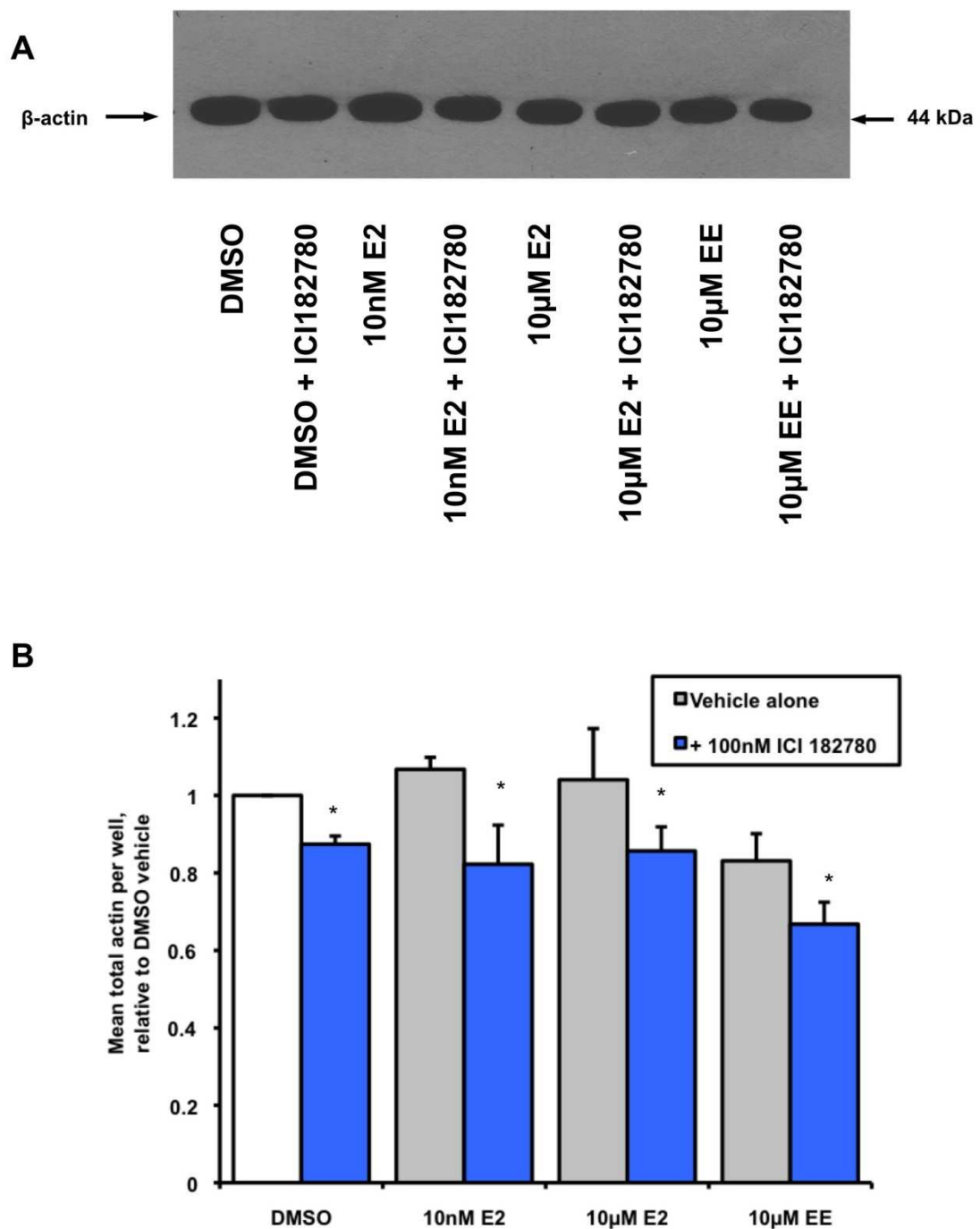


Figure 3.44 – Effect of E2 on the proliferation of biliary cell cultures. A. Western Blot for β -actin for a fixed volume of total protein taken from cell cultures isolated from the rat biliary structure following treatment with 10nM/10 μ M E2 or DMSO vehicle, +/- 100nM ICI 182780, for 5 days. 20 μ l of protein sample/lane **B.** Quantification of actin Western blot for a fixed volume of total protein taken from cell cultures isolated from the rat biliary structure following treatment with 10nM/10 μ M E2 or DMSO vehicle, +/- 100nM ICI 182780, for 5 days. Data are mean and SD of n=3. *= Significant decrease to control group. ($p < 0.05$) (Students t-test, two tailed).

To study whether treatment of cell cultures with estrogen has an effect on their differentiation, or rate of proliferation between cholangiocytes and fibroblasts, vimentin expression was quantified relative to total actin. The results shown in Fig 3.45A,B suggest that there is no change in the amount of vimentin relative to total actin in response to treatment with either E2 or ICI 182780, and therefore it is unlikely that there is a shift towards either fibroblasts or cholangiocytes in culture.

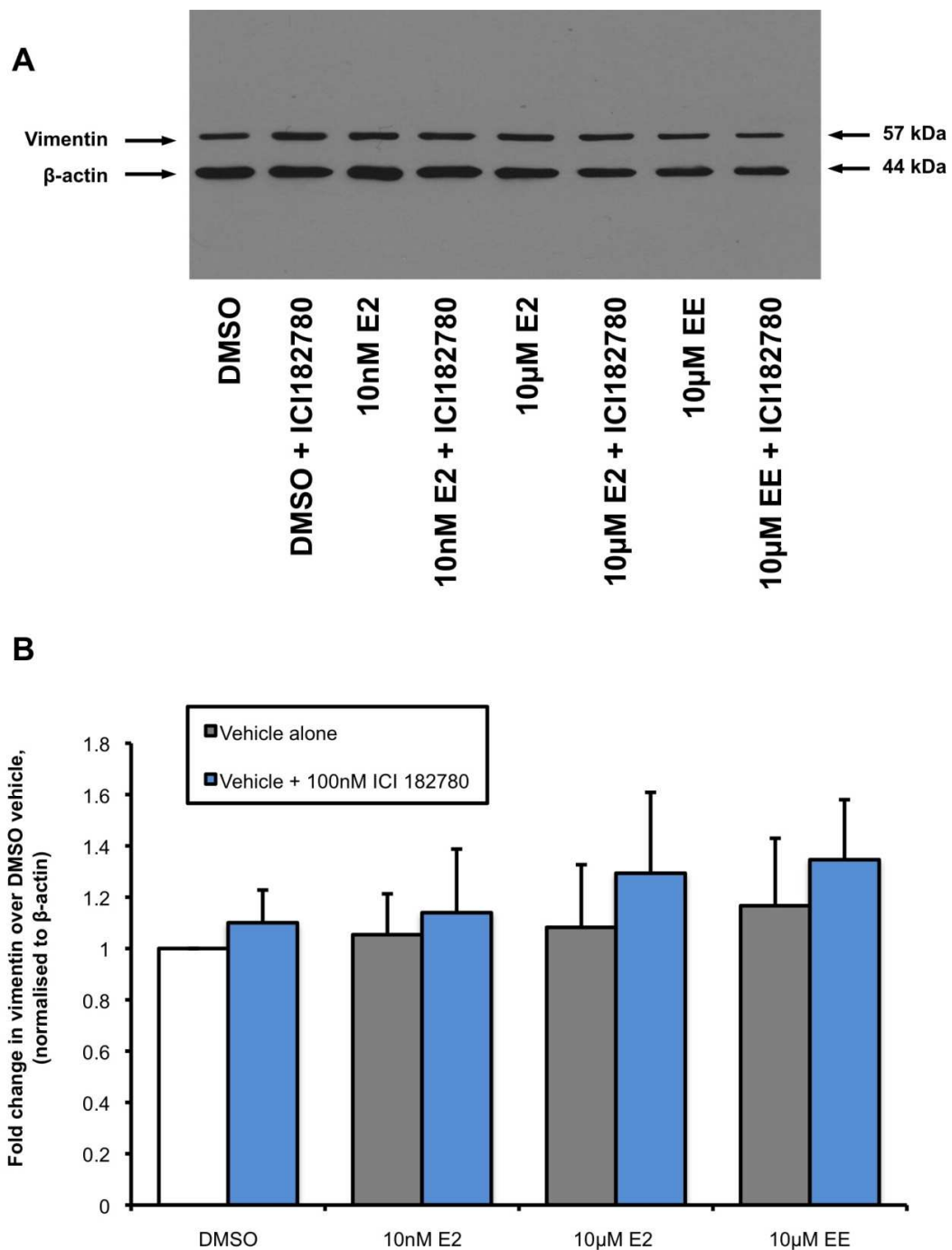


Figure 3.45 – Effect of E2 on the differentiation of biliary cell cultures. **A.** Western Blot for β-actin and vimentin for a fixed volume of total protein taken from cell cultures isolated from the rat biliary structure following treatment with 10nM/10µM E2 or DMSO vehicle, +/- 100nM ICI 182780, for 5 days. 20µl of protein sample/lane **B.** Quantification of vimentin Western blot expressed relative to total actin for a fixed volume of total protein taken from cell cultures isolated from the rat biliary structure following treatment with 10nM/10µM E2 or DMSO vehicle, +/- 100nM ICI 182780, for 5 days. Data are mean and SD of n=3.

3.5.5. Chapter 3.5 discussion

This chapter has described the isolation of cells from the intrahepatic biliary structure that proliferate to form a mixed population of cells, similar to that which may be found in the bile duct *in vivo*. These cell cultures were found to be positive for both OV-6 and albumin antigens, suggesting that the initial clusters of cells that were isolated have some stem cell like characteristics.

Further analysis of gene expression in these cell cultures revealed that they express Sox 17, a marker of progenitor cells whose fate may be endodermal epithelium, liver or pancreatic cell types. The cell cultures also expressed c-Myc and Klf4 up until the point of passage, and Sox 2 at the point of isolation. These transcription factors are thought to be essential in both native and induced pluripotency and their detection is further evidence of the presence of a form of liver progenitor cell within the cultures. Based on the expression of OV-6 which is widely regarded as a specific marker for oval cells, they may be identified as such. However, Oval cells are poorly defined and it is equally possible that OV-6 is a marker of a wider range of liver progenitor cells.

These cell cultures were discovered to be sensitive to estrogen exposure, which had some regulatory action upon their rate of proliferation, this may suggest that the mechanism of bile duct proliferation in estrogen cholestasis or PBC is as a direct response to the estrogen itself.

Estrogen was not found to alter the balance of fibroblasts to epithelial cells in culture so it may be possible that some other factor, possibly the toxicity of an environmental xenoestrogen, is required to induce fibrosis of the bile ducts seen in PBC.

4. General discussion

The initial aim of this research project was to identify xenobiotic compounds that may have the potential to initiate PBC through interactions with the ER. Although it has not been discussed at length in this thesis, the first method employed to achieve this specific aim was to find a reliable estrogen responsive gene in rat hepatocytes, the expression of which could be measured by quantitative PCR. It became apparent that this would not be possible as the response to a variety of different genes, previously reported to be estrogen responsive in the liver was found to be variable and inconsistent. The decision was made at that point to find an alternative method for measurement of transcriptional activity.

The subsequent development of an estrogen receptor-luciferase reporter construct was ultimately very beneficial. It allowed for thorough determination of the specificity of the resulting estrogen screening system and confirmation that transcriptional estrogenic activity mediated by both ER α and ER β . This method was coupled with the well-defined induction of TFF1 by estrogen receptor activation in MCF-7 cells. Estrogen induced TFF1 expression in estrogen responsive breast cancer cells has been investigated at length by cancer research groups⁹⁶ and was used to provide assurance the findings that emerged from the luciferase reporter work.

Primarily using the (ERE)₃pGL3-promoter luciferase screening system, groups of xenobiotics were assessed for transcriptional estrogenic activity in the MCF-7 breast carcinoma cell line. From these experiments, the transcriptional estrogenic activity of a number of compounds was discovered, and the activity

of other previously reported xenoestrogens was confirmed. These findings were corroborated by measurement of TFF1 expression. It is worth noting that some compounds appeared to inhibit the estrogen receptor in these experiments.

By performing dose-response investigations using the (ERE)₃-pGL3-promoter/MCF-7 system it became apparent that the potency of the identified xenoestrogens, sunset yellow, tartrazine, propyl paraben and butyl paraben was much lower (>50x lower) than E2. This suggested that whilst these compounds do appear to activate the human ER, a very high level of exposure might be required to produce comparable effects to those of pure estrogens *in vivo*.

Primary rat hepatocytes were used to study the effects of hepatic metabolism on the estrogenic activity of a smaller set of xenobiotics. These experiments proved difficult to perform as the estrogen response from different liver perfusions proved highly variable, and transfection of the necessary plasmids was inefficient. Despite these obstacles, the data obtained revealed that some xenobiotics, which were not estrogenic in MCF-7 cells, did appear to activate the rat ER in hepatocytes. This could be due to the requirement for metabolism to form reactive metabolites with estrogenic activity, or equally could indicate a species difference in substrate specificity between humans and rats. This could be explored further by repeating the investigation in primary human hepatocytes, an experiment that was attempted but the cells were repeatedly untransfected.

By utilising non estrogen responsive cell lines and ectopic expression of the different estrogen receptor subtypes, ER α and ER β , it was observed that tartrazine showed a greater affinity for ER β whilst sunset yellow was ER β specific in both MDA and H69 cells.

Following the identification of sunset yellow and tartrazine as hER activators, the effects of these compounds on mitochondrial function was investigated. The hypothesis was proposed that whilst the potency of the estrogenic activity of these xenobiotics was low in comparison to E2, if these compounds also caused a degree of mitochondrial toxicity they might be candidate triggers for PBC. It was discovered that sunset yellow caused a decrease in MTS reduction in primary rat hepatocytes, This was an indication that sunset yellow exposure may cause alterations to mitochondrial energetics, to which PDC enzymes are critical. Another clear difference between sunset yellow and tartrazine was observed, with the latter not producing the same hepatotoxic effects.

The inhibition of MTS reduction by sunset yellow was intensified in the presence of DTT. It is known that a major route of metabolism of azo dyes is via bacterial reduction in the gut¹⁰⁷. It is feasible that DTT may act as an electron donor to reduce sunset yellow further that is possible by cultures hepatocytes and that this reduced metabolite is more damaging to mitochondrial function. It is important to point out that it has been suggested previously that other enzymes including those involved in hepatic metabolism can also reduce MTS. It is not possible to conclude from this assay the precise effects of sunset yellow on mitochondrial viability. Another point of consideration is that MTS assay is a

colorimetric method, and despite careful experimental planning and normalisation to controls, there may be some degree of noise or interference.

A second measure of mitochondrial function was implemented. By measuring the localisation of TMRM following treatment, the mitochondrial membrane potential was examined. These data showed that treatment with relatively low concentrations of sunset yellow and tartrazine caused an accelerated loss of mitochondrial polarisation, supporting the evidence for these compounds to have a negative effect on mitochondrial function. Whilst these studies may imply that exposure to certain xenoestrogens causes a loss of mitochondrial function, it must be accepted that the effects seen in these assays may be due to cell death or proliferation effects resulting in a decreased number of mitochondria. Without performing cell proliferation/total protein it is impossible to clarify the underlying cause.

In a pilot study of estrogen exposure in the mouse, acute exposure to E2 was found to significantly increase PTI, this supports the previous work surrounding the cholestatic effect of estrogens. However this same earlier work has found similar effects following administration of EE, but in our model EE did not produce the same elevation in PTI as E2.

A range of xenobiotics, including sunset yellow and tartrazine, were tested for estrogenic activity using the classical mouse uterine bioassay. In this model only long-established xenoestrogens, such as methoxychlor, caused a significant acceleration in uterine development¹²³. Taking into account that ER β

is not deemed critical in sexual development it is reasonable to suggest that the uterotrophic assay is a screen for ER α activity¹²⁴. Having previously indicated that both sunset yellow and tartrazine appear to show higher affinity for the β receptor subtype *in vitro*, this offers an explanation to why they tested negative in the mouse assay.

In a separate *in vivo* model it was observed that tartrazine caused a similar cholestatic liver injury to E2, both treatments resulted in increased serum ALP activity, PTI and positive sirius red staining in the mouse. Despite not having an effect on uterine development, tartrazine produces a similar liver injury to E2. As the primary estrogen receptor in human cholangiocytes has been shown to be the β form, the expression of which is up regulated in cholestasis and in PBC, this is further evidence for the importance of ER β activation in cholestatic liver injury arising from estrogen/xenoestrogen exposure⁹².

Sunset yellow did not produce the same effect as tartrazine and E2, a potential explanation for this is that azo dyes are metabolised in part by reduction facilitated by gut bacteria, by administering these compounds by *i.p.* injection bypasses this system, which may be required for the bioactivation of some azo compounds. It would be worthwhile to repeat the same investigation and administer the treatment by oral gavage to investigate this further. The expression of a variety of membrane transport proteins were also analysed in this study. These data show that E2, tartrazine and sunset yellow all have effects on expression of the family of genes which encode MRP transporters and also other hepatic transport proteins. The expression of bile salt

transporters has been investigated previously in the context of estrogen cholestasis. Despite noticing alterations in expression of these genes, the results of our study did not always concur with previous work, high degree of variability between animals, and small group numbers may in some way accounted for this effect.

The expression of CYP3a11 in the mouse was analysed following treatment with xenoestrogens. It was found that both E2 and tartrazine caused a significant down regulation of this PXR dependant gene, implying a level of PXR antagonism. It has been previously documented that the PXR controls the expression of certain hepatic transport proteins, significantly MRP3¹¹⁵. The inhibition of Abcc3 gene (coding for MRP3) by E2 and tartrazine supports a theory of estrogenic PXR antagonism as a potential mechanism for the altered transport protein expression profile seen in estrogen cholestasis. As PXR activation has been reported to be beneficial in liver regeneration, its inhibition could cause a 'double hit' by also reducing the capacity for liver recovery.

The presence of AMA, or elevated serum antibody activity against PDC enzymes, is considered the hallmark of PBC. Following exposure to tartrazine, no significant increase in sera AMA activity over vehicle control was observed in the mouse. E2 did cause a significant increase in AMA activity, but again there was a lot of inter animal variability and small group numbers that reduced the statistical power of the study. A correlation was made between the serum AMA titre and the severity of liver injury in that animal. Remembering that AMA are

not detectable in all PBC patients, possibly AMA are not a causative factor in PBC, but merely an indication of the disease state.

Through the isolation of mixed cell populations from the intrahepatic biliary structure of the rat liver, it was possible to study the effect of estrogen exposure on growth and differentiation. It was observed that E2 caused an acceleration in the rate of proliferation of these cells, their differentiation was unchanged. It was not possible to examine the effects of the xenoestrogens tartrazine and sunset yellow, as the work with primary rat liver cells became impossible due to an unknown problem resulting in a decline in cell viability.

The *in vivo* studies of xenoestrogen exposure used exceptionally high doses of sunset yellow and tartrazine. Which were calculated based upon the EC₅₀ values from the *in vitro* screening systems. It is unrealistic that a person would ever be exposed to such a high concentration of a food dye. The maximum exposure to tartrazine, reported by the European food safety authority, is in the region of 8mg/kg body weight per day. There is potential for significant geographical variation in the exposure to azo compounds to occur. Those populations located close to industrial areas concerned with the dye industry, for example, may be exposed to significantly higher levels of azo dyes than other populations. And whilst it is already understood that there is an increased incidence of PBC in certain industrial areas, it would be interesting to map the incidence of PBC with the manufacture/use of these compounds.

During the course of the preparation of this thesis, the possible role of xenobiotic exposure in the initiation or progression of PBC has become more widely acknowledged. Research into geographical variance of the incidence of PBC has previously highlighted the north east of England as a 'hotspot' for PBC¹²⁵. Recent epidemiological studies amongst populations of PBC patients, such as those in the north east of England, have revealed a number of environmental risk factors, including the use of hair dyes and smoking. These same studies also show potential links between those who have previously been diagnosed with obstetric cholestasis¹²⁶.

More recently, research to understand the mechanisms by which chemical compounds may act to cause the development of PBC and more specifically the loss of tolerance to self PDC-E2 has suggested that some xenobiotics may disrupt the domain of PDC-E2 may disrupt the S-S disulphide. This may render it in a reduced state that could be susceptible to modification by any of a number of common electrophiles such as acetaminophen and other non-steroidal anti-inflammatory drugs (NSAIDs)¹²⁷.

This thesis has described how certain xenobiotics, routinely found in products, to which the frequent use of has been linked to increased incidence of PBC, can activate the human ER and cause a cholestatic liver injury in the mouse. This may cause an increase in ER β expression alongside PXR antagonism, both of which may form a positive feedback mechanism causing and intensifying and perpetuating cholestatic condition.

Whilst no definitive answers have been proposed, the evidence presented suggests that exposure to certain environmental xenoestrogens may be one of multitude of factors, including genetic susceptibility and predisposition to estrogen cholestasis or cholestatic liver disease, implicated in the development and progression of PBC.

5. References

1. Deroo BJ, Korach KS. Estrogen receptors and human disease. *The Journal of Clinical Investigation* 2006;116:561-570.
2. Hess RA, Bunick D, Bahr J. Oestrogen, its receptors and function in the male reproductive tract -- a review. *Molecular and Cellular Endocrinology* 2001;178:29-38.
3. Huet G, MÈrot Y, Le Dily F, Kern L, FerriÈre F, Saligaut C, Boujrad N, Pakdel F, MÈtivier R, Flouriot G. Loss of E-cadherin-mediated cell contacts reduces estrogen receptor alpha (ER[alpha]) transcriptional efficiency by affecting the respective contribution exerted by AF1 and AF2 transactivation functions. *Biochemical and Biophysical Research Communications* 2008;365:304-309.
4. pEGFP-N. www.liv.ac.uk.
5. e-Learning Unit St Georges University of London. *Liver Structure and Function*, 2006.
6. The Liver Centre, www.thelivercentre.com/au. 2003.
7. John Hopkins Gastroenterology and Hepatology, 2011.
8. Clemens DL. *Use of cultured cells to study alcohol metabolism*, 2006.
9. Cunningham C, Van Horn C. Energy availability and alcohol-related liver pathology. *Alcohol Res Health* 2003;27:291-9.
10. Li C, Wu Q. Adaptive evolution of multiple-variable exons and structural diversity of drug-metabolizing enzymes. *BMC Evolutionary Biology* 2007;7:69.
11. Nilsson S, Gustafsson JA. Estrogen Receptors: Therapies Targeted to Receptor Subtypes. *Clin Pharmacol Ther* 2011;89:44-55.
12. *Mechanisms of assembly and enzym.* www.chemistry.uah.edu
13. Bossard R, Stieger B, O'Neill B, Fricker G, Meier PJ. Ethinylestradiol treatment induces multiple canalicular membrane transport alterations in rat liver. *The Journal of Clinical Investigation* 1993;91:2714-20.
14. McGraw-Hill. AccessScience. www.accessscience.com

15. Friedman SL. Mac the knife? Macrophages, the double-edged sword of hepatic fibrosis. *The Journal of Clinical Investigation* 2005;115:29-32.
16. Lee JM, Trauner M, Soroka CJ, Stieger B, Meier PJ, Boyer JL. Expression of the bile salt export pump is maintained after chronic cholestasis in the rat. *Gastroenterology* 2000;118:163-172.
17. Kuntz E, Kuntz HD. *Hepatology: textbook and atlas : history, morphology, biochemistry, diagnostics, clinic, therapy*. Springer, 2008.
18. Gray H, Lewis WH. *Anatomy of the human body*. Lea & Febiger, 1918.
19. Wallace K, Burt AD, Wright MC. Liver fibrosis. *Biochem J* 2008;411:1-18.
20. Kiernan F. *The Anatomy and Physiology of the Liver*. *Philosophical Transactions of the Royal Society of London* 1833;123:711-770.
21. Rappaport AM, Wilson WD. The structural and functional unit in the human liver (liver acinus). *The Anatomical Record* 1958;130:673-689.
22. Ramadori G, Saile B. Portal tract fibrogenesis in the liver. *Lab Invest* 2003;84:153-159.
23. Woolf TF, Jordan RA. Basic Concepts in Drug Metabolism: Part I. *The Journal of Clinical Pharmacology* 1987;27:15-17.
24. Jordan R, Woolf T. Basic concepts in drug metabolism: Part II. *The Journal of Clinical Pharmacology* 1987;27:87-90.
25. Li Y. Steroid hormone biotransformation and xenobiotic induction of hepatic steroid metabolizing enzymes. *Chemico-Biological Interactions* 2004;147:233-246.
26. Zsembery A, Thalhammer T, Graf J. Bile Formation: a Concerted Action of Membrane Transporters in Hepatocytes and Cholangiocytes. *News Physiol Sci* 2000;15:6-11.
27. Aller M-A, Arias J-L, Garcia-Dominguez J, Arias J-I, Duran M, Arias J. Experimental obstructive cholestasis: the wound-like inflammatory liver response. *Fibrogenesis & Tissue Repair* 2008;1:6.
28. Pusl T, Beuers U. Intrahepatic cholestasis of pregnancy. *Orphanet Journal of Rare Diseases* 2007;2:26.

29. Jones DEJ. Pathogenesis of Primary Biliary Cirrhosis. *Clinics in Liver Disease* 2008;12:305-321.
30. Shuichi Terasaki YN, Masakazu Yamazaki, Masashi Unoura. Eosinophilic infiltration of the liver in primary biliary cirrhosis: A morphological study. *Hepatology* 1993;17:206-212.
31. Nakano T, Inoue K, Hirohara J, Arita S, Higuchi K, Omata M, Toda G. Long-term prognosis of primary biliary cirrhosis (PBC) in Japan and analysis of the factors of stage progression in asymptomatic PBC (a-PBC). *Hepatology Research* 2002;22:250-260.
32. Kumagi T, Heathcote EJ. Primary biliary cirrhosis. *Orphanet Journal of Rare Diseases* 2008;3:1.
33. Boberg K.M, Aadland E. Jahnsen J, Raknerud N, Stiris M, Bell H. Incidence and Prevalence of Primary Biliary Cirrhosis, Primary Sclerosing Cholangitis, and Autoimmune Hepatitis in a Norwegian Population. *Scandinavian Journal of Gastroenterology* 1998;33:99-103.
34. Reddy A. Tamoxifen: a novel treatment for primary biliary cirrhosis? *Liver International* 2004;24:194-197.
35. Masanori Abe MO. Natural history of primary biliary cirrhosis. *Hepatology Research* 2008;38:639-645.
36. Kaplan MM. Primary Biliary Cirrhosis. *New England Journal of Medicine* 1987;316:521-528.
37. Jones DEJ. Pathogenesis of primary biliary cirrhosis. *Postgraduate Medical Journal* 2008;84:23-33.
38. PBC foundation. 2011. www.pbcfoundation.org.uk
39. Poupon RE, Lindor KD, Cauch-Dudek K, Dickson ER, Poupon R, Heathcote EJ. Combined analysis of randomized controlled trials of ursodeoxycholic acid in primary biliary cirrhosis. *Gastroenterology* 1997;113:884 - 890.
40. Poupon RE, Bonnand AM, Chretien Y, Poupon R. Ten-year survival in ursodeoxycholic acid-treated patients with primary biliary cirrhosis. The UDCA-PBC Study Group. *Hepatology* 1999;29:1668 - 1671.

41. Corpechot C, Carrat F, Bonnard AM, Poupon RE, Poupon R. The effect of ursodeoxycholic acid therapy on liver fibrosis progression in primary biliary cirrhosis. *Hepatology* 2000;32:1196 - 1199.
42. Mauss, Berg, Rockstroh, Sarrazin, Wedemeyer. *Hepatology - A Clinical Textbook*, 2010.
43. Mitchison HC, Palmer JM, Bassendine MF, Watson AJ, Record CO, James OFW. A controlled trial of prednisolone treatment in primary biliary cirrhosis : Three-year results. *Journal of Hepatology* 1992;15:336-344.
44. Christensen E, Neuberger J, Crowe J, Altman DG, Popper H, Portmann B, Doniach D, Ranek L, Tygstrup N, Williams R. Beneficial effect of azathioprine and prediction of prognosis in primary biliary cirrhosis. Final results of an international trial. *Gastroenterology* 1985;89:1084-91.
45. Wiesner RH, Ludwig J, Lindor KD, Jorgensen RA, Baldus WP, Homburger HA, Dickson ER. A Controlled Trial of Cyclosporine in the Treatment of Primary Biliary Cirrhosis. *New England Journal of Medicine* 1990;322:1419-1424.
46. Bodenheimer HC, Schaffner F, Sternlieb I, Klion FM, Vernace S, Pezzullo J. A prospective clinical trial of D-penicillamine in the treatment of primary biliary cirrhosis. *Hepatology* 1985;5:1139-1142.
47. Hendrickse MT, Rigney E, Giaffer MH, Soomro I, Triger DR, Underwood JCE, Gleeson D. Low-dose methotrexate is ineffective in primary biliary cirrhosis: Long-term results of a placebo-controlled trial. *Gastroenterology* 1999;117:400-407.
48. Leuschner M, G,ld,tuna Sk, You T, H,bner K, Bhatti S, Leuschner U. Ursodeoxycholic acid and prednisolone versus ursodeoxycholic acid and placebo in the treatment of early stages of primary biliary cirrhosis. *Journal of Hepatology* 1996;25:49-57.
49. Leuschner M, Maier K-P, Schlichting J, Strahl S, Herrmann Gn, Dahm HH, Ackermann H, Happ J, Leuschner U. Oral budesonide and ursodeoxycholic acid for treatment of primary biliary cirrhosis: Results of a prospective double-blind trial. *Gastroenterology* 1999;117:918-925.
50. Leuschner M, Holtmeier J, Ackermann H, Leuschner U. The influence of sulindac on patients with primary biliary cirrhosis that responds

- incompletely to ursodeoxycholic acid: a pilot study. *European Journal of Gastroenterology & Hepatology* 2002;14:1369-1376.
51. Ikeda T, Tozuka S, Noguchi O, Kobayashi F, Sakamoto S, Marumo F, Sato C. Effects of additional administration of colchicine in ursodeoxycholic acid-treated patients with primary biliary cirrhosis: a prospective randomized study. *Journal of Hepatology* 1996;24:88-94.
 52. Poupon RE, Huet PM, Poupon R, Bonnand A, Van Nhieu JT, Zafrani ES. A randomized trial comparing colchicine and ursodeoxycholic acid combination to ursodeoxycholic acid in primary biliary cirrhosis. *Hepatology* 1996;24:1098-1103.
 53. Hoensch HP, Balzer K, Dylewicz P, Kirch W, Goebell H, Ohnhaus EE. Effect of rifampicin treatment on hepatic drug metabolism and serum bile acids in patients with primary biliary cirrhosis. *European Journal of Clinical Pharmacology* 1985;28:475-477.
 54. Harmsen S, Meijerman I, Beijnen J, Schellens J. Nuclear receptor mediated induction of cytochrome P450 3A4 by anticancer drugs: a key role for the pregnane X receptor. *Cancer Chemotherapy and Pharmacology* 2009;64:35-43.
 55. Beuers U, Kullak-Ublick G, Pusch T, Rauws E, Rust C. Medical Treatment of Primary Sclerosing Cholangitis: A Role for Novel Bile Acids and other (post-)Transcriptional Modulators? *Clinical Reviews in Allergy and Immunology* 2009;36:52-61.
 56. Marek CJ, Tucker SJ, Konstantinou DK, Elrick LJ, Haefner D, Sigalas C, Murray GI, Goodwin B, Wright MC. Pregnenolone-16 α -carbonitrile inhibits rodent liver fibrogenesis via PXR (pregnane X receptor)-dependent and PXR-independent mechanisms. *Biochem. J.* 2005;387:601-608.
 57. Axon A, Cowie DE, Mann DA, Wright MC. A mechanism for the anti-fibrogenic effects of the pregnane X receptor (PXR) in the liver: Inhibition of NF- κ B? *Toxicology* 2008;246:40-44.
 58. Haughton EL, Tucker SJ, Marek CJ, Durward E, Leel V, Bascal Z, Monaghan T, Koruth M, Collie-Duguid E, Mann DA, Trim JE, Wright MC. Pregnane X Receptor Activators Inhibit Human Hepatic Stellate Cell Transdifferentiation In Vitro. *Gastroenterology* 2006;131:194-209.

59. Christensen E, Gunson B, Neuberger J. Optimal timing of liver transplantation for patients with primary biliary cirrhosis: use of prognostic modelling. *J Hepatol* 1999;30:285 - 292.
60. Fregeau D, Davis P, Danner D, Ansari A, Coppel R, Dickson E, Gershwin M. Antimitochondrial antibodies of primary biliary cirrhosis recognize dihydrolipoamide acyltransferase and inhibit enzyme function of the branched chain alpha-ketoacid dehydrogenase complex. *The Journal of Immunology* 1989;142:3815-3820.
61. Hiromasa Y, Fujisawa T, Aso Y, Roche TE. Organization of the Cores of the Mammalian Pyruvate Dehydrogenase Complex Formed by E2 and E2 Plus the E3-binding Protein and Their Capacities to Bind the E1 and E3 Components. *Journal of Biological Chemistry* 2004;279:6921-6933.
62. Fukushima N, Nalbandian G, Van De Water J, White K, Ansari AA, Leung P, Kenny T, Kamita SG, Hammock BD, Coppel RL, Stevenson F, Ishibashi H, Gershwin ME. Characterization of recombinant monoclonal IgA anti—PDC-E2 autoantibodies derived from patients with PBC. *Hepatology* 2002;36:1383-1392.
63. Nishio A, Van de Water J, Leung PS, Joplin R, Neuberger JM, Lake J, Bjorkland A, Totterman TH, Peters M, Worman HJ, Ansari AA, Coppel RL, Gershwin ME. Comparative studies of antimitochondrial autoantibodies in sera and bile in primary biliary cirrhosis. *Hepatology* 1997;25:1085-1089.
64. Palmer JM, Doshi M, Kirby JA, Yeaman SJ, Bassendine MF, Jones DEJ. Secretory autoantibodies in primary biliary cirrhosis (PBC). *Clinical & Experimental Immunology* 2000;122:423-428.
65. M. Eric Gershwin . Primary biliary cirrhosis: an orchestrated immune response against epithelial cells. *Immunological Reviews* 2000;174:210-225.
66. Selmi C, Lleo A, Invernizzi P, Eric Gershwin M. Primary Biliary Cirrhosis and Autoimmune Cholangitis. *Liver Immunology*, 2007:235-247.
67. Christen U . Identification of the dihydrolipoamide acetyltransferase subunit of the human pyruvate dehydrogenase complex as an autoantigen in halothane hepatitis. *European Journal of Biochemistry* 1994;223:1035-1047.

68. Amano K, Leung PS, Rieger R, Quan C, Wang X, Marik J, Suen YF, Kurth MJ, Nantz MH, Ansari AA, Lam KS, Zeniya M, Matsuura E, Coppel RL, Gershwin ME. Chemical xenobiotics and mitochondrial autoantigens in primary biliary cirrhosis: identification of antibodies against a common environmental, cosmetic, and food additive, 2-octynoic acid. *J Immunol* 2005;174:5874 - 5883.
69. Gershwin ME, Selmi C, Worman HJ, Gold EB, Watnik M, Utts J, Lindor KD, Kaplan MM, Vierling JM. USA PBC Epidemiology Group. Risk factors and comorbidities in primary biliary cirrhosis: a controlled interview-based study of 1032 patients. *Hepatology* 2005;42:1194 - 1202.
70. Zein CO, Beatty K, Post AB, Logan L, Debanne S, McCullough AJ. Smoking and increased severity of hepatic fibrosis in primary biliary cirrhosis: A cross validated retrospective assessment. *Hepatology* 2006;44:1564 - 1571.
71. Arrese M, Macias RIR, Briz O, Perez MJ, Marin JJG. Molecular pathogenesis of intrahepatic cholestasis of pregnancy. *Expert Reviews in Molecular Medicine* 2008;10:null-null.
72. Reyes H. Sex hormones and bile acids in intrahepatic cholestasis of pregnancy. *Hepatology* 2008;47:376-379.
73. Huang P, Chandra V, Rastinejad F. Structural Overview of the Nuclear Receptor Superfamily: Insights into Physiology and Therapeutics. *Annual Review of Physiology* 2010;72:247-272.
74. McKenna NJ, O'Malley BW. Combinatorial Control of Gene Expression by Nuclear Receptors and Coregulators. *Cell* 2002;108:465-474.
75. Shu F-j, Sidell N, Yang D, Kallen CB. The tri-nucleotide spacer sequence between estrogen response element half-sites is conserved and modulates ER[alpha]-mediated transcriptional responses. *The Journal of Steroid Biochemistry and Molecular Biology* 2010;120:172-179.
76. Tsai MJ, O'Malley BW. Molecular mechanisms of action of steroid/thyroid receptor superfamily members. *Annual review of biochemistry* 1994;63:451-86.
77. DeNardo DG, Kim H-T, Hilsenbeck S, Cuba V, Tsimelzon A, Brown PH. Global Gene Expression Analysis of Estrogen Receptor Transcription Factor Cross Talk in Breast Cancer: Identification of Estrogen-

- Induced/Activator Protein-1-Dependent Genes. *Molecular Endocrinology* 2005;19:362-378.
78. Björnström L, Sjöberg M. Mechanisms of Estrogen Receptor Signaling: Convergence of Genomic and Nongenomic Actions on Target Genes. *Molecular Endocrinology* 2005;19:833-842.
 79. Levin ER. Cellular Functions of the Plasma Membrane Estrogen Receptor. *Trends in Endocrinology and Metabolism* 1999;10:374-377.
 80. Ellmann S, Sticht H, Thiel F, Beckmann M, Strick R, Strissel P. Estrogen and progesterone receptors: from molecular structures to clinical targets. *Cellular and Molecular Life Sciences* 2009;66:2405-2426.
 81. Thomas P, Dong J. Binding and activation of the seven-transmembrane estrogen receptor GPR30 by environmental estrogens: A potential novel mechanism of endocrine disruption. *The Journal of Steroid Biochemistry and Molecular Biology* 2006;102:175-179.
 82. Hall JM, Couse JF, Korach KS. The Multifaceted Mechanisms of Estradiol and Estrogen Receptor Signaling. *Journal of Biological Chemistry* 2001;276:36869-36872.
 83. Nilsson S, Gustafsson J-A. Estrogen receptor transcription and transactivation: Basic aspects of estrogen action. *Breast Cancer Res* 2000;2:360 - 366.
 84. Cowley SM, Hoare S, Mosselman S, Parker MG. Estrogen Receptors α and β Form Heterodimers on DNA. *Journal of Biological Chemistry* 1997;272:19858-19862.
 85. Subramanian S, Tovey M, Afentoulis M, Krogstad A, Vandenberg AA, Offner H. Ethinyl estradiol treats collagen-induced arthritis in DBA/1J mice by inhibiting the production of TNF- α and IL-1 β . *Clinical Immunology* 2005;115:162-172.
 86. Bolt HM. Metabolism of estrogens--natural and synthetic. *Pharmacology & Therapeutics* 1979;4:155-181.
 87. McDonnell DP, Wardell SE. The molecular mechanisms underlying the pharmacological actions of ER modulators: implications for new drug discovery in breast cancer. *Current Opinion in Pharmacology* 2010;10:620-628.

88. Brown AM, Jeltsch JM, Roberts M, Chambon P. Activation of pS2 gene transcription is a primary response to estrogen in the human breast cancer cell line MCF-7. *Proceedings of the National Academy of Sciences* 1984;81:6344-6348.
89. Westley B, May FE, Brown AM, Krust A, Chambon P, Lippman ME, Rochefort H. Effects of antiestrogens on the estrogen-regulated pS2 RNA and the 52- and 160-kilodalton proteins in MCF7 cells and two tamoxifen-resistant sublines. *Journal of Biological Chemistry* 1984;259:10030-10035.
90. Rubin BL, Dorfman AS, Black L, Dorfman RI. Bioassay of estrogens using the mouse uterine response. *Endocrinology* 1951;49:429-439.
91. Galey FD, Mendez LE, Whitehead WE, Holstege DM, Plumlee KH, Johnson B. Estrogenic Activity in Forages: Diagnostic Use of the Classical Mouse Uterine Bioassay. *Journal of Veterinary Diagnostic Investigation* 1993;5:603-608.
92. Alvaro D, Invernizzi P, Onori P, Franchitto A, De Santis A, Crosignani A, Sferra R, Ginanni-Corradini S, Grazia Mancino M, Maggioni M, Attili AF, Podda M, Gaudio E. Estrogen receptors in cholangiocytes and the progression of primary biliary cirrhosis. *Journal of Hepatology* 2004;41:905-912.
93. Vanparys C, Maras M, Lenjou M, Robbens J, Van Bockstaele D, Blust R, De Coen W. Flow cytometric cell cycle analysis allows for rapid screening of estrogenicity in MCF-7 breast cancer cells. *Toxicology in Vitro* 2006;20:1238-1248.
94. Prusakiewicz JJ, Harville HM, Zhang Y, Ackermann C, Voorman RL. Parabens inhibit human skin estrogen sulfotransferase activity: Possible link to paraben estrogenic effects. *Toxicology* 2007;232:248-256.
95. Jones DE, Palmer JM, Yeaman SJ, Kirby JA, Bassendine MF. Breakdown of tolerance to pyruvate dehydrogenase complex in experimental autoimmune cholangitis: A mouse model of primary biliary cirrhosis. *Hepatology* 1999;30:65-70.
96. May FE, Westley BR. Effects of tamoxifen and 4-hydroxytamoxifen on the pNR-1 and pNR-2 estrogen-regulated RNAs in human breast cancer cells. *Journal of Biological Chemistry* 1987;262:15894-15899.

97. Stewart AJ, Johnson MD, May FE, Westley BR. Role of insulin-like growth factors and the type I insulin-like growth factor receptor in the estrogen-stimulated proliferation of human breast cancer cells. *Journal of Biological Chemistry* 1990;265:21172-8.
98. May FEB, Semple JI, Prest SJ, Westley BR. Expression and mitogenic activity of TFF2 in human breast cancer cells. *Peptides* 2004;25:865-872.
99. Mgbonyebi OP, Russo J, Russo IH. Roscovitine Induces Cell Death and Morphological Changes Indicative of Apoptosis in MDA-MB-231 Breast Cancer Cells. *Cancer Research* 1999;59:1903-1910.
100. Chatagnon A, Ballestar E, Esteller M, Dante R. A Role for Methyl-CpG Binding Domain Protein 2 in the Modulation of the Estrogen Response of pS2/TFF1 Gene. *PLoS ONE* 2010
101. Amano K, Leung PSC, Rieger R, Quan C, Wang X, Marik J, Suen YF, Kurth MJ, Nantz MH, Ansari AA, Lam KS, Zeniya M, Matsuura E, Coppel# RL, Gershwin ME. Chemical Xenobiotics and Mitochondrial Autoantigens in Primary Biliary Cirrhosis: Identification of Antibodies against a Common Environmental, Cosmetic, and Food Additive, 2-Octynoic Acid. *The Journal of Immunology* 2005;174:5874-5883.
102. Gershwin ME, Selmi C, Worman HJ, Gold EB, Watnik M, Utts J, Lindor KD, Kaplan MM, Vierling JM. Risk factors and comorbidities in primary biliary cirrhosis: A controlled interview-based study of 1032 patients. *Hepatology* 2005;42:1194-1202.
103. Routledge EJ, Parker J, Odum J, Ashby J, Sumpter JP. Some Alkyl Hydroxy Benzoate Preservatives (Parabens) Are Estrogenic. *Toxicology and Applied Pharmacology* 1998;153:12-19.
104. Wallace K, Fairhall EA, Charlton KA, Wright MC. AR42J-B-13 cell: An expandable progenitor to generate an unlimited supply of functional hepatocytes. *Toxicology* 2010;278:277-287.
105. Gerasimenko JV, Gerasimenko OV, Palejwala A, Tepikin AV, Petersen OH, Watson AJM. Menadione-induced apoptosis: roles of cytosolic Ca²⁺ elevations and the mitochondrial permeability transition pore. *Journal of Cell Science* 2002;115:485-497.
106. Sweeney EA, Chipman JK, Forsythe SJ. Evidence for Direct-Acting Oxidative Genotoxicity by Reduction Products of Azo Dyes. *Environmental Health Perspectives* 1994;102:119-122.

107. Chung K-T, Stevens SE, Cerniglia CE. The Reduction of Azo Dyes by the Intestinal Microflora. *Critical Reviews in Microbiology* 1992;18:175-190.
108. Yamamoto Y, Moore R, Hess HA, Guo GL, Gonzalez FJ, Korach KS, Maronpot RR, Negishi M. Estrogen Receptor α Mediates 17 α -Ethinylestradiol Causing Hepatotoxicity. *Journal of Biological Chemistry* 2006;281:16625-16631.
109. Stieger B, Fattinger K, Madon J, Kullak-Ublick GA, Meier PJ. Drug- and estrogen-induced cholestasis through inhibition of the hepatocellular bile salt export pump (Bsep) of rat liver. *Gastroenterology* 2000;118:422-430.
110. Gu X, Manautou JE. Regulation of hepatic ABCC transporters by xenobiotics and in disease states. *Drug Metabolism Reviews* 2010;42:482-538.
111. Zelcer N, Wetering Kvd, Waart Rd, Scheffer GL, Marschall H-U, Wielinga PR, Kuil A, Kunne C, Smith A, Valk Mvd, Wijnholds J, Elferink RO, Borst P. Mice lacking Mrp3 (Abcc3) have normal bile salt transport, but altered hepatic transport of endogenous glucuronides. *Journal of Hepatology* 2006;44:768-775.
112. Gradhand U, Lang T, Schaeffeler E, Glaeser H, Tegude H, Klein K, Fritz P, Jedlitschky G, Kroemer HK, Bachmakov I, Anwald B, Kerb R, Zanger UM, Eichelbaum M, Schwab M, Fromm MF. Variability in human hepatic MRP4 expression: influence of cholestasis and genotype. *Pharmacogenomics J* 2007;8:42-52.
113. Simon FR, Fortune J, Iwahashi M, Qadri I, Sutherland E. Multihormonal regulation of hepatic sinusoidal Ntcp gene expression. *American Journal of Physiology - Gastrointestinal and Liver Physiology* 2004;287:G782-G794.
114. Thiebaut F, Tsuruo T, Hamada H, Gottesman MM, Pastan I, Willingham MC. Cellular localization of the multidrug-resistance gene product P-glycoprotein in normal human tissues. *Proceedings of the National Academy of Sciences* 1987;84:7735-7738.
115. Teng S, Jekerle V, Piquette-Miller M. Induction of Abcc3 (MRP3) by pregnane X receptor activators. *Drug Metabolism and Disposition* 2003;31:1296-1299.

116. Fausto N. Liver regeneration and repair: Hepatocytes, progenitor cells, and stem cells. *Hepatology* 2004;39:1477-1487.
117. Cardinale V, Wang Y, Carpino G, Cui C-B, Gatto M, Rossi M, Berloco PB, Cantafora A, Wauthier E, Furth ME, Inverardi L, Dominguez-Bendala J, Ricordi C, Gerber D, Gaudio E, Alvaro D, Reid L. Multipotent stem/progenitor cells in human biliary tree give rise to hepatocytes, cholangiocytes and pancreatic islets. *Hepatology* 2011:n/a-n/a.
118. Petersen BE, Goff JP, Greenberger JS, Michalopoulos GK. Hepatic oval cells express the hematopoietic stem cell marker thy-1 in the rat. *Hepatology* 1998;27:433-445.
119. Shiojiri N. Analysis of Differentiation of Hepatocytes and Bile Duct Cells in Developing Mouse Liver by Albumin Immunofluorescence. *Development, Growth & Differentiation* 1984;26:555-561.
120. Sinner Db, Rankin S, Lee M, Zorn AM. Sox17 and β -catenin cooperate to regulate the transcription of endodermal genes. *Development* 2004;131:3069-3080.
121. Shi Y, Desponts C, Do JT, Hahm HS, Sch[^]ler HR, Ding S. Induction of Pluripotent Stem Cells from Mouse Embryonic Fibroblasts by Oct4 and Klf4 with Small-Molecule Compounds. *Cell Stem Cell* 2008;3:568-574.
122. Moretti A, Bellin M, Jung CB, Thies T-M, Takashima Y, Bernshausen A, Schiemann M, Fischer S, Moosmang S, Smith AG, Lam JT, Laugwitz K-L. Mouse and human induced pluripotent stem cells as a source for multipotent Isl1+ cardiovascular progenitors. *The FASEB Journal* 2010;24:700-711.
123. Tullner WW. Uterotrophic Action of the Insecticide Methoxychlor. *Science* 1961;133:647-648.
124. Krege JH, Hodgins JB, Couse JF, Enmark E, Warner M, Mahler JF, Sar M, Korach KS, Gustafsson J-Ö, Smithies O. Generation and reproductive phenotypes of mice lacking estrogen receptor β . *Proceedings of the National Academy of Sciences* 1998;95:15677-15682.
125. Metcalf JV, Bhopal RS, Gray J, Howel D, James OFW. Incidence and prevalence of primary biliary cirrhosis in the city of Newcastle upon Tyne, England. *International Journal of Epidemiology* 1997;26:830-836.

126. Prince MI, Ducker SJ, James OFW. Case-control studies of risk factors for primary biliary cirrhosis in two United Kingdom populations. *Gut* 2010;59:508-512.
127. Naiyanetr P, Butler JD, Meng L, Pfeiff J, Kenny TP, Guggenheim KG, Reiger R, Lam K, Kurth MJ, Ansari AA, Coppel RL, Lopez-Hoyos M, Gershwin ME, Leung PSC. Electrophile-modified lipoic derivatives of PDC-E2 elicits anti-mitochondrial antibody reactivity. *Journal of Autoimmunity* 2011;37:209-216.

6. Communication and Awards

COMMUNICATION

- NEPG Conference 2011
- ISHSR 2011
- BTS Autumn Conference 2011
- ISHSR 2010
- BTS annual congress 2009

AWARDS

- The British Toxicology Society Best Presentation Award 2011
- BTS Travel Award Bursary 2011
- ISHSR Travel Award Bursary 2010
- BTS travel award bursary 2009

7. Publications and abstracts